

https://dspace.org/

Water-gas shift reaction over supported metal oxides with special reference to the cobalt manganese oxide system

2015-01-22
http://hdl.handle.net/10539/16690

Downloaded from a DSpace repository. https://dspace.org/

WATER-GAS SHIFT REACTION OVER SUPPORTED METAL OXIDES WITH SPECIAL REFERENCE TO THE COBALT MANGANESE OXIDE SYSTEM

Frank Michael Gottschalk

A Dissertation Submitted to the Faculty of Science, University of the Witwatersrand, Johannesburg in fulfilment of the requirements for the degree of Doctor of Philosophy

Johannesburg, December 1989

25×

ABSTRACT

The water-gas shift reaction ($H_2O + CO \rightleftharpoons H_2 + CO_2$) is used extensively in a number of industrial processes either to produce the large tonnages of hydrogen required in the manufacture of ammonia, or to adjust the CO/H_2 ratio of synthesis gas for the manufacture of chemicals. At present most production units operate a two stage process involving an Fe/Cr oxide high temperature shift catalyst (to reduce the CO content of gas derived synthesis gas from about 10 mole % to ca. 3 mole %) followed by a low temperature shift unit which utilises a Cu/Zn oxide catalyst (to further reduce the CO content to ca. 0.3 mole %). However, as the Cu/Zn oxide catalyst is readily poisoned by sulphur, it cannot be operated successfully with coal derived synthesis gas.

This Thesis presents the results of a study involving the development of various novel high temperature water-gas shift catalysts with significantly improved activity and sulphur resistivity when compared to current industrial formulations. Co/Mn oxide, Cu/Mn oxide and Co/Cr oxide catalysts were prepared by co-precipitation from their respective metal nitrates and tested for water-gas shift activity using a laboratory scale (2g catalyst) testing rig. Catalytic

activity was found to be mainly a function of the metal ratios as well as operating temperature. Under optimum conditions, all three catalyst systems were found to give appreciably higher activity when compared to an existing Fe/Cr based commercial catalyst.

Kinetic and mechanistic investigations revealed that the water-gas shift reaction proceeded via the formation of surface formate intermediates over all three catalyst systems tested. Furthermore, a regenerative "Temkin type" mechanism was suspected to occur at a high partial pressure of CO over the Co/Mn oxide and the Co/Cr oxide catalysts.

Sulphur poisoning studies were also carried out by co-feeding different levels of sulphur (i.e 1 ppm and 240 ppm total S). The results indicated that only the Cu/Mn oxide catalyst showed signs of deactivation after prolonged exposure to these gases.

In summary, three novel high activity water-gas shift catalyst systems were identified, and their chemical behaviours studied under a variety of experimental conditions. Both the Co/Mn oxide and the Co/Cr oxide proved to be potentially valuable as substitute commercial high temperature water-gas shift catalysts.

DECLARATION

I declare that this dissertation is my own, unaided work. It is being submitted for the degree Doctor of Philosophy in the University of the Witwatersrand, Johannesburg. It has not been submitted before for any degree or examination in any other University.

P.L. Yelland

20th day of December, 1989

To My Parents

ACKNOWLEDGEMENTS

I would like to thank the following people and institutions for their ever present support. Without them this thesis would not have been written.

- *Prof. G.J. Hutchings* and Prof. R.G. Copperthwaite, my supervisors for their constant assistance, guidance and encouragement at all times.

- Prof. N.J. Coville, Dr. R.H. Hunter and Dr. S.W. Orchard for their valuable discussions and input to this Thesis.

- To my family for their constant support and encouragement in the more difficult phases of the project.

- To my fellow students and friends in the catalysis laboratory, for creating a pleasant working atmosphere.

- Acknowledgements are also due to the staff of the Chemistry Department of the University, particularly Agnes Pointeer, Margret Crabb, Barry Fairbrother, John Hughes, Steve van der Schyff, Les Henwood and Basil Chassoulas.

- The support of four related Honours projects in the fields of potassium promotion of Co/Mn oxide catalysts (Sa Colley), Co/Cr oxide catalysts (Tarnya Sangiorgio), mechanistic studies over Co/Cr oxide (John Mellor) and Cu/Mn oxide catalysts (Mariam Rhemtula) is also greatly appreciated.

- Finally, I would like to thank AECI Ltd. for their generous financial and personal support for the entire duration of this project.

LIST OF ABBREVIATIONS

AAS	- Atomic Absorption Spectroscopy
BET	- Brunauer, Emmett, Teller (surface area)
DSC	- Differential Scanning Calorimetry
EDTA	- *Ethylenediaminetetraacetic acid*
FCC	- Faced Centred Cubic
FID	- Flame Ionisation Detector
FT	- Fischer Tropsch
FTIR	- Fourier Tranisform Infra Red
GC	- Gas Chromatograph
GHSV	- Gas Hourly Space Velocity
HCP	- Hexagonal Closest Packed
HDS	- Hydrodesulphurisation
SS	- Stainless Steel
TCD	- Thermal Conductivity Detector
TGA	- Thermogravimetric Analysis
XRD	- X-ray Diffractometry

CONTENTS

	Page
LIST OF ABBREVIATIONS	viii
LIST OF TABLES	xv
LIST OF FIGURES	xviii
1. INTRODUCTION	1
1.1 History of catalysis	1
1.2 The water-gas shift reaction	3
1.3 Applications of the water-gas shift reaction	4
1.4 Catalysts used for the water-gas shift reaction	6
1.4.1 High temperature water-gas shift catalysts	6
1.4.2 Copper based low temperature water-gas shift catalysts	10
1.4.3 Sulphided cobalt molybdenum based water-gas shift catalysts	13
1.4.4 Homogeneous water-gas shift catalysts	14
1.5 Mechanisms for the water-gas shift reaction	17
1.5.1 The redox mechanism	18

Page

1.5.2 Surface intermediate type mechanisms 20

1.5.2.1 Reagent adsorption onto catalyst sites 21

1.5.2.2 The formation of the central intermediate 22

1.5.3 Other mechanisms 26

1.5.4 Summary of the proposed mechanisms 30

1.6 The kinetics of the water-gas shift reaction 31

1.7 Outline of thesis 36

2. EXPERIMENTAL 40

2.1 Catalyst preparation 40

2.2 Catalyst pretreatment 42

2.3 Catalyst testing 43

2.4 Product gas analysis, data evaluation and calculations 44

2.5 Catalyst characterisation 45

3. COBALT MANGANESE OXIDE WATER-GAS SHIFT CATALYSTS 46

3.1 Introduction 46

3.2 Experimental 50

Page

3.3 Effect of Co:Mn ratios on the water-gas shift activity 51

3.3.1 Catalyst activity and lifetime studies 51

3.3.2 Temperature dependent studies 55

3.4 Effect of potassium promotion on the water-gas shift activity and CH_4 production 59

3.5 Effect of reagent feed rates on the water-gas shift activity 63

3.6 Structural characterisation 65

3.7 Competition between carbon monoxide hydrogenation and water-gas shift activity 72

3.7.1 Carbon monoxide hydrogenation 72

3.7.2 Water-gas shift activity 73

3.7.3 Discussion 77

3.8 Summary 78

4. COPPER AND IRON MANGANESE OXIDE WATER-GAS SHIFT CATALYSTS 80

4.1 Introduction 80

4.1.1 The iron manganese oxide catalyst system 80

4.1.2 The copper manganese oxide catalyst system 81

Page

4.2 Comparison of the water-gas shift activities of the Cu/Mn oxide, Fe/Mn oxide and Co/Mn oxide catalysts 83

4.2.1 Specific catalyst activities 85

4.2.2 *Activation energy calculations* 87

4.3 Effect of Cu:Mn ratios on catalytic activity 89

4.3.1 Effect of temperature on catalytic activity 89

4.3.2 Stability studies involving Cu/Mn oxide catalysts 91

4.3.3 Effect of reagent feed rate on catalytic activity 94

4.4 Effect of potassium promotion on the water-gas shift activity of a Cu:Mn = 1:3 catalyst 96

4.5 Structural characterisation of Cu/Mn oxide and Fe/Mn oxide catalysts 97

4.5.1 The Fe/Mn oxide system 97

4.5.2 The Cu/Mn oxide system 98

4.5.3 Thermometric analysis of a Cu/Mn oxide catalyst 103

4.6 Summary 104

Page

5. COBALT CHROMIUM OXIDE BASED WATER-GAS SHIFT CATALYSTS 108

5.1 Introduction 108

5.2 Activity studies 109

5.2.1 Temperature dependence 110

5.2.2 Stability studies 113

5.2.3 Surface area determinations 114

5.3 Methane by-product formation under water-gas shift reaction conditions 115

5.4 Structural studies 120

5.5 Summary 127

6. A KINETIC AND MECHANISTIC STUDY OF THE Co/Mn OXIDE, Cu/Mn OXIDE AND Co/Cr OXIDE WATER-GAS SHIFT CATALYSTS 129

6.1 Introduction 129

6.2 Experimental techniques 130

6.3 Kinetic studies 132

6.3.1 The effect of the partial pressure of H_2O on the rate of the reaction 132

6.3.2 The effect of the partial pressure of CO on the rate of the reaction 134

6.3.2.1 The Langmuir-Hinshelwood mechanism 137

25×

Page

6.4 Model reagent mechanistic studies 143

6.4.1 Reaction of formic acid over various catalyst systems 144

6.4.2 Reaction of methanol over various catalyst systems 150

6.5 Reaction mechanism 156

6.6 Summary 161

7. SULPHUR POISONING STUDIES 163

7.1 Introduction 163

7.2 Experimental 169

7.3 Results 170

7.4 Discussion 172

7.4.1 The Co/Mn oxide and Co/Cr oxide catalyst system 172

7.4.2 The Cu/Mn oxide catalyst system 173

7.5 Summary 176

8. CONCLUSION 178

REFERENCES 181

Appendix 1 : Co-precipitation method 203

Appendix 2 : Impregnation or "Incipient Wetness" method 207

	Page
Appendix 3 : Catalyst pretreatment	209
Appendix 4 : Stainless steel reactor assembly used for catalyst testing	211
Appendix 5 : Glass reactor assembly for the mechanistic co-feeding experiments	217
Appendix 6 : Product analysis	220
Appendix 7 : Data evaluation and calculations	223
Appendix 8 : Catalyst characterisation	226
Appendix 9 : List of Publications	228

LIST OF TABLES

		Page
Table 1.1	: Characteristics of currently used water-gas shift catalysts	37
Table 2.1	: Experimental parameters used for the preparation of the various catalyst systems tested	204
Table 2.2	: Calcination temperatures during catalyst pretreatments	209
Table 2.3	: Reduction conditions for the various catalysts tested	210
Table 3.1	: BET surface areas of pure Co and Co:Mn = 3:1 catalyst	55
Table 3.2	: Temperature dependence of K_p and equilibrium conversion of CO	57
Table 3.3	: BET surface areas of potassium promoted Co/Mn oxide catalysts	61
Table 3.4	: Bulk structure of a Co/Mn oxide catalyst	67
Table 3.5	: Lattice parameters of MnO present in an active Co/Mn oxide catalyst	71
Table 3.6	: Carbon monoxide hydrogenation over a Co/Mn oxide catalyst	73
Table 3.7	: Water-gas shift/CO hydrogenation activity of a Co:Mn = 1:1 catalyst	74

LIST OF TABLES (continued)

		Page
Table 3.8	: Reaction of a carbon monoxide, hydrogen and water feed mixture	75
Table 4.1	: Pseudo first order rate constants for X:Mn = 1:1 catalysts (X=Cu, Fe or Co)	84
Table 4.2	: Surface areas determined by the BET method for the various manganese oxide catalysts tested	85
Table 4.3	: Specific catalyst activity for the *various metal/manganese oxide* catalyst systems	86
Table 4.4	: Apparent activation energies of the various manganese oxide catalysts tested	89
Table 4.5	: BET surface areas of discharged Cu/Mn oxide catalysts	93
Table 4.6	: Bulk surface structure of Cu/Mn oxide catalysts as determined by X-ray diffractometry	99
Table 4.7	: Ionic radii of Co, Cu and Mn cations	102
Table 4.8	: Lattice parameters for pure and catalytically active MnO	102
Table 5.1	: Apparent activation energies for the various Co/Cr oxide catalysts studied	112

LIST OF TABLES (continued)

		Page
Table 5.2	: Surface areas for Co : Cr = 1:1 catalyst for the various stages of pretreatment	115
Table 5.3	: Bulk structure of Co/Cr oxide catalysts	121
Table 6.1	: Reaction of formic acid over the various catalysts tested	148
Table 6.2	: Reaction of methanol over the various catalysts studied - (i) Organic product distribution	151
Table 6.3	: Reaction of methanol over the various catalysts studied - (ii) Inorganic product distribution	152
Table 7.1	: Composition of sulphur-containing feed gas	170
Table 7.2	: Surface area determined by the BET method for the various manganese oxide catalysts after sulphur exposure experiments	175

LIST OF FIGURES

		Page
Figure 1.1	: Heats of adsorption of CO versus metal activity at 300°C	21
Figure 1.2	: Water-gas shift reaction sequence proposed by Amenomiya and Pleitzer (65)	23
Figure 1.3	: Formation of water-gas shift intermediate as proposed by Grenoble et. al. (8)	24
Figure 1.4	: Water-gas shift mechanism as proposed by Shopov and Andreev (66)	25
Figure 1.5	: Mechanistic steps for the homogeneously catalysed water-gas shift reaction as proposed by Ford (55)	28
Figure 1.6	: Water-gas shift reaction cycle proposed by Elliott (69)	30
Figure 2.1	: Schematic representation of the experimental set-up used for co-precipitation method	205
Figure 2.2	: Stainless steel reactor assembly layout	212
Figure 2.3	: Schematic diagram of evaporator	213
Figure 2.4	: Details of reactor design	215

LIST OF FIGURES

		Page
Figure 2.5	: Valve system used to select individual product streams	216
Figure 2.6	: Glass reactor used for mechanistic studies	217
Figure 2.7	: Pneumatically operated gas chromatographic sample valve	220
Figure 2.8	: Chromatogram of a typical permanent gas analysis	223
Figure 3.1	: Synergic bonding model of carbon monoxide onto a catalytic surface	50
Figure 3.2	: Effect of metal ratio on water-gas shift activity	53
Figure 3.3	: Effect of temperature on CO conversion for the various Co/Mn oxide catalysts tested	56
Figure 3.4	: Effect of temperature on CH_4 by-product levels	58
Figure 3.5	: Effect of potassium addition on CO conversion for a Co:Mn = 3:1 catalyst	60
Figure 3.6	: Effect of potassium addition on the rate of CH_4 formation for a Co:Mn = 3:1 catalyst	62

LIST OF FIGURES (continued)

		Page
Figure 3.7	: Effect of CO : H_2O ratio on the catalytic performance	64
Figure 3.8	: Effect of CO GHSV on catalytic activity	65
Figure 3.9	: DSC plot for Co/Mn oxide catalyst reducing under hydrogen	68
Figure 3.10	: TGA plot for Co/Mn oxide catalyst reducing under hydrogen	69
Figure 4.1	: CO conversion as a function of temperature for the Cu/Mn oxide catalysts tested	90
Figure 4.2	: Stability of various Cu/Mn oxide catalysts	92
Figure 4.3	: Effect of CO GHSV on catalytic performance for the various Cu/Mn oxide catalyst tested	94
Figure 4.4	: Effect of H_2O : CO feed ratio on catalytic performance of the various Cu/Mn oxide catalysts tested	95
Figure 4.5	: Potassium promotion of a 1:3 Cu/Mn oxide catalyst	96
Figure 4.6	: Structural differences between calcined Cu/Mn oxide and calcined Co/Mn oxide catalysts	101

LIST OF FIGURES (continued)

		Page
Figure 4.7	: DSC trace for Cu/Mn oxide catalyst reducing under hydrogen	103
Figure 4.8	: TGA trace for the 1:3 Cu/Mn oxide catalyst reducing under hydrogen	105
Figure 5.1	: Effect of temperature on the water-gas shift activity for the various Co/Cr oxide catalysts studied	110
Figure 5.2	: Stability of Co/Cr oxide catalysts	113
Figure 5.3	: Methane by-product formation over various Co/Cr oxide catalysts operated under water-gas shift reaction conditions	116
Figure 5.4	: Effect of introducing potassium or manganese on the levels of methane formation over a Co:Cr = 3:1 catalyst	118
Figure 5.5	: Effect of introducing potassium or manganese on the water-gas shift activity over a Co:Cr = 3:1 catalyst	119
Figure 5.6	: A comparison of the $CuMn_2O_4$ spinel to the $CoCr_2O_4$ spinel	122

LIST OF FIGURES (continued)

		Page
Figure 5.7	: DSC plot for the reduction of a $CoCr_2O_4$ catalyst under hydrogen	126
Figure 6.1	: Rate of H_2O conversion as a *function of* P_{H2O} *for the* various catalysts tested	133
Figure 6.2	: Effect of CO partial pressure on the rate of CO conversion for the various catalysts tested	135
Figure 6.3	: A comparison between experimental and theoretical rates of CO conversion at constant H_2O partial pressure for the Co/MnO and $CoCr_2O_4$ catalysts	141
Figure 6.4	: Decomposition of formic acid over metal oxide catalysts	149
Figure 6.5	: The formation of methyl formate over the various catalysts studied	153
Figure 6.6	: Water-gas shift reaction mechanism over the Co/MnO and the $CoCr_2O_4$ catalyst systems investigated	158

LIST OF FIGURES (continued)

Page

Figure 6.7 : Water-gas shift reaction mechanism over the Cu/MnO catalyst system 160

Figure 7.1 : Schematic diagram of a coal-based *ammonia synthesis plant* 164

Figure 7.2 : Hydrodesulphurisation reaction sequence over a CoMox catalyst proposed by Topsoe et. al. (195) 168

Figure 7.3 : Stability studies of various catalysts using coal-derived feed gas containing 1 ppm sulphur 171

Figure 7.4 : Stability studies of various catalysts using coal-derived feed gas containing 240 ppm sulphur 172

1. INTRODUCTION

1.1 History of catalysis

" Catalytic power actually means that substances are able to awake affinities which are asleep at this temperature by their mere presence and not by their own affinity "

This was part of the definition first proposed by Berzelius (1) in 1836 about an unexplainable power that has turned out to be a major driving force in the chemical industry. Berzelius was referring to the observations made in the early 19th century, when it was noticed that a number of chemical reactions were affected by the presence of trace amounts of foreign substances that did not take part in the reaction itself. Considering what little was known about chemical reactivity at the time and comparing it with today's definition (1) of a catalyst, which states that

" a catalyst is a substance that increases the rate at which a chemical system approaches equilibrium, without being consumed in the process "

one can see that Berzelius expressed his view on catalysis with a definite degree of perception Even though, this appeared to be the first attempt at

25×1C

describing the function of catalysts, the first use of catalysts had already been made by man thousands of years ago. This was the time when wine, vinegar and soap were made using catalytic techniques, although their workings were not entirely understood.

It was only in 1746 when modern industrial catalysis as we know it came into being with the introduction of the "lead chamber process" for the manufacture of sulphuric acid. In this method nitric acid was used to oxidise SO_2 to SO_3 in an aqueous environment. Almost 70 years later, in 1831, the above mentioned oxidation of SO_2 was carried out over a platinum surface and was patented by Phillips. It was first carried out on a commercial scale by Squire and Messel in 1875. By this time the catalytic production of chlorine gas from HCl and air over a supported $CuCl_2$ catalyst (2) had been introduced by Deacon in 1860. From then onwards followed a never ending surge of developments of catalytic processes operated on an industrial scale.

It was the understanding brought to the subject by the Nobel prize winners Bosch and Haber (introducing the catalytic production of ammonia from hydrogen and nitrogen in 1913), and Ziegler and Natta, who in 1955 developed a catalyst that could polymerise ethylene at low pressures, which transformed the "black art" of catalysis into the science as we know it today.

The production of ammonia,

$$N_2 + 3\ H_2 \rightleftharpoons 2\ NH_3 \qquad (1.1)$$

can be considered as one of the earliest major catalytic processes to be introduced on an industrial scale. With it came the need for supplementary technology - hydrogen needed to be produced on a large scale. Before the advent of the Haber-Bosch process, hydrogen was manufactured by means of electrolysis or by dissolving iron in sulphuric acid (3). However, these processes only allowed for the production of hydrogen on a small scale. Thus the need for large-scale hydrogen production was recognised.

1.2 The water-gas shift reaction

Already before the turn of the century, it was known that if carbon monoxide and steam were passed over catalytic materials such as red hot refractories (4) one obtained hydrogen and carbon dioxide. This reaction became known as the water-gas shift reaction or the CO shift reaction.

$$CO_{(g)} + H_2O_{(g)} \rightleftharpoons H_{2\ (g)} + CO_{2\ (g)} \qquad (1.2)$$

This reaction is an exothermic ($\Delta H = -40.6$ kJ/mol) chemical change controlled by a thermodynamic

equilibrium, which can be accelerated by a catalyst. One should note, that as there is no change in molar volume during the reaction, the equilibrium constant is therefore independent of pressure.

1.3 Applications of the water-gas shift reaction

The water-gas shift reaction has become a well studied reaction of industrial importance (5-8), as it not only produces hydrogen, but can also be utilised to remove any unwanted carbon monoxide. It was these two applications that ensured this reaction an integral part in many large scale chemical operations.

The most important use of the water-gas shift reaction will always be in the production of ammonia, where it not only produces sufficient hydrogen, but also removes unwanted carbon monoxide, which would otherwise poison the ammonia synthesis catalyst. However, there are far more areas where the water-gas shift reaction is utilised. For example, in the 1930's hydrogen was produced in the USA by reacting methane with steam, according to the following reaction:

$$CH_4 + H_2O \rightleftharpoons 3\ H_2 + CO \qquad (1.3)$$

The water-gas shift reaction was then used to "shift" the unwanted carbon monoxide together with more steam to produce more hydrogen and carbon dioxide. The carbon dioxide could then be easily removed in a cryogenic "rectisol" unit.

Further applications can be found in the Fischer-Tropsch industry, where, for the hydrogenation of carbon monoxide, a feed gas containing about two parts hydrogen and one part carbon monoxide is required. Synthesis gas derived from various sources (eg. coal gasification or steam reforming of hydrocarbons) yield a H_2 : CO ratio of about 1 : 1. The water-gas shift reaction is then used to convert the excess CO and produce more hydrogen so that the required H_2 : CO ratio is reached.

Other applications of the water-gas shift reaction include the detoxification of town gas (9) and automotive emission control (10) where the lowering of CO levels is required. Some speculation and research (12) has also been aimed at employing the CO-shift reaction for hydrogenation by using H_2O as the hydrogenation agent instead of H_2. Here the hydrogenation of coal could bring about a new means of hydrocarbon production. With the ever increasing demand for hydrogen, the water-gas shift reaction is certain to continue as an important industrial process.

1.4 Catalysts used for the water-gas shift reaction

It has been found that the water-gas shift reaction is catalysed heterogeneously by many metals and metal oxides and recently the academic interest in homogeneous water-gas shift catalyst systems has increased (40, 44-46). Moe (13) and Grenoble et.al. (8) give accounts of the activity of various metals for the water-gas shift reaction. Grenoble found the activity of alumina supported metal catalysts (at 300° C) to decrease in the following order :

Cu > Re > Co > Ni > Pt > Os > Au > Fe > Pd > Rh > Ir

However, only two classes of catalysts are currently used on an industrial scale, namely the Fe-based "high temperature" shift catalysts, and the Cu-based "low temperature" shift catalysts, which have only been utilised since the late 1960's.

1.4.1 High temperature water-gas shift catalysts

The history of the Fe based high temperature shift catalysts can be traced back to 1913, when BASF claimed the use of an iron oxide based catalyst that could be promoted with other metal oxides including thoria. It was soon found that these iron based catalysts could be

operated successfully in the temperature range : 320 to 450 ^{o}C - hence the name "high temperature" shift catalysts. These catalysts were found to contain about 70 - 74 % Fe_2O_3 and 8 - 10 % Cr_2O_3 and other volatiles (14) in their precursor stage. However, Markina et. al. (15) showed that the optimum Cr_2O_3 content appeared to be about 14 % (wt). It is generally believed that the Cr_2O_3 only acts as a stabiliser to prevent deactivation due to high temperature sintering, and not as a catalytic promoter. This finding is best supported by the work of Singh et. al. (16) who observed that catalysts prepared without Cr_2O_3 lost catalytic activity much faster than the Cr_2O_3 supported Fe_2O_3 catalysts.

Before use, the high temperature water-gas shift catalysts have to be activated by means of partial reduction of Fe_2O_3 to form Fe_3O_4. This step has to be carried out under controlled conditions as the formation of metallic Fe must be avoided because it catalyses the highly exothermic methanation reaction (17) shown below.

$$CO + 3\ H_2 \rightleftharpoons CH_4 + H_2O \qquad (1.4)$$

Gonzalez et. al. (18) give a good discussion of the influence of thermal pretreatment and reduction

conditions on the activity of various high temperature water-gas shift catalysts. They concluded that the use of pure hydrogen gas or a gas mixture comprising hydrogen, nitrogen, carbon monoxide and water vapour were best suited as reducing agents to obtain a highly active Fe_3O_4 / Cr_2O_3 water-gas shift catalyst. Furthermore, they claimed that the use of these two reducing mixtures eliminated an over-reduction as long as the temperatures were kept below 500 ^{o}C. These findings are also in agreement with those of Bohlbro et. al. (19), who recommended a reduction temperature in the range of 250 to 400 ^{o}C, claiming that higher temperatures result in decreased catalytic activity due, presumably, to sintering of the active phase.

Another feature of these ferrochrome catalysts is their very long lifetimes, with continuous industrial operations of more than two years having been achieved (20). Nevertheless, these catalysts do show some deactivation with time-on-line, and this problem has been the subject of numerous studies (21-24) with many theories being proposed as to the causes. Ahmed et. al. (23) for example claimed that the deactivation was due to various temperature and time-on-stream factors. A more detailed explanation is given by Chinchen et. al. (24), who reported two forms of decay - the initial

fast decay and the subsequent slow decay of activity. They attributed these forms of decay to the rapid sintering of Fe_3O_4 crystallites which are in contact with each other. They then claimed that after some time Cr_2O_3 crystallites will separate the Fe_3O_4 crystallites and the deactivation process will slow down. In practice, the loss of activity of a high temperature shift catalyst is compensated for by increasing its operating temperature (5), which in turn restores the catalytic activity.

In contrast to the copper-based low temperature shift catalysts, which shall be discussed later in this chapter, the ferrochrome catalysts are not very susceptible to poisons, thus making them ideal choices for plants operating on oil-based or coal-based feedstock, which contain sulphur compounds. Bohlbro et. al. (19) found that small levels of sulphur (i.e. < 10 ppm) had next to no effect on the catalytic activity, but that at sulphur levels higher than 100 ppm the catalysts' activities decreased approximately as the square root of the sulphur concentration. They also found that other poisons like chlorine, phosphorous and silicon could only be tolerated at levels of about 1 ppm, before having adverse effects on the catalytic activity.

From this discussion of the high temperature ferrochrome shift catalysts, it can be seen that they are adequately suited for operation on current chemical plants. They represent a generation of catalysts which are not only reasonably economical to manufacture, but also show good water-gas shift activity and resistance to potential catalyst poisons when operated under plant conditions. However, iron is not the most active water-gas shift material and thus the attraction of developing a yet more active catalytic material, which otherwise has the same advantages as the Fe-based catalysts, still exists.

1.4.2 Copper based low temperature water-gas shift catalysts

Copper based materials have been known to catalyse various reactions carried out on an industrial scale, such as carbon monoxide oxidation (25), methanol synthesis (26, 27), and nitrous oxide decomposition (28). However, in the field of water-gas shift catalysis, the use of these copper based materials was only reported in the literature in the mid 1960's, when Uchida et. al. (29) reported an active zinc oxide-copper oxide catalyst for carbon monoxide shift conversion. They found that the optimum Cu/Zn atomic ratio for their type of catalyst was about 0.4.

Studies have since been carried out to determine the various phases present in this catalyst system. In more recent years, Garbassi et. al. (30) used X-ray photoelectron spectroscopy to study the unreduced copper-zinc system. They found evidence for the existence of a non equilibrium solid solution of Cu(II) in ZnO. Structural studies have also been carried out on the active form of the Cu/ZnO catalysts. These studies have shown that if the catalyst is not reduced prior to use free Cu^{+} ions are the active phase under reaction conditions (31). Again, ZnO was claimed to be the other major phase present. However, upon reduction, the formation of Cu metal has been observed and it has been shown (32) that a Cu catalyst supported on alumina showed the same activity as a Cu catalyst containing significant amounts of ZnO. Thus, it now be concluded that Cu metal seems to be the active phase and it appears that ZnO acts as a structural support in order to stabilise the surface area of the Cu metal. This theory is also supported by Uchida et. al. (33), who used X-ray diffraction analysis to confirm the presence of Cu metal and ZnO as the only major phases present in their active low temperature water-gas shift catalyst.

The Cu/ZnO catalysts are generally operated at much lower temperatures than the Fe based high temperature

shift catalysts. Typical operating temperatures range from about 210°C to 240°C (34). As Cu is known to sinter readily at elevated temperatures (35, 36), an operating temperature of higher than 280°C should be avoided in order to prevent catalyst deactivation (5).

Even though the low temperature shift catalysts are highly active if operated properly (c.f. Cu being the most active water-gas shift material (8,13)), they are also very susceptible to poisoning, especially by sulphur and chlorine (34, 37). Hawker (5) described how sulphur and chlorine poisoning cause catalyst deactivation and how to minimise these effects. He suggested that in order to counteract the effect of sulphur poisoning, the catalyst should contain a high surface area of unbound zinc oxide, as it will absorb sulphur, by reacting to form zinc sulphide and water. Thus in an industrial water-gas shift reactor, operating with a Cu/ZnO catalyst, it is possible, that the upper part of the catalyst bed will only be used to remove any sulphur impurities by absorbing them onto the ZnO, and the lower part of the bed will be used for the CO shift reaction. Hawker furthermore described chlorine, which is generally present in the form of HCl, as a more severe poison than sulphur, as it increased the sintering rate of the Cu/ZnO catalyst. It thereby reduced the overall surface area of the catalyst, leading to loss of activity.

This short discussion on copper containing low temperature shift catalysts has shown that these are highly active water-gas shift catalysts, which use Cu metal as their active component, and ZnO as a structural support. They are, however, not ideal, particularly for coal derived synthesis gas, because they are susceptible to high temperature sintering and irreversible poisoning by both sulphur and chlorine.

1.4.3 Sulphided Cobalt Molybdenum based water-gas shift catalysts

Sulphided cobalt molybdenum catalysts have proved themselves highly active hydrodesulphurisation catalysts (38,39). For this process, the active phases are claimed to be a mixture of Co_9S_8 and MoS_2 supported on γ - Al_2O_3 (40), but due to the complexity of the sulphided form there still exists disagreement as to the precise structural features.

Apart from catalysing various hydrodesulphurisation reactions, this type of material has also been found to be active as a water-gas shift catalyst (41). The major advantage of this class of catalyst, which contains about 1-2 % Co and about 7 % Mo, is complete insensitivity to sulphur poisoning. In fact, this type of catalyst is only active in its sulphided form (41).

Activation is generally carried out by pretreating the calcined Co-Mo-Al_2O_3 precursor material with a gas mixture of H_2S and H_2 at an elevated temperature (42).

Comparing the sulphided Co-Mo-Al_2O_3 catalysts with the Fe-based and the Cu-based water-gas shift catalysts, Newsome (7) used data to show that at 404°C and even at 300°C the water-gas shift activity of a Cs promoted Co-Mo-Al_2O_3 catalyst is superior to the activity of both the Fe-based and the Cu-based catalyst systems. However, in order for this sulphided type of catalyst to remain active, the feed gas has to contain sulphur compounds at levels higher than normally found in process gas. Furthermore, the required presence of sulphur in the gas stream might be harmful to other catalyst systems, which are generally operated in conjunction with the water-gas shift reaction. These last two observations could explain why the sulphided Co-Mo-Al_2O_3 material is not yet operative as an industrial water-gas shift catalyst.

1.4.4. Homogeneous Water-Gas Shift Catalysts

The introduction of homogeneous catalyst systems started with the "Oxo process", which was developed by Roelen in Germany in 1938-1946. It involved the

reaction of an olefin with carbon monoxide and hydrogen to produce aldehydes and fatty acids, using a cobalt carbonyl catalyst (43).

The first indication of a homogeneous water-gas shift catalyst in the literature was made in 1953 by Reppe et. al. (44), who suggested the use of $Fe(CO)_5$ as a catalyst. However, their study only seemed to be of a theoretical nature. The reaction was thought to proceed according to the following cycle:

$$H_2Fe(CO)_4 + CO \longrightarrow Fe(CO)_5 + H_2 \quad (1.5)$$

$$Fe(CO)_5 + H_2O \longrightarrow H_2Fe(CO)_4 + CO_2 \quad (1.6)$$

$$CO + H_2O \longrightarrow CO_2 + H_2$$

It was not until the early 1970's that more information appeared in the literature in the form of patents, which described the use of a variety of group VIII metals in conjunction with phosphine, arsine or stibine ligands as homogeneous water-gas shift catalysts (45). Further advancement in the field was made in 1977 when several researchers discovered new catalyst systems for the water-gas shift reaction. Eisenberg et. al. (46) showed that a catalyst derived from $[Rh(CO)_2Cl]_2$, HCl and NaI in glacial acetic acid was an active homogeneous water-gas shift catalyst at as low a temperature as 80°C. On the other hand, Ka et. al. (47) and Laine et. al. (48) developed h[illegible]geneous

water-gas shift catalysts which were active in a basic medium.

At this time it was obvious that the water-gas shift reaction could be catalysed under homogeneous conditions and the development of new homogeneous catalyst systems increased at a rapid rate. A system based on platinum chloride - tin chloride was first reported by Cheng and Eisenberg (49). This followed the introduction of numerous other catalysts based on metals such as platinum (50) and nickel (51).

Numerous other homogeneous systems, mainly consisting of metal carbonyls have been found to exhibit water-gas shift activity. Laine and Wilson (45) give a good review on the composition and working of these systems. The major advantage of all these homogeneous systems is that they can successfully be operated at temperatures much lower than 200°C, which would be the cut-off temperature for the Cu-based low temperature heterogeneous water-gas shift catalyst. For example, Laine and Wilson (45) also showed that an amine-promoted $Ru_3(CO)_{12}$ complex run in an alkaline solvent showed outstanding water-gas shift activity at a temperature of only 100°C.

However, significant disadvantages of these catalyst

systems include their susceptibility to sulphur poisoning and the unfavourable costs involved in producing and operating such systems on an industrial scale.

1.5. Mechanisms for the water-gas shift reaction

The classical definition of the term "mechanism" as found in many textbooks (52, 53), includes all the individual collisional or other elementary processes involving molecules, atoms, radicals and ions that take place simultaneously or consecutively in producing the observed overall reaction. Nevertheless, one should not loose track of the fact that a proposed mechanism can only explain the experimental data that was available at the time. One might even find that the current data can account for the existence of several plausible mechanisms. In such cases, more experimentation is required to at least eliminate some of the possibilities. Thus, a mechanism should only be seen as a tool in the quest to understand and describe the entire reaction.

Due to the importance of the water-gas shift reaction as a source of high purity hydrogen, this reaction has been the subject of many theoretical and mechanistic

studies (7,45,54,55). However, to this day there is still considerable controversy as to the exact mechanism operating in the water-gas shift reaction. A short review of mechanistic aspects will now be given.

1.5.1 The Redox Mechanism

At first sight the water-gas shift reaction appears to be an oxygen transfer reaction, as an oxygen atom is transferred from a water molecule to a carbon monoxide molecule as shown below :

$$CO + H_2O \xrightarrow{\text{catalyst}} CO_2 + H_2 \qquad (1.7)$$

This type of transfer is known as the reduction-oxidation mechanism (56-58). It was first proposed by Temkin et. al. (59) in 1949 for the water-gas shift reaction over an iron based catalyst. The overall reaction was envisaged to proceed as follows:

reduction :

$$H_2O_{(g)} + \text{Red.} \rightleftharpoons H_{2\,(g)} + \text{Ox} \qquad (1.8)$$

oxidation :

$$CO_{(g)} + \text{Ox} \rightleftharpoons CO_{2\,(g)} + \text{Red} \qquad (1.9)$$

Where Ox = Oxidised species of the active catalyst component

Red = Reduced species of the active catalyst component

As has been mentioned previously, Fe_3O_4 appeared to be the active phase for the standard high temperature shift catalyst. Boreskov et. al. (60) have shown that the required reduction of Fe_3O_4 and the subsequent oxidation of the reduced species is possible under normal reaction conditions. If one now assumes that the oxidised and reduced species of the active catalytic material are Fe_3O_4 and FeO respectively, then the water-gas shift reaction will proceed over the high temperature Fe-based catalysts as follows according to this redox type mechanism (61) :

$$H_2O_{(g)} + 3\ FeO \rightleftharpoons H_{2(g)} + Fe_3O_4 \quad (1.10)$$

$$CO_{(g)} + Fe_3O_4 \rightleftharpoons CO_{2(g)} + 3\ FeO \quad (1.11)$$

There still exists a great deal of uncertainty as to the catalytically active species involved in the redox mechanism over the Cu-based low temperature shift catalysts, especially since van Herwijnen et. al. (61) reported that the required oxidation of copper is thermodynamically not favourable at normal operating temperatures. However, Salmi et. al. (58) have claimed that a redox type mechanism was significant at the beginning of the reaction period over the Cu-based catalysts, but that the main reaction pathway probably proceeds via the formation of a surface intermediate.

1.5.2 Surface Intermediate type Mechanisms

These type of mechanisms incorporate the build-up of the reagent species on the surface of the catalytic material with the subsequent formation of a central intermediate. This intermediate will then react in such a way as to form the product species. The following scheme gives an example of such a mechanism, which was proposed by Yur'eva et. al. (62) to occur on a copper-chromite catalyst :

$$CO_{(g)} \rightleftharpoons CO_{(ads.)}$$

$$H_2O_{(g)} \rightleftharpoons H_2O_{(ads.)}$$

$$CO_{(ads.)} + H_2O_{(ads.)} \rightleftharpoons [\ ]^* \rightleftharpoons CO_{2\,(ads.)} + H_{2\,(ads.)}$$

$$CO_{2\,(ads.)} \rightleftharpoons CO_{2\,(g)}$$

$$H_{2\,(ads.)} \rightleftharpoons H_{2\,(g)}$$

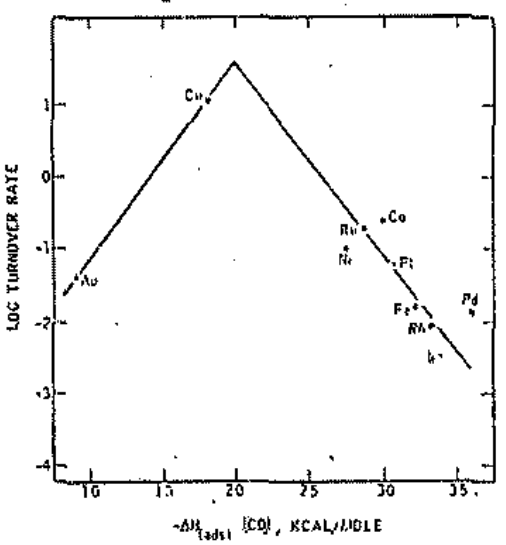
where $[\ ]^*$ denotes the central intermediate of unknown composition. It is thus of relevance to consider previous studies conducted to determine the identity of this central intermediate. These studies

involve specifically the adsorption of both CO and H_2O onto the surface sites of the catalyst.

1.5.2.1 Reagent adsorption onto catalyst sites

Grenoble et. al. (8) considered that it would be reasonable to expect a relationship between the water-gas shift activity of the metal catalyst and the strength of interaction of CO with the catalyst surface. Using the heats of adsorption obtained by Vannice et. al. (63), they were able to draw a correlation between the heats of adsorption of CO and the metal activity at 300°C as shown in Figure 1.1.

Figure 1.1 : Heats of adsorption of CO versus metal activity at 300°C [a]



a : from reference 8

Grenoble concluded that for the adsorbed CO there should be an optimum strength of interaction between CO and the catalytic surface. If this interaction is too weak, (as is the case for Au), the catalytic activity will be low, due to the fact that the surface concentration of adsorbed CO will be low. On the other hand, if the interaction between CO and the metal is too strong, (as is the case for Pd or Ir, for example), then the adsorbed CO intermediate becomes so stable that subsequent reaction to form the central water-gas shift reaction intermediate slows down considerably.

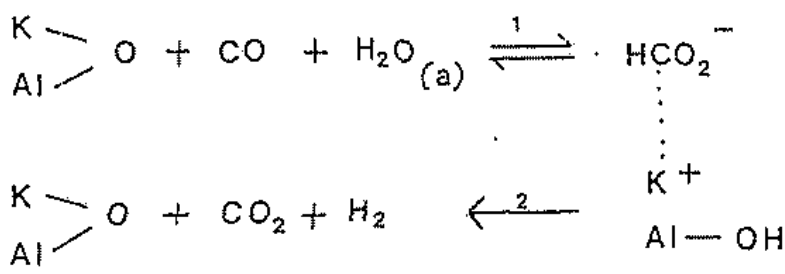
Furthermore, when Grenoble et.al. (8) considered the interaction of H_2O with the catalyst surface, th concluded that for SiO_2-and Al_2O_3-supporte catalysts the support had a much stronger effect towards reactions requiring the activation of H_2O. They finally concluded that the water-gas shift reaction occurred bifunctionally with the active metal activating the CO and that the support activating the H_2O.

1.5.2.2 The formation of the central intermediate

The identity of the central intermediate has always been an area of great discussion. This dates back to as

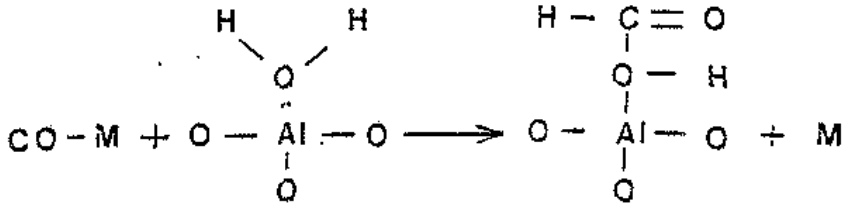
early as 1920, when Armstrong and Hilditch (64) suggested the central intermediate in the water-gas shift reaction over a Cu/ZnO catalyst to be formic acid. Since then their claim has been backed up by other researchers. Amenomiya and Pleitzer (65) argued that on promoted alumina catalysts a formate intermediate had formed. Backing their claim by infra-red spectroscopy, they proposed following reaction sequence shown in Figure 1.2 for the water-gas shift reaction :

Figure 1.2 : Water-gas shift reaction sequence proposed by Amenomiya and Pleitzer (65)



The formation of a formic acid complex as the central intermediate was also reported by Grenoble et.al. (8) who suggested the mechanism given in Figure 1.3 for the formation of such an intermediate over alumina-supported metal catalysts.

Figure 1.3 : Formation of water-gas shift reaction intermediate as proposed by Grenoble et. al. (8)

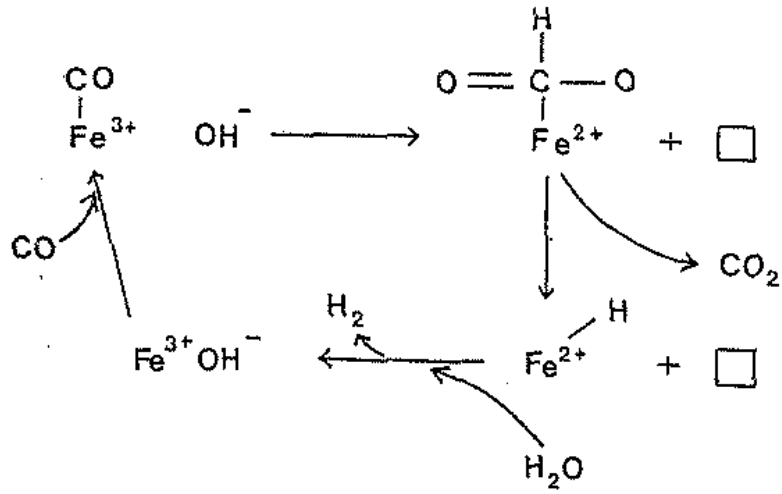


They also reported that the formic acid must "shift" from the support to the active metal component of the catalyst, before the decomposition of the formic acid to the products CO_2 and H_2 could take place. According to this proposal, the rate of the reaction is governed by the accessibility of the vacant surface site on the metal M made available by insertion of CO into the O-H bond on the alumina support. More credibility to the presence of a formate intermediate was given by the results published by van Herwijnen and de Jong (61). These workers also reported the existence of a central intermediate over a Cu/SiO_2 catalyst having the same stoichiometry as formic acid.

Taking the idea of a formate intermediate one step further, recent work of Shopov and Andreev (66)

combined the theories of a redox mechanism with the formation of a formate intermediate over a cobalt oxide promoted iron-chromium catalyst. These authors proposed a mechanism which assumes the participation of lattice oxygen and change in the degree of oxidation of iron in accordance with the redox mechanism. Further indication of the participation of the hydroxyl groups in the formation of the surface formate complex was also made. Their mechanism is depicted in Figure 1.4.

Figure 1.4 : Water-gas shift mechanism as proposed by Shopov and Andreev (66)



One could extend this review of the long list of researchers who proposed the presence of the formate ion as the central reaction intermediate by quoting the names of other researchers (eg. Tamaru (67)), but this would merely result in reproducing the reaction schemes already presented in this section.

Summarising the facts presented here, it can be said that the formate ion most probably is the central intermediate found on a variety of catalysts, and especially on copper containing low temperature water-gas shift catalysts, which, as mentioned previously, operate in the temperatures range of about 200 - 250°C.

1.5.3 Other mechanisms

In his review on the water-gas shift reaction, Newsome points out that some of the most fundamental mechanistic studies on iron-based catalysts involved the "stoichiometric number" method as devised by Oki et. al. (7). Thermodynamic calculations, the assignments of stoichiometric numbers and a rate-determining step were used to propose plausible elementary steps which then made up the overall reaction. The value of the stoichiometric number implied the number of times an elementary step had to be repeated to obtain the overall stoichiometric equation for the reaction. It is interesting to note, that by using this method, Oki concluded that the redox mechanism for the iron based catalysts was incompatible with his experimental data. Instead, he proposed that

the following two mechanisms, made up of elementary steps were theoretically possible:

Mechanism 1:

$$CO \rightleftharpoons CO(a)$$
$$H_2O \rightleftharpoons 2\,H(a) + O(a)$$
$$CO(a) + O(a) \rightleftharpoons CO_2(a)$$
$$CO_2(a) \rightleftharpoons CO_2$$
$$2\,H(a) \rightleftharpoons H_2$$

Mechanism 2:

$$CO \rightleftharpoons CO(a)$$
$$H_2O \rightleftharpoons OH(a) + H(a)$$
$$CO(a) + OH(a) \rightleftharpoons COOH(a)$$
$$COOH(a) \rightleftharpoons CO_2(a) + H(a)$$
$$CO_2(a) \rightleftharpoons CO_2$$
$$2\,H(a) \rightleftharpoons H_2$$

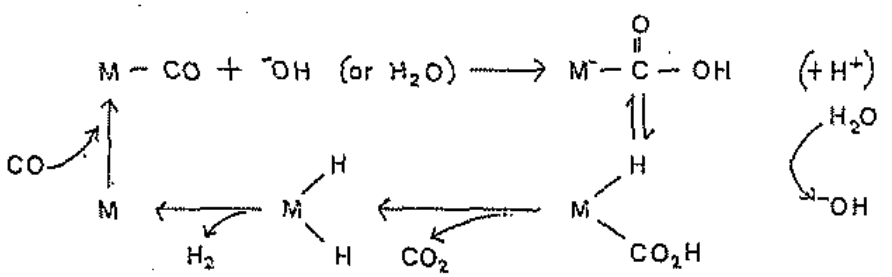
where (a) represents species adsorbed on the active site

Again, it can be seen that mechanism 2 incorporated the presence of a formate intermediate. Mechanism 1 looks very similar to the redox mechanism proposed earlier, but differs in that it does not include the involvement

of lattice oxygen, as was the case for the redox mechanism proposed by Temkin et. al. (59).

In section 1.4.4 it was shown that the water-gas shift reaction could be catalysed homogeneously. It was also in this field that an immediate interest as to the sequence of the reaction mechanism was apparent. An interesting mechanistic proposal involving nucleophilic activation of CO by reaction with H_2O or OH^- under moderately alkaline conditions was proposed by Ford (55). The mechanistic steps of this are shown in Figure 1.5 below.

Figure 1.5 : Mechanistic steps for the homogeneously catalysed water-gas shift reaction as proposed by Ford (55)



The outstanding feature in this proposed mechanism is

that the formate intermediate was this time bonded to the metal site of the catalyst via the carbon atom of the formate species and not via the acidic oxygen atom as was the case in the mechanisms described previously.

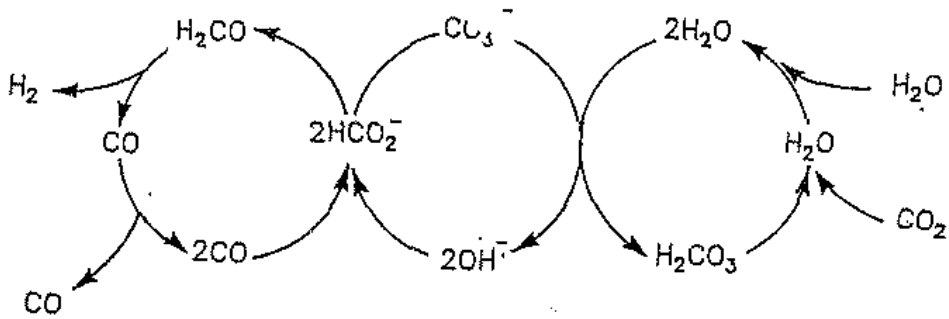
In a later paper published by Ford (68), he extended his mechanistic ideas so as to get a generalisation to other homogeneous catalyst intermediates. Many of these systems can be represented by the general formula

$$M_X(CO)_Y$$

where M is the active metal. Modifying his earlier reaction scheme by substituting $M(CO)_{Y-1}$ for M, Ford then presented a mechanistic case study for $Ru_3(CO)_{12}$ and $Fe(CO)_5$.

Even though most of the mechanisms discussed up to now involved the presence of a formate intermediate in some form or another, this type of intermediate is not the only crucial species required in the water-gas shift reaction. Elliott et. al. (69) showed in their cyclic mechanistic system, that, in addition to the formate intermediate, the presence of two other intermediate anions are required to complete the reaction; carbonate and hydroxide. The complete mechanism, which they claimed could proceed in the presence of any basic catalyst precursor which could generate one of these catalytic species is shown in Figure 1.6.

Figure 1.6 : Water-gas shift reaction cycle proposed by Elliott et. al. (39)



1.5.4 Summary of the proposed mechanisms

Examining the information in section 1.5 it is apparent that to this day there still exists a degree of uncertainty as to the exact mechanistic steps operative on the individual water-gas shift catalysts. However, two main mechanistic routes can be categorised. Firstly, we most probably have the regenerative redox mechanism working with a high temperature iron based catalyst, even though this pathway is disputed by Oki and his research team. In Oki's defence, it must be said that he proposed a very similar pathway from water-gas shift reagents to products involving either oxygen transfer or the presence of a formate intermediate.

It was the presence of a central formate intermediate which was also recognised by many other researchers that have contributed to studies on the water-gas shift reaction mechanism. It is without doubt that one can conclude that in the presence of a copper containing catalyst, the formate species forms the backbone of the central intermediate. This idea can, for all practical purposes also be extended to the homogeneous catalyst systems. All the other steps required to complete the water-gas shift reaction cycle appear to be straight forward adsorption and desorption steps.

1.6 The kinetics of the water-gas shift reaction

A kinetic study deals with the rate of the chemical reaction and with all the factors that influence this rate (52). Even though it is purely a study of how fast reagents are transformed to the product state, it nevertheless provides us with a means of analysing a reaction mechanism. The link between kinetic and mechanistic studies lies in the fact that any acceptable mechanism has to conform to the observed rate law. For example, if a reaction was thought to be a simple bimolecular process, then the kinetics will be have to be second order. However, the reverse does not necessarily hold true; for if the kinetics are second

order, then the reaction mechanism does not have to be a bimolecular process - it could also be complex. The study of kinetics should thus only be regarded as a valuable tool to obtain clues about the reaction mechanism.

However, in order use this kinetic tool effectively, one often has to deal with complex mathematical expressions and the introduction of a catalyst to a reaction system can only be considered to further complicate such studies. As kinetic rate expressions involving catalytic processes are dependent on a number of factors such as catalyst preparation techniques, reagent gas composition and operating conditions, it is not surprising that different research workers devised different mathematical rate expressions for the same chemical process. Here the rate expressions derived for the water-gas shift reaction over certain catalysts are no exception.

A number of kinetic expressions have been derived for both the iron based high temperature shift catalyst (70) and the copper based low temperature shift catalyst (61). As can be expected, kinetic expressions differed significantly and some were even of a contradictory nature. It would be a repetitive exercise to list all of these expressions, and so only a summary

of the more important expressions will follow in this section.

Kinetic formulae may be of a very simple nature such as the one derived by Sahay et. al. (71), using the variance method for the Fe-Cr-O system, which is shown below.

$$r = k\,[CO]^{0.9}\,[H_2O]^{0.1}$$

On the other hand, complex equations such as the one shown below, which was also derived for the Fe-Cr-O water-gas shift catalyst system by Temkin et. al. (72) also form part of the long list of published kinetic expressions.

$$r = k\,P_{H2O}\,P_{CO} - \frac{(K_{eq.}^{-1}\,P_{CO2}\,P_{H2})}{A\,P_{H2O} + P_{CO2}}$$

where k = rate constant

r = reaction rate

P_i = partial pressure of component i

A = constant

$K_{eq.}$ = equilibrium constant

In his review, Newsome (7) considered the previous rate equation as the best power expression derived for the high temperature water-gas shift catalysts.

In order to simplify matters and to steer away from complex mathematical models, which could still describe the water-gas shift reaction over a Fe-Cr-O catalyst adequately, Chinchen et. al. (73) modified a rate equation based on a Langmuir-Hinshelwood model by operating the catalyst at sufficiently small CO conversions, so that the overall gas composition could be considered to be constant. They thus managed to reduce the rate equation to the expression shown below:

$$r = \frac{k\ P^2}{(1 + B\ P)^2}$$

where k and B = constants

r = reaction rate

P = total operating pressure

Chinchen then used experimental results obtained at 350°C and found the values of k and B to be as follows:

$$k = 0.00227\ bar^{-1}s^{-1}$$

$$B = 0.227\ bar^{-1}$$

For the copper-based, low temperature water-gas shift catalysts a similar situation exists - in that numerous kinetic expressions have been published. It is however interesting to note that an expression which is identical to the last equation derived by Temkin et.

al. (72) for the Fe/Cr oxide catalyst was also found to describe accurately the kinetics of the water-gas shift reaction over a Cu/Zn oxide catalyst (7). This finding is very surprising, especially since the water-gas shift reaction over the iron-based catalyst is considered to proceed via the regenerative redox mechanism, whereas the same reaction over the copper-based catalyst is considered to proceed via a formate intermediate. To this date, no explanation as to why the same equation accounts for the kinetics of the water-gas shift reaction over different catalyst systems has been found.

Finally, the kinetics over a sulphur tolerant Co/Mo oxide catalyst system will be discussed. Here again a link to the kinetics of the other two catalyst systems already described is apparent in the way that kinetic data obtained by Hou et. al. (41) was interpreted in terms of a Langmuir-Hinshelwood surface reaction. The kinetic expression obtained by these researchers is shown below:

$$r = k \frac{K_1 K_2 [CO]\,[H_2]}{\{\,1 + K_1[H_2O] + K_2[CO]\,\}^2}$$

where r = reaction rate

k = rate constant

K_1 = equilibrium constant for H_2O adsorption

K_2 = equilibrium constant for CO adsorption

This expression fitted the experimental data in as far as that, with increasing H_2O feed rate, the reaction rate increased at first, then went through a maximum and finally settled into a plateau region, as would be predicted by the equation.

Even though the field of chemical kinetics does not seem to be documented as accurately as the field of reaction mechanisms, it nevertheless remains an integral part of our understanding of the reaction system as a whole.

1.7. Outline of thesis

Following the discussion presented in sections 1.2 to 1.6, it can clearly be seen that even though the water-gas shift reaction is a very important catalytic and industrial process, the development of the catalysts and the understanding of their operation is still not fully optimised and understood. Gaps in the network of catalyst development still exist, even though some of the technology is more than 100 years old. The major drawbacks of currently used catalysts that can be identified are summarised in Table 1.1.

Taking all these points into account, there definitely exists a need to develop a water-gas shift catalyst

Table 1.1 : Characteristics of currently used water-gas shift catalysts

	Fe-based catalyst	Cu-based catalyst	Co/Mo oxide catalyst
Activity	medium	high	high
Stability	slow decay with time-on-line	sinters easily	only active in sulphided phase
Sulphur poisoning sensitivity	moderate	very high	totally insensitive

that has the following attributes:

- high activity
- structural stability
- sulphur poisoning insensitivity

Chapter 2 of this Thesis deals with the theoretical developments and small scale preparation and testing of three such catalyst systems. The methods of catalyst preparation and testing are also described. The systems investigated include Co/Mn oxide, Cu/Mn oxide as well as Co/Cr oxide.

Initial optimisation studies on catalytic performance as well as comparisons to existing catalyst systems are made in chapters 3, 4 and 5. These studies probe the effect of catalytic composition, operating conditions and alkali promoters on the water-gas shift activity of the various catalyst systems. A further investigation on the CO hydrogenation ability of the Co/Mn oxide system is also discussed in chapter 3 as van der Riet et. al. (74) have shown evidence of this catalyst system having CO hydrogenation activity.

In order to obtain more information on the workings of the three catalyst systems investigated, kinetic as well as model reagent co-feed experiments were carried out and the results and discussions of this work are presented in chapter 6. Based on these, mechanisms, as well as kinetic expressions, were derived for the various catalyst systems.

Finally, to determine whether these novel high activity catalysts could also be operated in a coal based plant, which contains sulphur impurities in its feed gases, sulphur co-feeding experiments were carried out. For these studies the feed gases were spiked with low levels of H_2S and the effect was monitored. The outcome of these experiments is reported in chapter 7.

As a whole, this thesis will describe the development, preparation, and testing of novel high activity water-gas shift catalysts and will show that the goals set out in this section were met on a laboratory scale of operation.

2. EXPERIMENTAL

2.1 Catalyst preparation

A number of methods are available for the production of catalytically active materials. These methods, their merits and disadvantages are well documented in the open literature (75-78) and shall therefore not be discussed here. Techniques involving leaching selected components from solids, gel preparation, decomposition of salts or hydrates with gas evolution, sintering of metal oxides as well as precipitation and impregnation are available to scientists for the preparation of catalysts. It is the choice of the preparation method that will later determine the catalyst's physical and chemical properties.

For the work presented in this Thesis the following two techniques of catalyst preparation were chosen:

- co-precipitation
- impregnation, or the "incipient wetness" method

The reason for selecting these specific methods were twofold. Firstly, the co-precipitation method allowed for the preparation of catalysts, consisting of an active phase as well as a structural support phase. Secondly, this method was found to be reproducible

under carefully controlled reaction conditions (eg. temperature, pH, reagent flow rate) and only requires fairly simple and readily available equipment. As the name of this method implies, it involves the controlled precipitation of two, or more metal salts (eg. metal nitrates) by means of an alkaline precipitating agent (eg. dilute ammonia solution). The use of sulphate and chloride salts was avoided as sulphur and chlorine are both known water-gas shift catalyst poisons (Section 1.4). The detailed experimental procedure for the preparation of the various catalysts is given in Appendix 1. It should be pointed out that despite the fact that this method only allowed for a low recovery ratio of reagents (eg. to produce 5 g of a cobalt manganese oxide catalyst with a Co : Mn molar ratio of 1:1, 22 g of $Co(NO_3)_2 \cdot 6H_2O$ and 19 g of $Mn(NO_3)_2 \cdot 4H_2O$ starting material were required), it was nevertheless chosen as it repeatedly produced a high surface area type catalyst. The low recovery factor was of secondary importance as only small quantities of catalytic material were required.

The "incipient wetness" method was used in order to introduce a catalytic promoter (eg. potassium) to the catalysts. A detailed description of this technique is given in Appendix 2. This catalytic promoter was added to the pores of the dried co-precipitated catalysts by

"wetting" the material with a solution containing the required amount of the promoter dissolved in a minimum amount of water, and then drying the catalyst. However, this method could only be used to introduce small amounts (eg. 2 % (m/m)) of such a promoter to the catalytic material, as this promoter is only deposited on the catalyst's surface.

Thus, the reasons for preparing catalysts by the co-precipitation and the "incipient wetness" methods are that these methods yielded high surface area catalysts, which could be produced using common laboratory equipment and techniques.

2.2 Catalyst pretreatment

The co-precipitated catalytic material was subjected to the following sequence of pretreatments:

- pelleting
- calcination
- in-situ reduction
- quenching under nitrogen
- introduction of reagent gases

The exact procedures for these steps are outlined in Appendix 3. Catalyst pelleting was carried out by

pressing the dried material into discs with the aid of a hydraulic press (20 tons/cm^2). The disc was then broken down and the particles were sieved to obtain a particle size distribution ranging from 0.500 mm to 1.180 mm.

Calcination and reduction of the catalytic materials was found to be necessary in order to obtain increased catalyst surface area (eg. 10 m^2g^{-1} for freshly co-precipitated Co/MnO catalysts vs. 46 m^2g^{-1} for calcined and reduced Co/MnO catalysts). Once the catalytic material had undergone in-situ reduction (at 400°C for the Co based catalysts and at 250°C for the Cu based catalysts), the reactor was flushed with nitrogen and the temperature was dropped to 200°C before the introduction of the reagent gases to the reactor.

2.3 Catalyst testing

All catalyst testing, except for the mechanistic co-feeding studies, was carried out in a stainless steel micro-reactor assembly, which is described in Appendix 4. This facilitated the controlled introduction of reagent gases, temperature control, and allowed for independently testing three different

catalysts at one time. This assembly comprised three individual micro-reactors units connected to a gas chromatographic analysis section. The mechanistic co-feeding experiments were carried out in a glass micro-reactor of similar design. The layout is described in Appendix 5. This glass reactor assembly differed from the stainless steel ones as it also allowed for the introduction of organic liquids by controlled evaporation. The glass reactor was also linked to the same gas chromatographic system as the stainless steel reactors. An additional off-line gas chromatograph was used to analyse for the various organic compounds formed during these reactions.

2.4 Product gas analysis, data evaluation and calculations

Product analysis was done by gas-solid chromatography, using the instrumentation described in Appendix 6. Use was made of an on-line Hewlett Packard 5730A isothermal gas chromatograph with a thermal conductivity detector (TCD) and an automated injection system to analyse for the inorganic gases. An off-line Pye Unicam Series 204 temperature programmable gas chromatograph with a flame ionisation detector (FID) and a manually operated sample valve was used to analyse the organic product spectrum.

A Spectraphysics SP4290 electronic integrator was used to evaluate all gas chromatographic data obtained and also to control certain pre-programmed external events functions (eg. sample injections, switching of the reactor valves). The integrator's software contained built-in data evaluation programs, whose operations are explained in Appendix 7. These programs were routinely used to obtain quantitative product analyses.

2.5 Catalyst characterisation

Catalysts were characterised using techniques such as powder X-ray diffractometry (XRD) (Phillips PW 1050), differential scanning calorimetry (DSC), thermal gravimetric analysis (TGA) (Dupont 9900 thermal analyser), as well as surface area measurements (Carlo Erba Sorptomatic Series 1800). The reduced or active catalysts were kept under nitrogen during the transfer process from the reactor to the various instruments. Experimental details of these techniques are given in Appendix 8.

3. COBALT MANGANESE OXIDE WATER-GAS SHIFT CATALYSTS

3.1 Introduction

A literature search showed that even though cobalt manganese oxide had been used for carbon monoxide oxidation, no application dedicated to the water-gas shift reaction had been reported, with the exception of a paper by Varma et. al. (87).

In the early 1970's a number of patents had appeared claiming the use of materials containing both cobal oxide as well as manganese oxide for the treatment of automotive exhaust gases (10,88,89). The main functions of these catalysts were to oxidise CO, "NO_x" in the presence of O_2 and hydrocarbons present in these gases. As the catalysts also contained other metal oxides (eg. CuO, NiO or Al_2O_3), it cannot be concluded that the catalytic properties were primarily due to the cobalt and the manganese present. However, in a later article, Ivanova et. al. (90) reported the catalytic oxidation of butane using a Co-Mn-O system, thus providing evidence that this type of system could be used for oxidative purposes.

Even though, cobalt metal supported on alumina (8) as well as sulphided cobalt molybdenum based catalysts (41) had both been found to be active water-gas shift catalysts, no detailed information is available on the effect of supporting cobalt on manganese oxide as a water-gas shift catalyst. However, Varma et. al. (87) did suggest that a cobalt manganese oxide catalyst exhibited high water-gas shift activity, but presented no experimental data to support their claim. They based their claim on the observed formation of carbon dioxide during carbon monoxide hydrogenation experiments.

In this chapter, experimental data is presented to show that the cobalt manganese oxide system showed high water-gas shift activity under various conditions. Catalysts with different Co:Mn metal ratios were prepared and tested and their activity was compared to a standard high temperature water-gas shift catalyst (ICI 15/4 HD). The effect of the addition of alkali promoters (i.e. potassium) as well as structural characteristics of this type of catalyst system are also discussed here.

As mentioned previously, work carried out by Varma et. al. (87) had shown that cobalt manganese oxide was an active CO hydrogenation catalyst. Given the fact that both CO and H_2 are present during the water-gas shift

reaction, the hydrogenation of unreacted CO could take place inside a water-gas shift reactor, leading to the formation of unwanted hydrocarbon by-products. In order to obtain more information on the feasibility of this side reaction (occurring simultaneously with the water-gas shift reaction), a detailed investigation on the competition between these two reactions over a cobalt manganese oxide catalyst was carried out, and the results obtained are also presented in this chapter.

In order to control the selectivity of a chemical reaction, chemical promoters are usually incorporated into catalysts in order to enhance desirable and retard undesirable reactions. For the studies presented here, it would be beneficial if such a promoter could enhance the water-gas shift activity and at the same time retard the CO hydrogenation activity of the cobalt manganese oxide catalysts. Various researchers have reported that the addition of alkali salts causes an increase in catalytic activity for carbon monoxide related reactions (91-93), with the efficiency of promotion being in decreasing activity order :

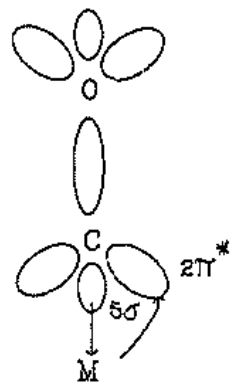
$$Cs > K > Na > Li$$

The influence of potassium promotion had been under

investigation as early as 1931 when it was shown that K_2O lowered the work function iron (94). Subsequent research work carried out in this field showed that the addition of a potassium promoter to a metal oxide catalyst enhanced the electron donating abilities of such a system (95, 96).

Carbon monoxide is known to synergistically bond to a catalytic surface (97-99) as shown in Figure 3.1. The overlapping of the occupied 5 σ orbital of CO with the unoccupied metal orbitals, results in a donation of electrons to the metal, with the back donation of electrons from occupied metal orbitals to the antibonding 2 π^* orbitals of CO making up the second component. The 5 σ orbital is non bonding in the isolated CO molecule (100) and donation of electrons from this orbital should not effect the C-O bond strength. This back donation into the antibonding 2 π^* orbitals of the CO molecule will, however, result in a weakening of the C-O bond. This donation is the apparent reason for the dissociative adsorption of CO on transition metal surfaces. Catalytic systems with enhanced electron donating abilities (eg. potassium promoted metal catalysts) would therefore aid the dissociation of the chemisorbed CO molecule and thereby activate it and explain their increased catalytic activities for CO related reactions.

Figure 3.1 : Synergic bonding model of carbon monoxide onto a catalytic surface



3.2 Experimental

All catalysts investigated were prepared and tested in accordance with the methods outlined in Chapter 2 of this Thesis. During the course of catalyst testing, a sequence of changing experimental parameters, as shown below was followed, in order to fully investigate the catalytic performance under different experimental conditions:

1) The catalyst was placed on-line at the relevant start-up temperature

2) The catalyst was allowed to stabilise at start-up condition for about 150 hours
3) The effect of variation in temperature was investigated
4) The effect of CO GHSV was investigated
5) The effect of CO : H_2O feed ratio was investigated

After every step mentioned above, the experimental conditions were returned to those used at the start-up of the catalyst, in order to restore the original level of activity of the system before proceeding with further testing.

All catalysts were evaluated for both water-gas shift activity and carbon monoxide hydrogenation activity at atmospheric pressure (i.e. 620 mm/ Hg in Johannesburg, South Africa), and it should be noted, that blank thermal reactions in the absence of any catalyst were found to be negligible, as was the formation of iron carbonyls in the stainless steel reactors.

3.3 Effect of Co : Mn ratio on the water-gas shift activity

3.3.1 Catalyst activity and lifetime studies

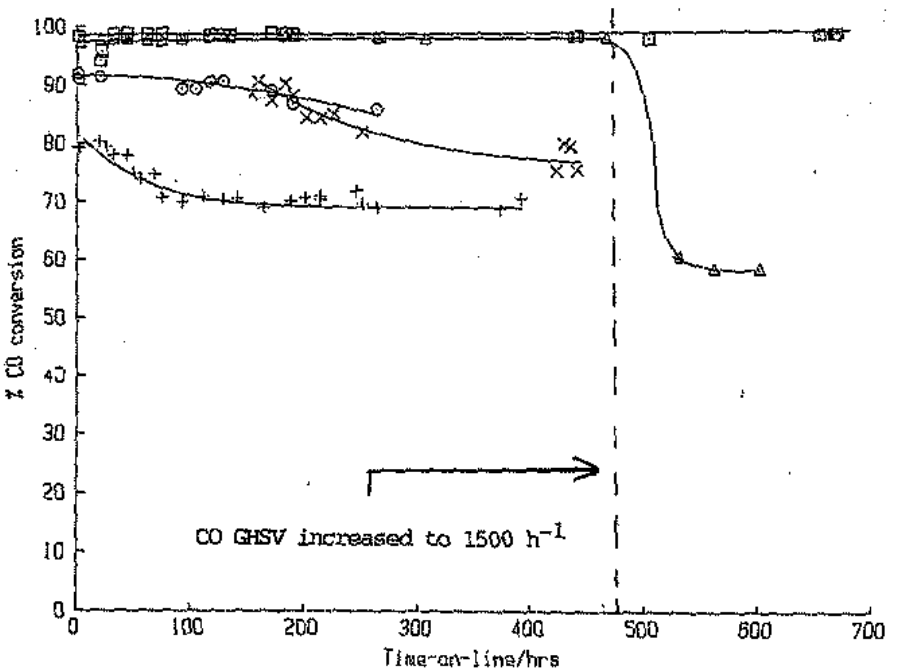
Cobalt manganese oxide catalysts with Co : Mn ratios of

1:3, 1:1, 3:1 as well as a pure Co catalyst were prepared and tested respectively. In order to assess catalyst stability, each sample was exposed to constant reaction conditions (400^{o}C ; CO GHSV = 510 / hr ; and a CO:H_2O = 1:4.5 ,in order to drive the water-gas shift equilibrium towards the product side) for a prolonged period of time. During the course of these studies, the activities of the respective cobalt manganese oxide catalysts was monitored periodically and the results are shown in Figure 3.2. Furthermore, Figure 3.2 also includes data points obtained for a standard high temperature iron chromium oxide based water-gas shift catalyst (ICI 15/4 HD) which was tested in the same microreactor under identical experimental conditions. This curve can thus be used as an activity reference line as compared to the novel cobalt manganese oxide catalysts.

From the results shown in Figure 3.2, it can be seen that for these type of catalysts, there appears to be a relationship between their water-gas shift activity and the amount of cobalt loading as both the Co : Mn = 3:1 and the pure Co catalysts showed a high and stable degree of water-gas shift activity under these experimental conditions. However, the pure Co catalyst decayed rapidly and irreversibly in activity after it was exposed to a higher reagent feed rate (400^{o}C ; CO GHSV= 1500 / hr) at about 450 hours on-line, whereas

the Co : Mn = 3:1 catalyst retained its high degree of activity after being exposed to the same high feed rate.

Figure 3.2 : Effect of metal ratios on water-gas shift activity[a]



Δ = Co only ; ⊡= Co : Mn = 3:1 ; ⊙ = Co : Mn = 1:1

× = Co : Mn = 1:3 ; + = ICI 15/4 HD

a : Temperature = 400°C ; $CO:H_2O$ = 1:4.5 ;
CO GHSV = 510 h^{-1}

This loss in activity was believed to have been due to the build up of "hot-spots" on the catalytically active

surface, brought about by the increased number of adsorbed H_2O molecules per unit area per unit time. As still enough H_2O molecules were present to react with the CO molecules (CO : H_2O = 1:1.5 at CO GHSV= 1500 / hr), a rate increase of the exothermic water-gas shift reaction could take place, thus leading to a rapid increase in temperature on the catalyst's surface. This rapid temperature increase ultimately causes thermal sintering and deactivation of the catalyst. Surface area measurements (as shown in Table 3.1) of the discharged Co only catalyst showed a definite loss of surface area after exposure to the high CO flow rates. Such a loss in surface area would be characteristic of catalyst sintering and thus lend support to the above hypothesis.

From these results, it can be concluded that the addition of manganese structurally stabilises the catalyst system and that cobalt appeared to be the active catalyst component.

It also should be noted that during the entire course of the stability studies, the Co : Mn = 3:1 catalyst showed a higher degree of water-gas shift activity than the standard iron chromium oxide ICI 15/4 HD water-gas shift catalyst.

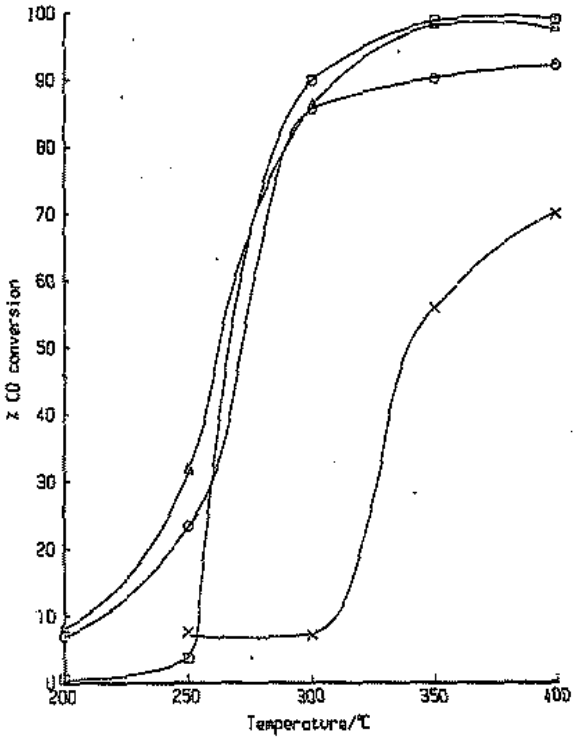
Table 3.1 : BET surface areas of pure Co and Co:Mn = 3:1 catalyst

	BET surface area / m^2/g	
	pure Co	Co : Mn = 3:1
before being exposed to G H S V = 1500 / hr at 400°C	63.4	62.7
after being exposed to G H S V = 1500 / hr at 400°C	20.3	64.0

3.3.2 Temperature dependent studies

Data obtained on the temperature dependence for the various catalysts studied is shown in Figure 3.3. For all the catalysts investigated, a sharp increase in catalyst activity at temperatures in excess of 300°C was observed, indicating that the cobalt manganese oxide system could be classified as a typical high temperature water-gas shift catalyst. Again note should be taken that both the pure Co and the Co : Mn = 3:1 catalysts achieved CO conversions higher than 98 %, which would be highly desirable for any industrial operation of such a catalyst system.

Figure 3.3 : Effect of temperature on CO conversion for the various Co/Mn oxide catalysts tested[a]



Δ = Co only ; $\boxdot$ = Co : Mn = 3:1 ; $\odot$ = Co : Mn = 1:1

$\times$ = Co : Mn = 1:3

a : CO GHSV = 510 h^{-1}; CO:H_2O = 1:4.5

As the water-gas shift reaction is an exothermic reaction, the conversion of carbon monoxide is enhanced by lower operating temperatures. Numerical data on the temperature dependence of the equilibrium constant (K_p) for the water-gas shift reaction has been published in the literature (101) and was used to determine the equilibrium conversion of CO for the

reaction conditions used for the data presented in Figure 3.3. The results for these calculations are shown in Table 3.2.

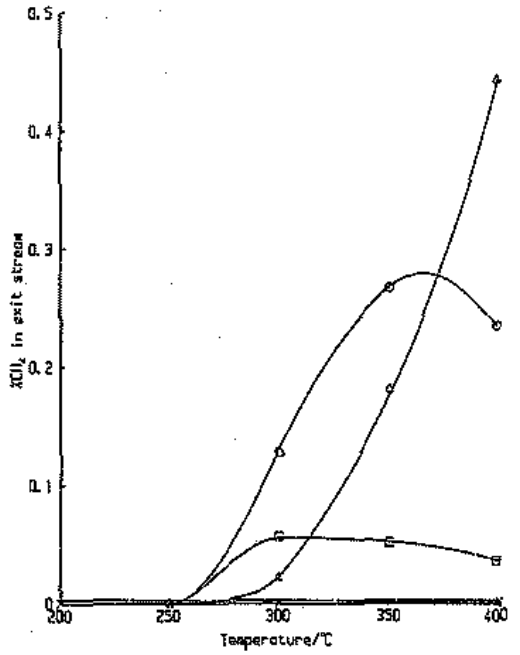
Table 3.2 : Temperature dependence of K_p and equilibrium CO conversion[a]

Temperature / °C	K_p	% CO conversion	
		calculated at equilibrium	observed
200	200	99.86	7.0
250	96	99.70	23.5
300	52	99.45	87.0
350	34	99.18	91.3
400	16	98.28	93.8

a : Co:Mn = 1:1 ; CO GHSV = 510 h^{-1} ; CO : H_2O = 1:4.5

It was observed that the % CO conversion tended towards an equilibrium value with increasing temperature. However, at temperatures lower than 300 °C, a large difference between the observed % CO conversion and the equilibrium value existed. This discrepancy indicated that at these lower temperatures the reaction was probably influenced by diffusion limiting factors, which could have prevented the reagent molecules from reaching the active sites in the catalytic network structure.

Figure 3.4 : Effect of temperature on CH_4 by-product levels[a]



△ = Co only ; ⊡ = Co : Mn = 3:1 ; ⊙ = Co : Mn = 1:1

✕ = Co : Mn = 1:3

a : CO GHSV = 510 h^{-1}; $CO:H_2O$ = 1:4.5

In contrast to the iron chromium oxide commercial catalyst, the cobalt manganese oxide catalysts were found to produce low selectivities for CH_4 as a by-product, (presumably formed by CO hydrogenation). A general increase of CH_4 production with temperature was observed, and levels of about 0.2 % (m/m) of CH_4 were typically produced at temperatures of 350°C, as

is shown in Figure 3.4. It is also interesting to note that no hydrocarbons higher than CH_4 were produced under any of the conditions investigated. More details on the interplay between the CO hydrogenation and the CO shift reaction over a cobalt manganese oxide are given in section 3.7 of this chapter.

3.4 Effect of potassium promotion on the water-gas shift activity and CH_4 production

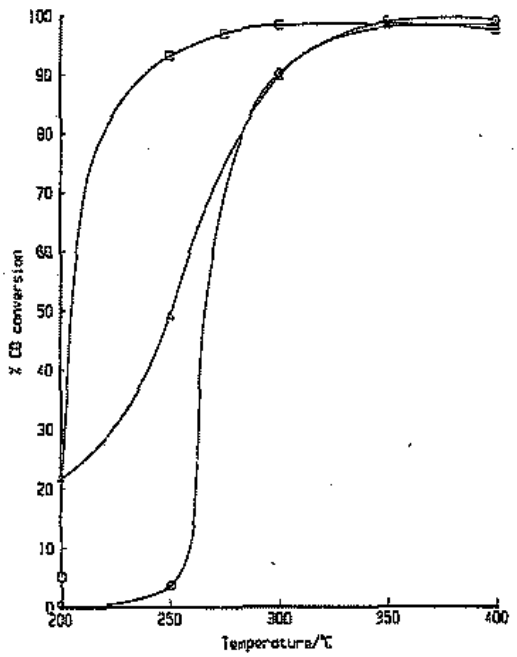
In order to investigate the effect of alkali promotion on a cobalt manganese oxide catalyst, potassium carbonate was added to catalytic material having a Co : Mn ratio of 3:1 by the incipient wetness technique as described in section 2.1.

The potassium promoted (1 % and 2 % (m/m) K^+ based on cobalt) cobalt manganese oxide catalysts were then tested for water-gas shift activity and the results obtained are shown in comparison to an unpromoted catalyst in Figure 3.5.

From these results it can be seen that the addition of potassium significantly enhanced the rate of CO conversion at temperatures less than 300°C, with the best catalytic activity being given by the cobalt manganese oxide catalyst containing 1 % (m/m) K^+. The

BET surface areas for the various catalysts studied are given in Table 3.3. A significant decrease in surface area was observed for the 2 % (m/m) K^+ promoted catalyst as compared to the 1 % (m/m) K^+ promoted and unpromoted catalysts.

Figure 3.5 : Effect of potassium addition on CO conversion for a Co : Mn = 3:1 catalyst[a]



$\triangle$ = 2 % (m/m) K ; $\boxdot$ = 1 % (m/m) K ; $\odot$ = 0 % (m/m) K

a : CO GHSV = 510 h^{-1}; CO:H_2O = 1:4.5

Table 3.3 : BET surface areas [a] of potassium promoted Co/Mn oxide catalysts

% K^+ (m/m)	Surface Area / m^2g^{-1}
0	64.0
1	62.7
2	52.5

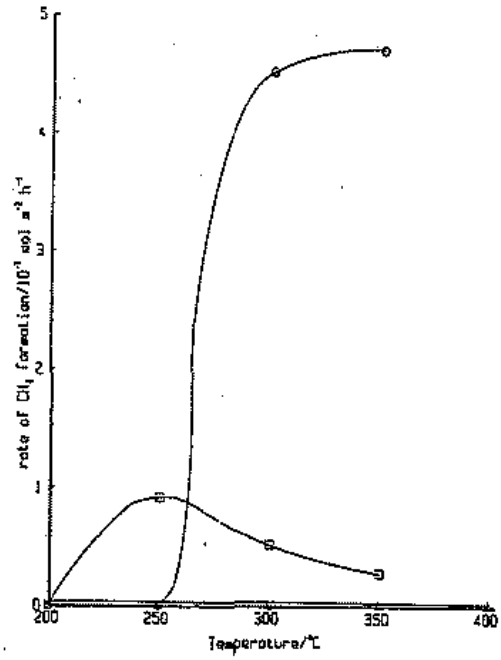
a : Data taken after catalysts had been on-line for about 600 hours

This decrease in surface area is indicative that a saturation point of K^+ promotion had been reached on the cobalt manganese oxide catalyst containing 2 % (m/m) K^+. Such a saturation point, where a monolayer of potassium ions has formed on the surface had also been reported by Amenomiya et. al. (65) for a potassium promoted alumina catalyst, where this point was observed after 9 % (m/m) of K_2CO_3 had been added to the catalyst.

Another significant aspect concerning the promotion of the 3:1 cobalt manganese oxide catalyst with potassium was that a decrease in the rate of formation of by-product CH_4 was observed at temperatures higher than 250°C as is shown in Figure 3.6.

..s, the results obtained with the promoted cobalt manganese oxide catalyst clearly indicate that the

Figure 3.6 : Effect of potassium addition on the rate of CH_4 formation for a Co : Mn = 3:1 catalyst[a]



Δ = 2 % (m/m) K ; $\boxdot$ = 1 % (m/m) K ; $\odot$ = 0 % (m/m) K

a : CO GHSV = 510 h^{-1}; CO:H_2O = 1:4.5

addition of potassium to the catalyst not only enhances the rate of the desired water-gas shift reaction, but also inhibits the rate of the unwanted CO hydrogenation reaction.

A weakening of the carbon-oxygen bond would activate

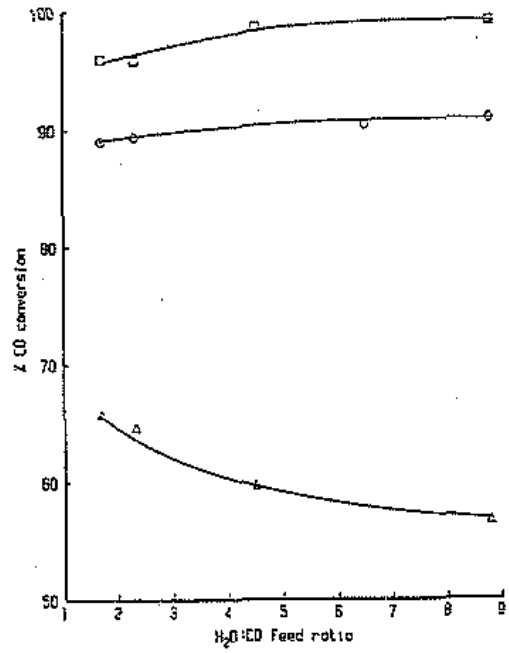
the chemisorbed CO molecule, allowing for an easier formation of a reaction intermediate, and thereby explaining the enhanced water-gas shift activity observed for the K^+ promoted cobalt manganese oxide catalyst. The formation of such an intermediate will be discussed in chapter 6.

In order to explain the decrease in the CO hydrogenation ability for the K^+ promoted catalyst, the role of surface bonded hydrogen will have to be considered. It has been found that chemisorbed hydrogen donates electrons to the catalytic material (102). As potassium acts as an electron donor, it would enhance the chemisorption of CO, but on the other hand it also discourages the chemisorption of H_2 (103, 104). Thus, the decrease in surface bonded hydrogen could explain the observed decrease in the rate of CO hydrogenation for the potassium promoted cobalt manganese oxide catalyst.

3.5 Effect of reagent feed rates on the water-gas shift activity

The effect of the variation of the H_2O feed rate on the water-gas shift activity has been investigated for various Co/Mn oxide catalysts and the results are shown in Figure 3.7.

Figure 3.7 : Effect of CO : H_2O ratio on the catalytic performance[a]



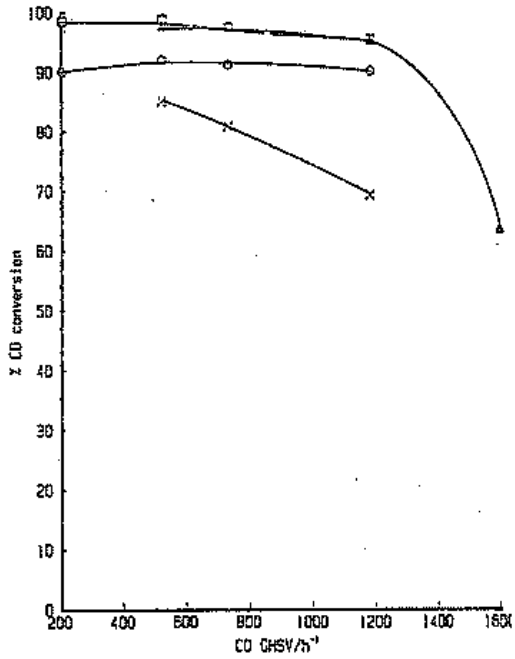
Δ = Co only ; ⊡ = Co : Mn = 3:1 ; ⊙ = Co : Mn = 1:1

a : CO GHSV = 510 h^{-1}; Temperature = 400°C

As can be seen, no significant improvement in the catalyst's performance was observed, even after the H_2O feedrate had been increased to give a CO : H_2O feed ratio of 1 : 8.8.

Similarly, increasing the CO feedrate showed no significant enhancement in activity as can be seen from the results presented in Figure 3.8.

Figure 3.8 : Effect of CO GHSV on catalytic activity[a]



△ = Co only ; □ = Co : Mn = 3:1 ; ⊙ = Co : Mn = 1:1

× = Co : Mn = 1:3

a : Temperature = 400°C ; $CO:H_2O$ = 1:4.5

The fact that the pure cobalt catalyst showed a sign of deactivation at the high CO GHSV was attributed to a loss of surface area brought about by catalytic sintering, which has already been discussed in section 3.3.

3.6 Structural characterisation

The bulk properties of cobalt manganese oxide catalysts

were examined using the following techniques:

- X-ray powder diffractometry (XRD)
- Differential scanning calorimetry (DSC)
- Thermogravimetric analysis (TGA)

It was found that the bulk structures of the catalysts in their various stages of pretreatment were made up of different phases as shown in Table 3.4.

Both the Co_2MnO_4 and the $CoMn_2O_4$ spinel phases observed for the precipitated and calcined catalysts display similar structures to the tetragonal system of Hausmannite, Mn_3O_4. In this mixed oxide system, which can also be represented as $MnO \cdot Mn_2O_3$, the manganese occupies both the tetrahedral (i.e. MnO) and the octahedral (i.e. Mn_2O_3) sites.

For the Co_2MnO_4 and the $CoMn_2O_4$ spinels present in the precipitated and calcined catalyst precursors, cobalt is exclusively substituted into either the tetrahedral site (i.e. $CoO \cdot Mn_2O_3$) or the octahedral site (i.e. $MnO \cdot Co_2O_3$). However, for the mixed spinel, $(Co,Mn)(Co,Mn)_2O_4$, the substitution of cobalt into the lattice sites is random, and the number of sites occupied depends on the number of cobalt atoms present in the catalyst (i.e. the Co:Mn ratio).

Table 3.4 : Bulk structure of a Co/Mn oxide catalyst[a]

Catalyst state	Phases present
Precipitated and dried (110°C)	Co_2MnO_4 spinel $CoMn_2O_4$ spinel $(Co,Mn)(Co,Mn)_2O_4$ mixed spinel
Calcined (500°C, air)	as for precipitated and dried state, but increased peak intensities indicated a higher degree of crystallinity
Reduced (400°C, H_2)	CoO and MnO as major phases α Co (hcp) as the minor phase
Active catalyst[b]	α Co , Co (fcc) and MnO

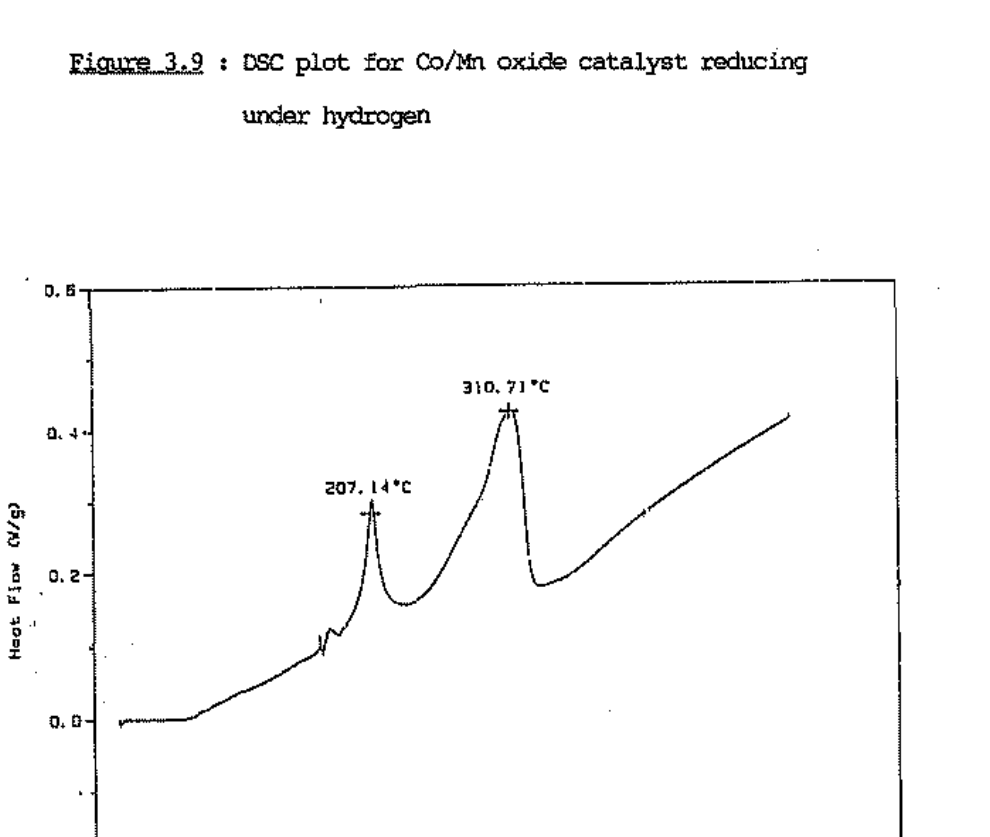
a : Co:Mn = 1:1 on a molar basis

b : data taken after catalyst had been on-line for 600 hours

It was also found that the addition of a potassium promoter or a change in the Co:Mn ratio did not significantly affect the bulk structure of the catalyst.

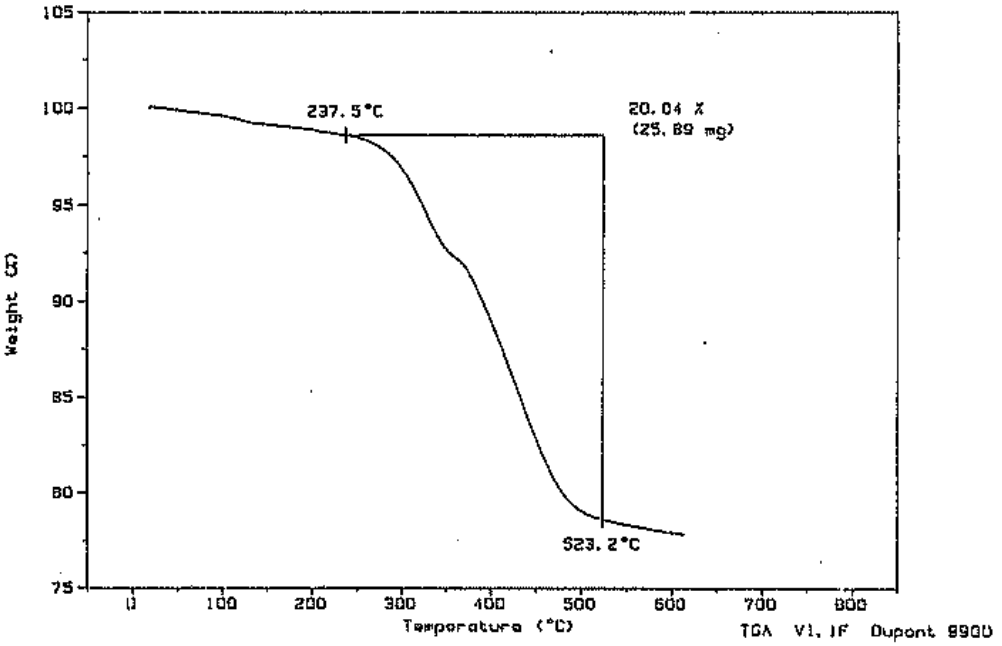
The phases identified for the calcined cobalt manganese catalysts have also been observed by Kuznetsova et. al. (105), who reported the presence of a $Co_xMn_{3-x}O_4$ mixed oxide after calcining in air at 400°C.

Figure 3.9 : DSC plot for Co/Mn oxide catalyst reducing under hydrogen



DSC and TGA were used to investigate the effects of reducing a calcined cobalt manganese oxide catalyst (Co:Mn = 3:1) under hydrogen. The catalyst was heated from room temperature to 550°C at a rate of 5°C/min under a hydrogen flow of 20 ml/min and the results obtained are shown in Figures 3.9 (DSC) and 3.10 (TGA).

Figure 3.10 : TGA plot for Co/Mn oxide catalyst reducing under hydrogen



From Figure 3.9, it can be seen that the reduction of the catalyst involved a two-stage process in which phase changes occurred at 207°C and 311°C. The overall mass loss observed during this process was found to be 20.0% (Figure 3.10). Thus, the reduction process under hydrogen can be represented as follows:

$$(Co,Mn)(Co,Mn)_2O_4 \xrightarrow{H_2} \text{intermediates}^a \longrightarrow CoO + 2\,MnO + H_2O$$

a : the identity of the intermediates are unknown, but most probably consist of mixed cobalt and manganese oxides.

For the active Co/MnO catalyst, a shift in the lattice parameter for the MnO phase from that of pure MnO was observed as shown in Table 3.5. This shift indicated that a solid solution of cobalt cations in the MnO lattice was present. In contrast to this observation, Copperthwaite et. al. (80) found that the bulk structure of a cobalt manganese oxide catalyst as used for CO hydrogenation consisted of the $(Co,Mn)(Co,Mn)_2O_4$ mixed spinel as the major active phase, thereby indicating that non-metallic cobalt appeared to be the active phase for CO hydrogenation, which in[illegible]l the formation of methane. Furthermore, in section 3.4, it was shown that the addition of K^+

to the Co/MnO catalyst decreased the rate of methane formation. Thus, the addition of K^+ tended to selectively poison CO hydrogenation sites, which appear to be associated with non-metallic cobalt.

Table 3.5 : Lattice parameters of MnO present in an active Co/Mn catalyst[a]

I/I_0	d-spacing / A	
	Co/MnO catalyst	pure MnO
100	2.212	2.223
80	2.550	2.568
60	1.562	1.571

a : Co:Mn = 3:1 , Catalyst had been on-line for 600 hours

The decrease in the rate of methane formation which was observed for a potassium promoted Co/MnO water-gas shift catalyst can now be attributed to the following factors:

-the electronic effect of K^+ on CO and H_2 adsorption onto the catalytic surface as described in section 3.4

and -the selective poisoning (or blocking) of non-metallic cobalt sites by K^+

3.7 Competition between carbon monoxide hydrogenation and water-gas shift activity

Cobalt manganese oxide catalysts with low cobalt loadings (i.e. < 50 % (mol) Co) have been shown to exhibit carbon monoxide hydrogenation activity (79, 80, 87). Typical results obtained by van der Riet et. al. (79) over a cobalt manganese oxide catalyst (Co:Mn = 1:1 on a molar basis) indicated that, particularly at elevated pressures, (eg. 600 - 850 kPa) C_3 hydrocarbons were the dominant species in the organic product spectrum. Carbon monoxide conversions were of the order of 35 - 45 % (mol) and no water-gas shift activity had been observed under their reaction conditions (CO : H_2 feed = 1:1 ; GHSV = 264 h^{-1} ; temperature = 190°C ; Pressure = 600 kPa). The effect of introducing water to a CO : H_2 feed mixture was investigated in order to obtain more information on the interplay between the CO hydrogenation and the water-gas shift reactions.

3.7.1 Carbon monoxide hydrogenation

Van der Riet et. al. (79, 81) have thoroughly investigated the carbon monoxide hydrogenation activity of various cobalt manganese oxide catalysts, and typical results obtained for a range of reaction pressures are shown in Table 3.6.

Table 3.6 : Carbon monoxide hydrogenation over a Co/Mn oxide catalyst[a,b]

Pressure /kPa	GHSV /h^{-1}	CO conversion mol %	Hydrocarbon selectivity /mass %				
			CH_4	C_2	C_3	C_4	C_{5+}
85	263	13.0	10.4	5.4	10.8	10.8	62.6
350	100	23.7	5.9	3.9	7.0	4.8	77.9
600	264	38.6	11.5	10.0	21.5	12.9	43.8
850	354	44.3	10.5	9.3	22.8	13.1	43.2

a : Data from reference 79

b : Co:Mn = 1:1 ; Catalyst temperature = 190°C ;
CO : H_2 = 1:1

3.7.2 Water-gas shift activity

Results for the water-gas shift activity for various cobalt manganese oxide catalysts have already been presented in section 3.3 of this chapter and have shown that this catalyst system exhibited considerable water-gas shift activity at temperatures higher than 300°C. To supplement these results, a Co : Mn = 1:1 catalyst was tested for both water-gas shift and Co hydrogenation activity, using a $CO:N_2:H_2O$ = 1:1:4.5

feed ratio (molar basis) and the results are shown in Table 3.7.

Table 3.7 : Water-gas shift / CO hydrogenation activity of a Co : Mn = 1:1 catalyst[a]

Time on line /hrs	Temp. / °C	CO conversion (mol %)		Hydrocarbon selectivity /mass %	
		to CO_2	to hydrocarbons	CH_4	C_{2+}
24	400	92.4	0.1	100	0
673	400	89.0	0.9	100	0
264	350	87.7	0.5	100	0
351	300	84.2	0.4	100	0
434	250	23.2	0.0	-	-

a : $CO:N_2:H_2O$ = 1:1:4.5 ; GHSV = 510 h^{-1}

Pressure = 85 kPa

The results presented in Table 3.7 indicated that whilst the cobalt manganese oxide catalyst was active for the water-gas shift reaction, only very low conversions (eg. maximum of 0.9 % (mass)) of carbon monoxide to hydrocarbons was observed. Also, as methane was the only hydrocarbon produced, no carbon-carbon bond formation was observed under these reaction conditions. This is in contrast to van der Riet's

results presented in Table 3.6, where considerable carbon-carbon bond formation had occurred when the catalyst was reacted with CO/H_2 in the absence of water. To further demonstrate that C-C bond formation and the water-gas shift reaction do not occur simultaneously to any appreciable extent, a series of experiments in which the $CO/H_2:H_2O$ ratio was varied at a temperature at which both these reactions were known to display a reasonable degree of activity (i.e. 300°C), and the results obtained are shown in Table 3.8.

Table 3.8 : Reaction of a carbon monoxide, hydrogen and water feed mixture[a]

Time on line /hrs	$CO:H_2:H_2O$ mol ratio	CO conversion (mol %)	
		to CO_2	to hydrocarbons
53	1 : 1 : 0	0	26.8
145	1 : 1 : 0	0	12.1
164	1 : 1 : 2.0	6.1	1.8
170	1 : 1 : 3.8	6.6	1.8
189	1 : 1 : 7.2	6.9	1.5
212	1 : 1 : 10.8	5.4	1.1
310	1 : 1 : 0	2.8	5.9

a : Temperature = 300°C ; CO GHSV = 250 h^{-1}

Table 3.8 (continued)

$CO:H_2:H_2O$	Hydrocarbon selectivity / mass %						
mol ratio	CH_4	C_2H_4	C_2H_6	C_3H_6	C_3H_8	C_4	C_{5+}
1:1: 0	22.2	2.3	19.7	10.5	13.5	15.3	16.5
1:1: 0	34.8	2.0	23.7	6.8	12.6	9.4	10.7
1:1: 2.0	78.3	1.4	9.9	1.6	1.9	1.0	5.9
1:1: 3.8	85.1	1.0	8.3	1.2	1.6	0.8	2.0
1:1: 7.2	96.4	0.1	1.4	0.3	0.1	0.7	1.0
1:1:10.8	96.7	0.8	0.8	0.3	0.1	0.8	0.5
1:1: 0	27.6	2.7	26.9	8.7	13.6	10.6	10.0

a : Co:Mn = 1:1 ; Temperature = 300°C ; CO GHSV = 250 h^{-1} ; Pressure = 85 kPa

Carbon monoxide hydrogenation activity, but no water-gas shift activity was observed as the catalyst was stabilised for the first 145 hours, and a range of hydrocarbons higher than C_2 were produced. However, upon addition of H_2O to the feed gases, a significant increase in the water-gas shift activity and a decrease in the CO hydrogenation activity were apparent immediately. Also, a shift in the hydrocarbon selectivity away from the formation of C_{2+} hydrocarbons was observed. The absence of water largely restored the hydrocarbon product selectivity to the

original values, but CO hydrogenation activity also decreased.

3.7.3 Discussion

The results presented in this study indicated that the water-gas shift reaction and carbon-carbon bond formation for the CO hydrogenation reaction did not occur simultaneously to any significant extend over a 1:1 cobalt manganese oxide catalyst. As water was added to the CO/H_2 feed stream, CH_4 was found to be the major (>75 % (mass) selectivity) hydrogenation product. This is probably due to an increase in the concentration of H_2 produced by the water-gas shift reaction and which was present on the catalyst's surface. The rate of CO hydrogenation was also found to decrease by an order of magnitude. An explanation can be found, in terms of a competition between the various molecules adsorbing onto the surface. Water being a highly polar molecule, will adsorb strongly and thereby compete favourably with carbon monoxide and hydrogen for available surface sites. Thus, the observations of a shift in the hydrocarbon selectivity towards CH_4 and the decrease in CO hydrogenation activity upon the addition of water to the feed stream, could be explained as follows:

Observation	Explanation
high CH_4 selectivity	enhanced H_2 concentration on catalytic surface brought about by additional H_2 (H_2 produced by the water-gas shift reaction)
lower CO hydrogenation activity	H_2O in the feed stream competes favourably with active sites (i.e H_2O can displace CO and/or H_2)

3.8 Summary

The results and discussion presented in this chapter indicate that the cobalt manganese oxide system exhibits a high degree of water-gas shift activity in the high temperature region (i.e. 350 - 400°C) under a variety of reaction conditions. Addition of a potassium promoter at a level of 1 % (m/m) to the cobalt manganese oxide catalyst (Co:Mn = 3:1) was found not only to further enhance the catalyst's activity, but also to decrease the rate at which the undesired CH_4 by-product was formed through the CO hydrogenation reaction. The origins of this observation were also discussed in this chapter.

The bulk structural determinations carried out by XRD indicated that the active cobalt manganese oxide

catalyst comprised Co metal and MnO, in which some Co^{2+} ions were found to be in a solid solution in the MnO lattice.

Finally, experimental data based on the reaction of various $CO:H_2:H_2O$ feed mixtures over a Co : Mn = 1:1 catalyst was presented to show that the CO hydrogenation reaction to form C_{2+} products and the water-gas shift reaction did not proceed simultaneously over this catalyst.

4. COPPER AND IRON MANGANESE OXIDE WATER-GAS SHIFT CATALYSTS

4.1 Introduction

This chapter extends the studies on cobalt manganese oxide water-gas shift catalysts to copper manganese (Cu/Mn) oxide and iron manganese (Fe/Mn) oxide catalysts. Again, optimisation studies formed the basis of this chapter and structural, thermometric as well as alkali promotion studies further supplemented the results.

Both the copper manganese and the iron manganese oxide systems have been known to catalyse various reactions (used on an industrial scale).

4.1.1 The iron manganese oxide catalyst system

The main use of iron manganese oxide catalysts documented in the literature (106-109) describes their Fischer-Tropsch activities. In contrast to the classical potassium promoted iron oxide based catalyst, the manganese supported catalysts were found to be particularly selective for the production of low molecular weight olefins (106, 107).

However, Kreitman et. al. (107) and Ledakowicz et. al. (108) observed the formation of significant CO_2 levels under typical Fischer-Tropsch operating conditions (i.e. Temperature = 242°C ; Pressure = 7.9 bar). Although, CO_2 was generally considered as a secondary product in the Fischer-Tropsch reaction (110), Kreitman et. al. (107) still found that the CO_2 levels were excessively high for the iron manganese oxide catalysts as compared to an iron silica catalyst. They thus attributed the CO_2 to the water-gas shift reaction, and also argued that the shift equilibrium was very favourable under their reaction conditions. In summary, water-gas shift activity had already been reported for an iron manganese oxide catalyst, which was operated under reducing Fischer-Tropsch reaction conditions.

However, no detailed results on the degree of water-gas shift activity have been reported in the literature. In this chapter, results are presented which show that the iron manganese oxide catalyst also had some degree of water-gas shift activity in an oxidising environment (i.e. where water was present).

4.1.2 The copper manganese oxide catalyst system

The catalytic activity of manganese oxide had been

discussed in the open literature, where its oxidation activity of carbon monoxide and the decomposition of hydrogen peroxide had been reported (111). Furthermore, copper oxides dispersed on different supports are known to catalyse processes such as methanol synthesis (26, 27), NO_x removal (28), as well as CO oxidation in air (25). However, only a few processes are catalysed by copper oxide supported on a manganese oxide matrix - eg. the hydrogenation of 1,5,9 - cyclododecatriene isomers (112), as well as CO oxidation, where various publications have appeared (113-116). It is also interesting to note that no publication describing the use of a copper manganese oxide catalyst for the water-gas shift reaction has appeared, especially as copper is known as a highly active water-gas shift metal (see section 1.4.2) when dispersed on an alumina support.

In chapter 3, it was already shown that cobalt supported on a manganese oxide matrix exhibited high water-gas shift activity. Now, also taking into account that Grenoble et. al. (8) showed that copper had a higher degree of water-gas shift activity than cobalt when supported on alumina, one can already see that a copper manganese oxide catalyst has the potential to be a highly active water-gas shift catalyst.

In this chapter, detailed results are presented and discussed on the performance of such a catalyst system under water-gas shift reaction conditions. The results obtained will be contrasted to the two other manganese oxide supported catalyst systems, namely the iron manganese oxide and the cobalt manganese oxide system.

4.2. Comparison of the water-gas shift activities of the Cu/Mn oxide, Fe/Mn oxide, and Co/Mn oxide catalysts

Catalysts of the type X : Mn = 1 : 1 mole ratio (X = Cu, Fe or C) were prepared and pretreated by the methods described in chapter 2. The catalytic activities of these catalysts were then examined as a function of temperature (CO GHSV = 510 h^{-1} ; CO : N_2 : H_2O = 1:1:4.5). The results which are shown in Table 4.1 were mathematically converted and expressed as pseudo first order rate constants using the formula shown below:

$$k_1 = \frac{F}{m\,P} \ln \frac{1}{1 - X_A}$$

where k_1 = pseudo first order rate constant / moles $s^{-1}g^{-1}atm.^{-1}$

F = molar flow rate of CO

m = mass of the catalyst

P = pressure in atm.

X_A = fractional conversion of CO

The above formula was derived by Thomas and Thomas (117), and was claimed to be valid for both homogeneous and heterogeneous reactions taking place in a plug-type flow reactor where longitudinal diffusion can be considered to be negligible. Furthermore, the above equation is only valid if no change in molar volume during the reaction takes place (as is the case for the water-gas shift reaction). In general, the form of the above rate equation is similar to that for a first-order reaction in a static system.

Table 4.1 : Pseudo first order rate constants for X:Mn = 1:1 catalysts (X = Cu, Fe or Co)

Temperature / °C	k_1 / 10^{-7} mol g^{-1} atm^{-1} s^{-1}		
	Cu : Mn	Fe : Mn	Co : Mn
200	4.9	-	4.1
250	12.9	0	14.9
300	61.8	0.2	110.2
350	85.0	1.9	133.4
400	70.6	6.0	158.7

On the basis of the results presented in Table 4.1, a definite activity sequence for the three manganese oxide supported catalysts emerged, with a decreasing order of activity of:

Co / Mn > Cu / Mn >> Fe / Mn

at virtually all reaction temperatures studied.

The activity difference between the Fe/Mn oxide catalyst and the other two catalysts was such that the Fe/Mn oxide system could be considered as fairly inactive in the temperature range studied.

4.2.1 Specific catalyst activities

In order to be able to calculate the catalysts' specific activities, the surface areas as shown in Table 4.2 had to be determined.

Table 4.2 : Surface areas[a] determined by the BET method for the various manganese oxide catalysts tested

X : Mn	Surface Area / m^2g^{-1}
Co	45.1
Cu	6.0
Fe	10.2

a : Surface areas shown were determined after the catalysts had been utilised for ca. 600 hours

The low value obtained for the surface area for the Cu/Mn catalyst could be attributed to sintering at the high operating temperatures. Co melts at a much higher

temperature (i.e. 1480°C) than Cu (i.e. 1083°C). Thus, any Cu containing catalyst would be expected to sinter more easily than an equivalent Co containing catalyst.

Correcting the various catalysts' activities for surface area, specific catalyst activities as shown in Table 4.3 were obtained.

Table 4.3 : Specific catalyst activity for the various metal / manganese oxide catalyst systems[a]

Catalyst system	Specific activity / 10^{-4} mol CO converted m^{-2} h^{-1}
Cu / Mn	41.6
Co / Mn	8.68
Fe / Mn	0.56

a : data obtained at T = 350°C ; CO GHSV = 510 h^{-1};
CO : N_2 : H_2O = 1:1:4.5

Hence, according to the results presented in Table 4.3, the order of activity for these catalysts was as follows:

Cu / Mn > Co / Mn > Fe / Mn

This activity sequence was also found to be in

agreement with a previous comparative study carried out by Grenoble et. al. (8) on alumina-supported metal catalysts. As work carried out by Baltans et. al. (118) showed that CO was a weak adsorbate on supported manganese oxide catalysts, it can be concluded that the manganese oxide does not significantly contribute towards the catalysts' activity. Therefore, cobalt, copper or iron can be considered to be the active phase for those three catalysts respectively.

4.2.2 Activation energy calculation

It is interesting to note that the Cu/Mn oxide catalyst already showed signs of activity in the 200°C - 300°C temperature region, whereas the Fe/Mn oxide catalyst only became active in the 300°C - 400°C temperature region. The Cu/Mn oxide catalyst then reached a maximum degree of activity at 350°C. Thus, this catalyst system is not a low temperature water-gas shift catalyst, which is in contrast to the copper zinc oxide system (section 1.4.2) which is operated on a commercial scale in the 200° - 250 °C temperature range.

Although, the 1 : 1 Cu / Mn catalyst was found to be a high activity water-gas shift catalyst at temperatures

of about 350°C, it nevertheless showed a loss in catalytic activity at the higher temperature of 400°C. This decrease in catalytic activity could be attributed to sintering at the higher temperature. The phenomenon of sintering is well known for copper containing catalysts (35, 36) and has already been described in section 1.4.2 of this Thesis.

Calculations to obtain the apparent activation energies of these manganese oxide supported catalysts were carried out. These calculations were based on the Arrhenius equation :-

$$k = A \exp \left\{ \frac{-E^*}{R\,T} \right\}$$

where k = rate constant

A = Pre-exponential factor

T = absolute temperature

E^* = activation energy

Activation energies for the Cu/Mn, Fe/Mn and the Co/Mn oxide catalysts were calculated and the results are shown in Table 4.4.

Table 4.4 : Apparent activation energies of the various manganese oxide catalysts tested

Catalyst system	Apparent activation energy / kJ mol^{-1}
Co / Mn	73
Cu / Mn	55
Fe / Mn	107
Fe_3O_4/Cr_2O_3	ca 130[a], 122[b]
Cu/ZnO	71[c]

a : comparative value calculated by Chinchen et. al. (119)

b : comparative value calculated by Salmi et. al. (57)

c : comparative value calculated by Campbell et. al. (120)

4.3 Effect of Cu : Mn ratio on catalyticity

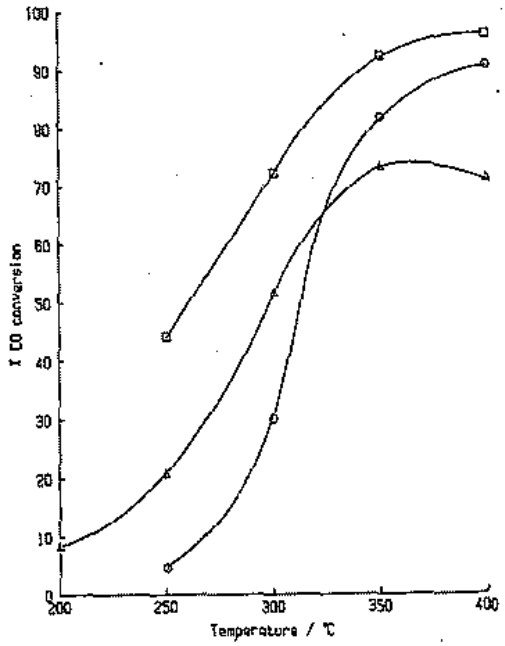
Catalysts with Cu:Mn mole ratios of 1:10, 1:3, and 1:1 were prepared and tested for water-gas shift activity under various operating conditions.

4.3.1 Effect of temperature on catalytic activity

The effect of temperature on CO conversion was

investigated keeping both the CO : N_2 : H_2O feed rate and the CO GHSV constant at 1:1:4.5 and 510 h^{-1} respectively. The results obtained are shown in Figure 4.1.

Figure 4.1 : CO conversion as a function of temperature for the Cu/Mn oxide catalysts tested[a]



△ = Cu : Mn = 1:1 ; □ = Cu : Mn = 1:3 ;

⊙ = Cu : Mn = 1:10

a : CO GHSV = 510 h^{-1} ; CO : N_2 : H_2O = 1:1:4.5

From the results it can be seen that all the copper

manganese oxide catalysts tested only became active at temperatures higher than 250°C and displayed their highest activity in the temperature range of 350°C - 400°C. This observation would classify the Cu/Mn catalysts as typical high temperature water-gas shift catalysts. Furthermore, it is apparent that in contrast to the Co/Mn catalysts, improved catalytic performance for the Cu/Mn catalysts was observed for manganese rich formulations, with an optimum Cu : Mn ratio of about 1:3.

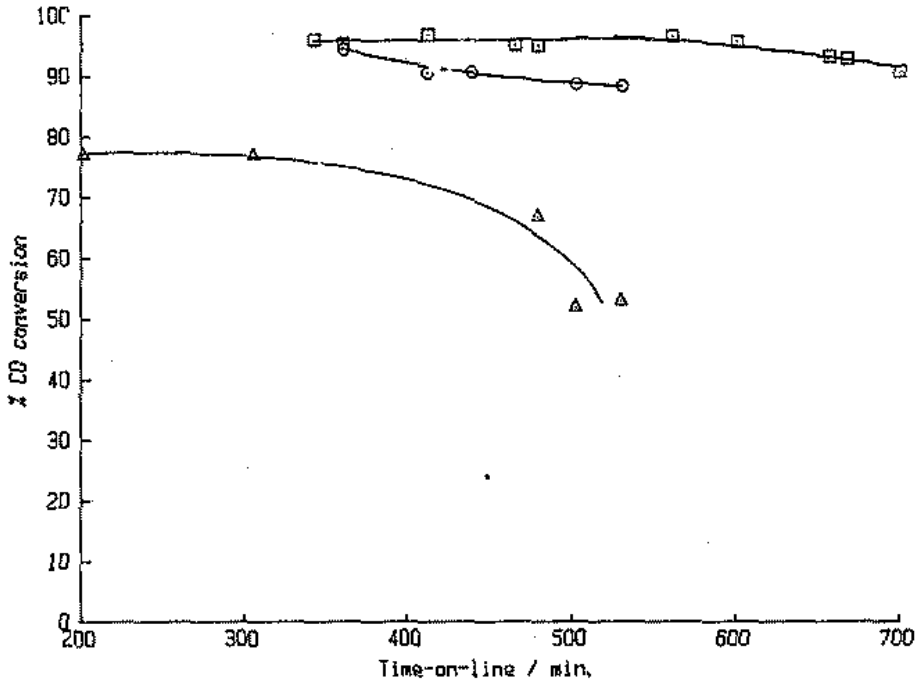
4.3.2 Stability studies involving copper manganese oxide catalysts

The catalyst stability at constant reaction conditions for the various Cu/Mn catalysts tested are shown in Figure 4.2.

It can be seen from the data presented in Figure 4.2, that both the Cu : Mn = 1:3 and the Cu : Mn = 1: 10 catalysts showed stable water-gas shift activity over a prolonged period of time (eg. about 200 hours). However, the Cu : Mn = 1:1 catalyst displayed a continuous loss in activity after being on-line for about 300 hours. An examination of the surface areas of the discharged catalysts, after they had been on-line for about 600 hours, revealed that for all of the Cu/Mn

catalysts tested, significantly lower values as compared to the Co/Mn catalysts were obtained (Table 4.5).

Figure 4.2 : Stability of various Cu/Mn oxide water-gas shift catalysts[a]



△ = Cu : Mn = 1:1 ; ⊡ = Cu : Mn = 1:3 ;

⊙ = Cu : Mn = 1:10

a : Temperature = 400°C ; CO GHSV = 510 h^{-1} ;

$CO:N_2:H_2O$ = 1:1:4.5

Although both the 1:10 and the 1:3 Cu : Mn catalysts showed a high degree of water-gas shift activity, a further improvement in catalytic performance could be obtained if it were possible to stabilise the catalysts' surface areas at high temperatures (eg. 350°C - 400°C).

Table 4.5 : BET surface areas of discharged Cu/Mn oxide catalysts

Cu : Mn mole ratio	Surface area[a] / m^2g^{-1}
1 : 3 (precipitated)	91.5
1 : 3 (calcined)	79.6
1 : 3 (reduced and calcined)	60.2
1 : 3	10.1
1 : 1	6.08
1 : 10	6.87
Co : Mn = 1 : 1[b]	45.1

a : data taken after the catalysts had been on-line for ca 600 hours

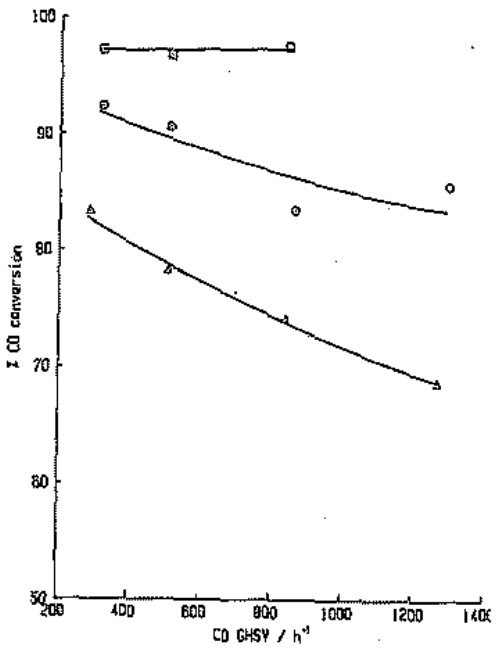
b : comparative value

It is also interesting to note that in contrast to the Co/Mn oxide catalysts, all the Cu/Mn oxide catalysts tested did not produce hydrocarbon by-products under any of the experimental conditions employed.

4.3.3 Effect of reagent feed-rate on catalytic activity

The effect of varying the CO and H_2O feed-rate on the catalysts' performances were investigated and the results are shown in Figures 4.3 and 4.4 respectively.

Figure 4.3 : Effect of CO GHSV on catalytic performance for the various Cu/Mn oxide catalysts tested[a]



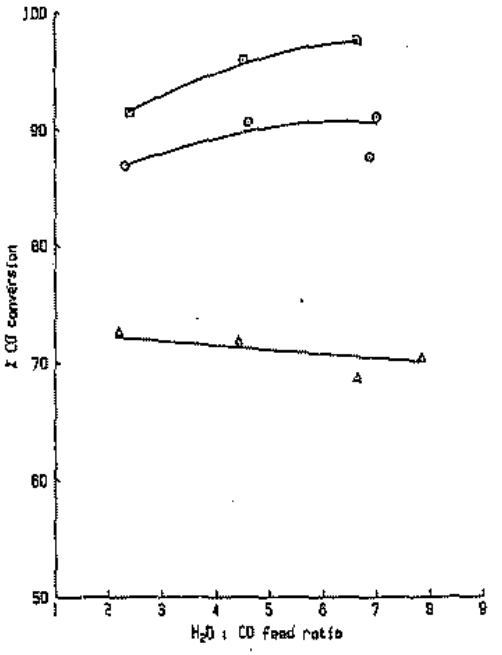
Δ = Cu : Mn = 1:1 ; □ = Cu : Mn = 1:3 ;

⊙ = Cu : Mn = 1:10

a : Temperature = 400°C

As can be seen from the results presented in Figures 4.3 and 4.4, variations in the feed-rate of both of the water-gas shift reagents (i.e. CO and H_2O) had no significant effect on catalytic performance.

Figure 4.4 : Effect of H_2O : CO feed ratio on catalytic performance of the various Cu/Mn oxide catalysts tested[a]

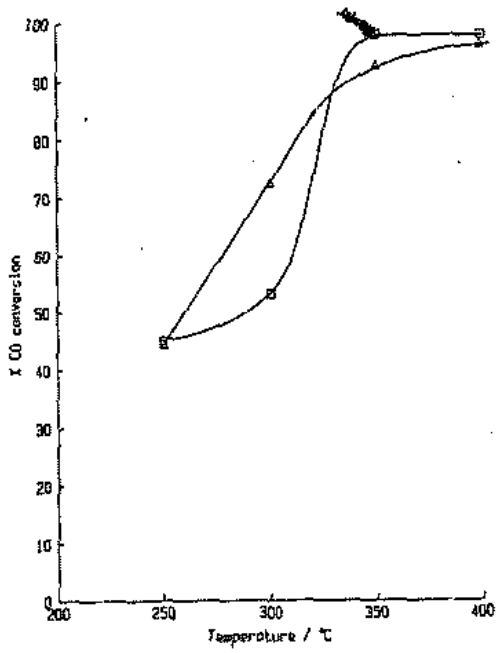


△ = Cu : Mn = 1:1 ; ⊡ = Cu : Mn = 1:3 ;

○ = Cu : Mn = 1:10

a : Temperature = 400°C ; CO GHSV = 510 h^{-1}

Figure 4.5 : Potassium promotion of a 1:3 Cu/Mn oxide catalyst[a]



Δ = Cu : Mn = 1:3 + 0 % K ; ⊡ = Cu : Mn = 1:3 + 0.6 % K

a : CO GHSV = 510 h^{-1} ; $CO:H_2O$ = 1:4.5

4.4 Effect of potassium promotion on the water-gas shift activity of a Cu : Mn = 1 : 3 catalyst

The effect of alkali promotion on the optimum catalyst formulation (i.e. Cu:Mn = 1:3) was investigated by

addition of a potassium carbonate solution to the calcined catalyst by means of the "incipient wetness" method. A similar enhancement in catalytic activity as for the Co/Mn catalyst system discussed previously (section 3.4) was observed for the Cu/Mn oxide catalyst. The results which are presented in Figure 4.5 indicated that a slightly higher % CO conversion was achieved for the 0.6 % (m/m) potassium promoted Cu/Mn oxide catalyst in the temperature range 350°C - 400°C, indicating that the addition of potassium stabilised the catalytic material and prevented a loss in activity due to the high temperature operation.

As had been noted in section 4.3.2, Cu/Mn oxide catalysts did not produce any hydrocarbon by-products under typical water-gas shift reaction conditions. The addition of potassium to the catalyst formulation did not affect this situation.

4.5 Structural characterisation of Cu/Mn oxide and Fe/Mn oxide catalysts

4.5.1 The Fe/Mn oxide system

The structure of the Fe/Mn catalyst system during reactor start up and during synthesis conditions for the Fischer Tropsch reaction had been described by

Lochner et. al. (109), who found hausmannite, alpha-iron, various iron-carbides, manganospinels and manganowurstites as the major structural components. In contrast to Lochner's observations, X-ray powder diffraction analysis of the Fe/Mn oxide catalyst (Fe:Mn = 1:1) which had been exposed to about 500 hours of water-gas shift reaction conditions showed that the catalyst comprised of Fe in solid solution in an MnO matrix together with Fe_3O_4.

As already mentioned in chapter 1, iron containing water-gas shift catalysts only displayed a medir degree of water-gas shift activity. It is thus possible that the low levels of water-gas shift activity with the Fe/Mn catalyst formulation could be attributed to the low levels of iron oxide present. It also appeared that the MnO support did not have any significant effect in promoting the catalyst's activity.

4.5.2 The Cu/Mn oxide system

X-ray diffraction, thermogravimetric analysis and differential scanning calorimetry were used to obtain more information on the catalysts' bulk structure. The results obtained from the X-ray diffraction studies are presented in Table 4.6.

It is again interesting to note that the catalysts'

bulk structures were not found to be affected by variables like Cu:Mn metal ratio or the presence of an alkali promoter.

Table 4.6 : Bulk structures of Cu/Mn oxide catalysts as determined by X-ray diffractometry

Catalyst state	Structure
precipitated	Largely amorphous with only $MnCO_3$ detected as a minor phase
calcined	copper (II) manganate (III) as the only phase detected *i.e.* $CuMn_2O_4$
reduced	Major phase : Cu (II) O Minor phase : Mn_5O_8
active[a]	major phases : Cu metal : MnO trace amounts : Cu_2O

a : after exposing the catalyst to water-gas shift reaction conditions for ca. 500 hours

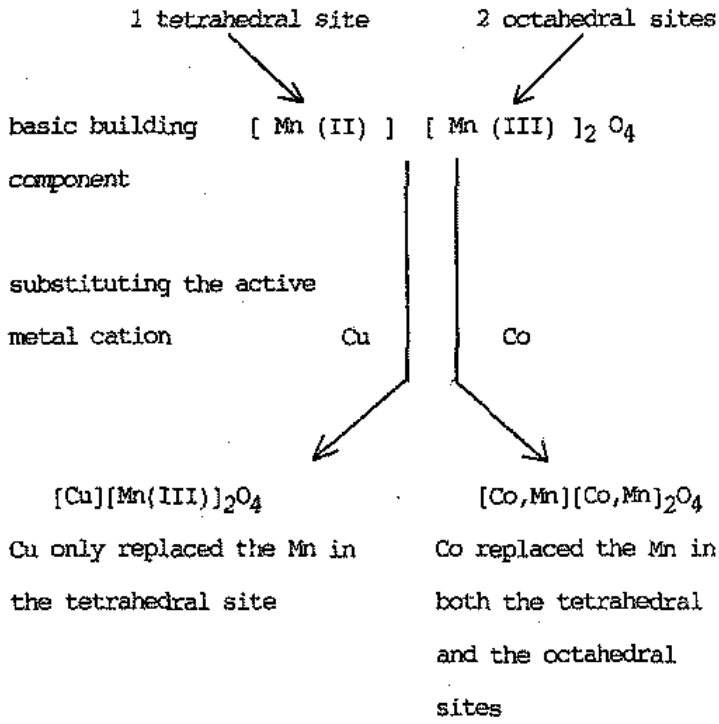
Furthermore, parallels can be drawn between the Cu/Mn

oxide catalysts' structures and the Co/Mn oxide catalysts' structures, (which had already been discussed in chapter 3). Upon calcination at 350°C in air, the Cu/Mn oxide catalysts were found to comprise $CuMn_2O_4$, a spinel in which the copper cations occupy only the tetrahedral sites and the manganese cations occupy only the octahedral sites. The presence of this $CuMn_2O_4$ spinel had also been reported by Kanungo (116) for Cu/Mn catalyst samples prepared from carbonates and which had then been calcined between 200°C and 300°C.

It can be seen that the mixed oxide, $Mn(II)Mn_3(III)O_4$, which also played an important role for the calcined Co/Mn oxide catalyst (section 3.6) forms the backbone for the calcined Cu/Mn oxide catalyst. Only this time, a difference in site substitution of the active metal component exists. A schematic representation of this substitution sequence, in which the copper cations are found to exclusively occupy the tetrahedral sites, is given in Figure 4.6.

An explanation as to why Cu (II) cations are only found to occupy the tetrahedral sites of the mixed manganese oxide spinel, can be based on the stereochemistry of this d^9 complex (121,122).

Figure 4.6 : Structural differences between calcined *Cu/Mn oxide and calcined Co/Mn oxide* catalysts



As the d^9 configuration makes Cu^{2+} subject to Jahn-Teller distortion, it has a profound effect on all its stereochemistry. When octahedrally coordinated, Cu^{2+} is severely distorted along one 4-fold axis, it leads to a situation which is indistinguishable from the tetrahedral coordination (123). This Jahn Teller distortion would thereby explain the observed tetrahedral coordination of the Cu^{2+} in the crystal lattice.

Table 4.7 : Ionic radii of Co, Cu, Fe and Mn cations[a]

Oxidation state	Ionic radius / Å			
	Co	Cu	Fe	Mn
+ 1	-	0.96	-	-
+ 2	0.74	0.72	0.74	0.80
+ 3	0.63	-	0.64	0.66

a : Data taken from reference 124

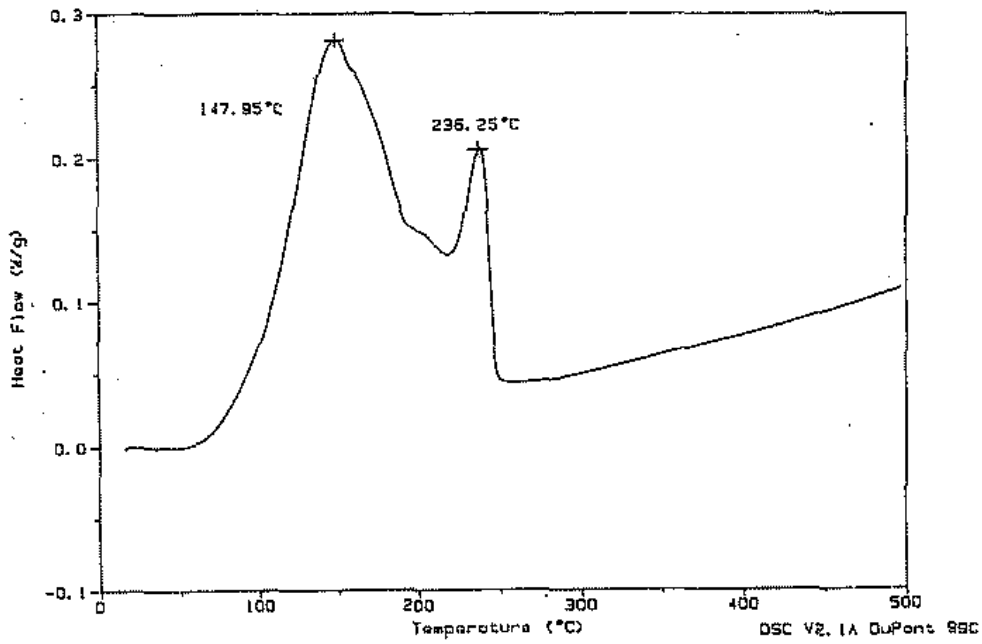
From a geometric point of view, Cu^{2+} and Co^{2+} have similar ionic radii (Table 4.7). This would imply that the selective occupation of the tetrahedral and octahedral sites did not take place on a size selective principle. It is also interesting to note that the active phase of the Cu/Mn oxide catalyst was present in a solution, whose presence was evident by a shift in the *d-spacing* of the MnO phase of the active catalyst (Table 4.8).

Table 4.8 : Lattice parameters for pure and catalytically active MnO[a]

I/I_o	d-spacing /Å	
	pure MnO	MnO in Cu/MnO catalyst
100	2.223	2.215
62	2.568	2.559
58	1.571	1.569

a : Discharged Cu/MnO catalyst ; Cu : Mn = 1:3 on a molar basis

Figure 4.7 : DSC trace for Cu/Mn oxide catalyst reducing under hydrogen[a]



a : Cu : Mn = 1:1 on a molar basis

4.5.3 Thermometric analysis of a Cu/Mn oxide catalyst

Two thermoanalytical techniques (DSC and TGA) were used to further supplement the structural information obtained by XRD. In these experiments, the reduction

process under hydrogen was simulated. The catalyst samples were heated from ambient to 550°C at a rate of 5°C/min under a hydrogen flow of 20 ml/min. Heat flow (DSC) as well as weight changes (TGA) were monitored during these experiments. The DSC and TGA results obtained are shown in Figures 4.9 and 4.10 respectively.

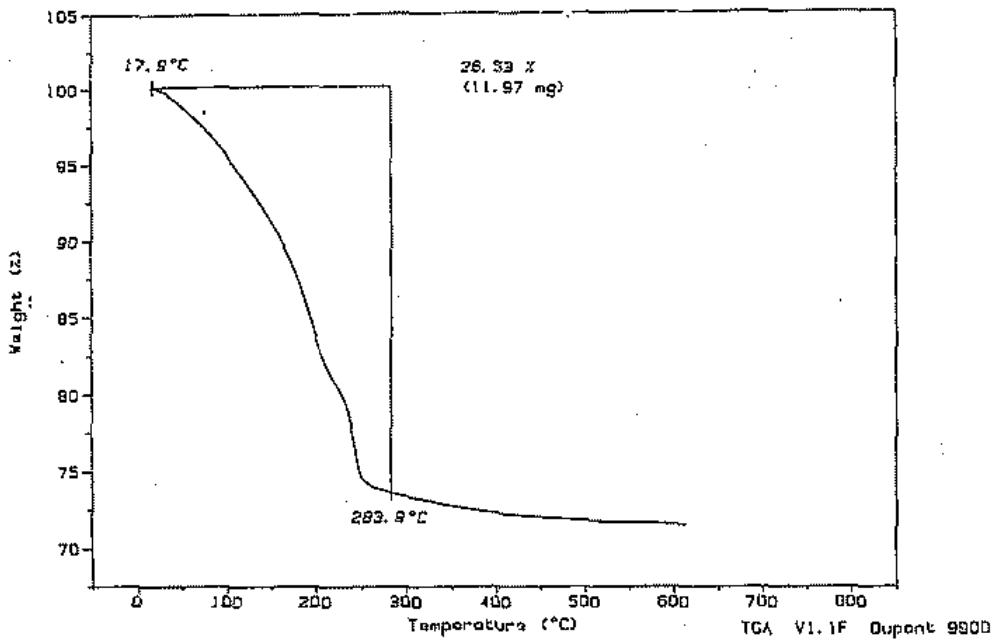
Comparing these results to the ones obtained for the Co/Mn oxide catalyst system (section 3.6), it can be seen that the reduction process under hydrogen for the Cu/Mn oxide catalyst was also found to be a 2-stage process with endotherms at 148°C and 236°C (viz. 207°C and 311°C for the 3:1 Co/Mn oxide catalyst) and an observed mass loss of 27 %.

4.6 Summary

In this chapter, results were presented which showed that the Cu/Mn oxide catalyst system can be regarded as a high activity water-gas shift system. The activity for a Cu:Mn = 1:1 catalyst was compared to Fe/Mn as well as Co/Mn oxide catalysts of similar composition and the following activity pattern emerged after correcting the results for surface areas:

Cu/Mn > Co/Mn > Fe/Mn

Figure 4.8 : TGA trace for the 1:3 Cu/Mn oxide catalyst reducing under hydrogen



It was also found, that all the Cu/Mn oxide catalysts tested did not produce any hydrocarbon by-products under any of the reaction conditions.

Calculations to determine the activation energies for M:Mn catalysts, where M = Co, Cu, or Fe, were carried

out and the results compared to literature values obtained.

Catalytic activity for the Cu/Mn oxide catalyst system was found to depend on a number of factors, the main ones being the Cu:Mn ratio, and operating temperature. The optimum Cu:Mn ratio appeared to be 1:3 and all the Cu/Mn catalysts tested displayed their highest activity in the temperature range 300°C - 400°C.

In contrast to the Cu/Mn oxide catalysts tested, the Fe/Mn oxide catalyst only displayed a low degree of water-gas shift activity. This lack of activity was attributed to the catalyst's bulk structure, which was only found to contain catalytically active Fe_3O_4 as a minor phase. The major phases detected by XRD were metallic Fe and MnO and it was thus concluded the Fe was a catalytically inactive water-gas shift phase. XRD studies furthermore revealed that the Cu/Mn oxide catalysts comprised of Cu and MnO in their active state and the addition of potassium to a Cu:Mn = 1:3 catalyst was found to further enhance the catalyst's water-gas shift activity without changing the catalyst's bulk structure.

As a final note, it should be mentioned that although Cu/Mn oxide catalysts demonstrated a significantly

higher specific activity than either the Co/Mn or the Fe/Mn oxide catalysts, they nevertheless were prone to loose catalytic activity due to a loss in surface area when operated continuously at 400°C for a prolonged period of time. In order to eliminate this problem, future studies should be aimed at stabilising the surface area of the Cu/Mn oxide formulation at these temperatures.

5. COBALT CHROMIUM OXIDE BASED WATER-GAS SHIFT CATALYSTS

5.1. Introduction

Fundamental studies of cobalt chromium oxide (Co/Cr oxide) catalysts have been well documented in the literature (125-129), and researchers have used bulk techniques such as Infra Red spectroscopy (126), X-ray diffraction studies (129) and surface techniques such as LEED - Auger measurements (128) to obtain more information at the molecular level of these catalyst systems.

Previous workers have established that materials containing cobalt and chromium oxide proved to be valuable catalysts, and numerous articles have appeared describing the use of such materials for processes ranging from ammonia oxidation (130, 131) to hydrocarbon oxidation (132-134) as well as exhaust or pollution control (135-137).

Although the use of Co/Cr oxide catalysts for carbon monoxide conversion had been shown by Rajwar et. al. (138) as well as Mekhandzhiev et. al. (139), the processes described in their studies were limited only to oxidation of carbon monoxide as shown below:

$$CO_{(g)} + 1/2\ O_{2(g)} \rightleftharpoons CO_2\ (g) \qquad (5.1)$$

Even though, it has been claimed in a patent (140) that materials containing the oxides of cobalt and chromium, catalyse the water-gas shift reaction, it must be pointed out, that iron oxides were the major phases present in these compounds and, therefore one cannot describe these materials as pure Co/Cr oxide catalysts; but one should rather refer to them as cobalt and chromium promoted iron based high temperature water-gas shift catalysts (141).

The use of various Co/Cr oxide water-gas shift catalysts which were operated under a variety of reaction conditions is described in this chapter. The results presented are compared and contrasted to the Co/MnO as well as to the Cu/MnO catalyst systems described previously.

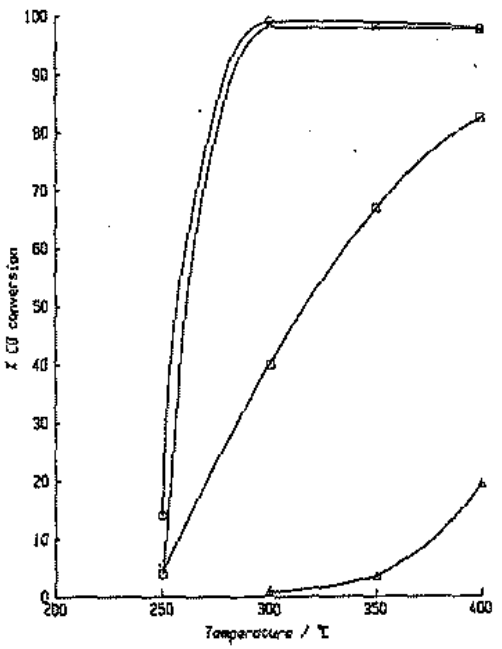
5.2. Activity Studies

Co/Cr oxide water-gas shift catalysts of various compositions were prepared and pretreated by the methods detailed in Chapter 2. All activity studies were carried out using the same micro-reactor and reaction conditions already described for the Co/MnO and the Cu/MnO catalysts in Chapters 3 and 4 respectively.

5.2.1 Temperature dependence

The effect of temperature on the water-gas shift activity for the various Co/Cr oxide catalysts tested is shown in Figure 5.1.

Figure 5.1 : Effect of temperature on the water-gas shift activity for the various Co/Cr oxide catalysts studied[a]



△ = Co : Cr = 1:10 ; □ = Co : Cr = 1:1 ;

⊙ = Co : Cr = 3:1 ; × = Co : Cr = 10:1

a : CO GHSV = 510 h^{-1} ; $CO:N_2:H_2O$ = 1:1:4.5 (on a molar basis)

The results presented in Figure 5.1 indicate that the Co : Cr metal ratio is a critical feature of the catalyst's activity. Activities for the catalysts of higher cobalt loading was found to increase sharply in the region of 250 - 300°C. The fact that all the Co/Cr oxide catalysts exhibited their highest degree of activity in the temperature range of 300 - 400°C indicated that, similarly to the Co/MnO and the Cu/MnO catalysts, the Co/Cr oxide catalyst system could also be classified as a high temperature shift catalyst.

These activity results were also in agreement with work carried out by Andreev et. al. (141), who reported the maximum degree of conversion of carbon monoxide with steam over a cobalt promoted iron-chromia catalyst in the temperature region of 320 - 420°C. Furthermore, Kadenatsi et. al. (129) showed that in the temperature region of 390 - 400°C CO could be oxidised completely over a $CoCr_2O_4$ spinel catalyst, thereby indicating that a Co/Cr oxide catalyst could be used for reactions involving CO activation.

The apparent activation energies for the various Co/Cr oxide catalysts in the temperature range 200 - 300°C were calculated by a similar method to that used in section 4.2.2 and are given in Table 5.1.

A general increase in activation energy with an

Table 5.1 : Apparent activation energies for the various Co/Cr oxide catalysts studied[a]

Co : Cr metal ratio	Activation energy / kJ mol^{-1}
1 : 10	117.2
1 : 1	125.2
3 : 1	167.7
10 : 1	218.4
Co : Mn = 1 : 1[b]	73
Fe/Cr[c]	ca. 130

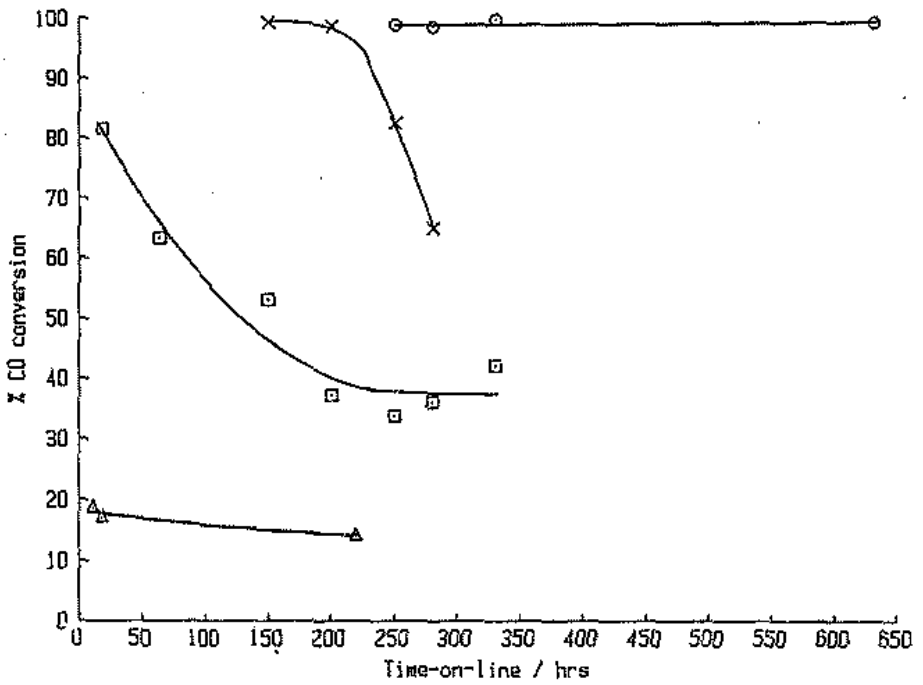
a : for the temperature range 200 - 300°C

b : comparative value

c : comparative value for a commercial high temperature water-gas shift catalyst (119)

increase in cobalt loading was observed for the Co/Cr oxide type catalysts. It is also interesting to note that the activation energies for all the Co/Cr oxide catalysts tested were not only higher than the comparative value shown for the Co/MnO catalyst, but they were also comparable with the value obtained (viz. 130 kJ/mol) for the Fe/Cr oxide catalyst by Chinchen et. al. (119). Based on these activation energy calculations, the mechanism by which the reaction intermediates form on a Co/Cr oxide catalyst appeared to be similar to that for a Fe/Cr oxide catalyst.

Figure 5.2 : Stability of Co/Cr oxide catalysts[a]



△ = Co : Cr = 1:10 ; ⊡ = Co : Cr = 1:1 ;

⊙ = Co : Cr = 3:1 ; × = Co : Cr = 10:1

a : Temperature = 400°C ; CO GHSV = 510 h^{-1} ;

$CO:N_2:H_2O$ = 1:1:4.5

5.2.2 Stability studies

The stability data of the various Co/Cr catalysts under water-gas shift reaction conditions are shown in Figure 5.2.

From these results, it is apparent that the formulations with Co:Cr = 1:1 and 3:1 both demonstrated high and stable activity for the water-gas shift reaction. It can also be seen that even though the Co:Cr = 1:10 catalyst showed a fairly constant pattern of activity, it never reached the high % CO conversions of the Co/Cr oxide catalysts with the higher Co loadings. Again, this can be taken as evidence that cobalt and not chromium is the active water-gas shift component in this catalyst system.

5.2.3 Surface area determinations

The surface areas for the various stages of catalyst preparation were determined for a Co:Cr = 1:1 catalyst (Table 5.2) and compared to the values for Co:Mn = 1:1, Cu:Mn = 1:1 and Fe:Mn = 1:1 catalysts.

The distinctly larger surface area for the Co:Cr =1:1 catalyst as compared to the other catalysts would explain the high water-gas shift activity observed for this system and could also account for the fact that this catalyst achieved CO conversions of 98 % at a temperature (300°C) where the other comparative catalysts returned a much lower value (chapter 4)

Table 5.2 : Surface areas for Co:Cr = 1:1 catalyst for the various stages of pretreatment

Catalyst state	Surface area / m^2/g
Precipitated	2.06
Calcined	27.8
Used[a]	85.9
Comparative catalysts	
Co:Mn = 1:1 (used)[a]	45.1
Cu:Mn = 1:1 (used)[a]	6.0
Fe:Mn = 1:1 (used)[a]	10.2

a : after the catalysts had been operated under water-gas shift conditions for ca. 600 hours

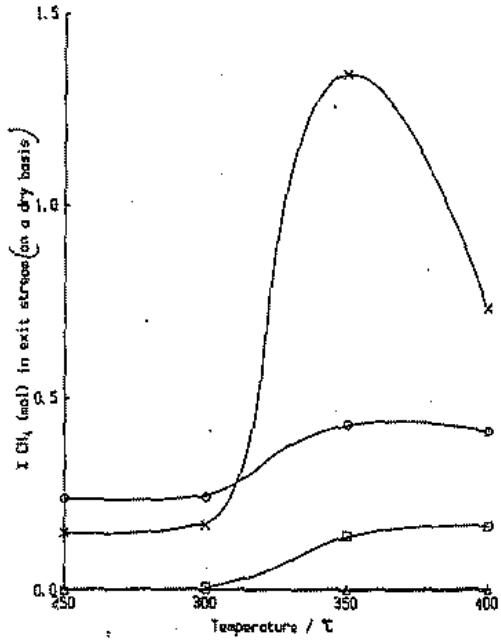
5.3 Methane by-product formation under water-gas shift reaction conditions

Cobalt chromium catalysts were found to produce significant levels of by-product methane under water-gas shift reaction conditions as is shown in Figure 5.3.

The levels at which methane was produced over these catalysts were considerably higher than those observed for the Co/MnO catalysts (section 3.7). In an attempt

to decrease the methane yield, alkali promotion (see section 3.1), as well as introducing manganese to the catalyst surface was investigated.

Figure 5.3 : Methane by-product formation over various Co/Cr oxide catalysts operated under water-gas shift reaction conditions[a]



△ = Co : Cr = 1:10 ; □ = Co : Cr = 1:1 ;

⊙ = Co : Cr = 3:1 ; × = Co : Cr = 10:1

a : Temperature = 400°C ; CO GHSV = 510 h^{-1} ;

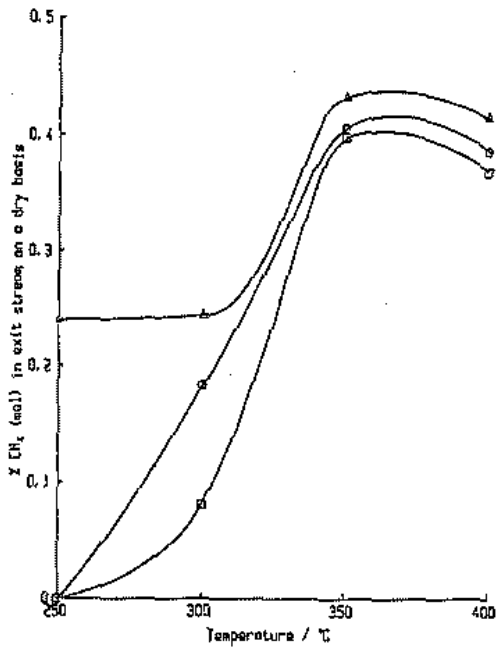
$CO:N_2:H_2O$ = 1:1:4.5

The effect of potassium promotion on the rate of methane formation (by its electron donating abilities to the chemisorbed CO molecule) has already been discussed in section 3.4 of this Thesis. The manganese promoter for the supression of methane by-product formation had been chosen because:-

Sachtler (142) has described a case where the addition of manganese to an iron-containing catalyst changed the CO hydrogenation selectivity towards oxygenates. He thereby provided evidence that the addition of manganese to a metal oxide catalyst enhanced such a catalyst's oxidation properties. Furthermore, the addition of manganese to an iron catalyst had been reported to increase the formation of the Fe_3O_{4-x} oxide phase, and since it was noted that CH_4 formation was believed to take place on the metallic phase (143), the addition of manganese should indirectly have reduced the rate of CH_4 formation over such a catalyst.

Kreitman et.al. (107) have also shown that the addition of MnO to a conventional Fe catalyst, which was then operated under FT conditions was more active for the water-gas shift reaction and less selective for methane as compared to the unpromoted Fe catalyst. They concluded that the MnO interacted with the Fe

Figure 5.4 : Effect of introducing potassium or, manganese on the levels of methane formation[a] over a Co:Cr = 3:1 catalyst



△ = Co : Cr = 3:1 + 0 % K ; ⊡ = Co : Cr = 3:1 + 1 % K

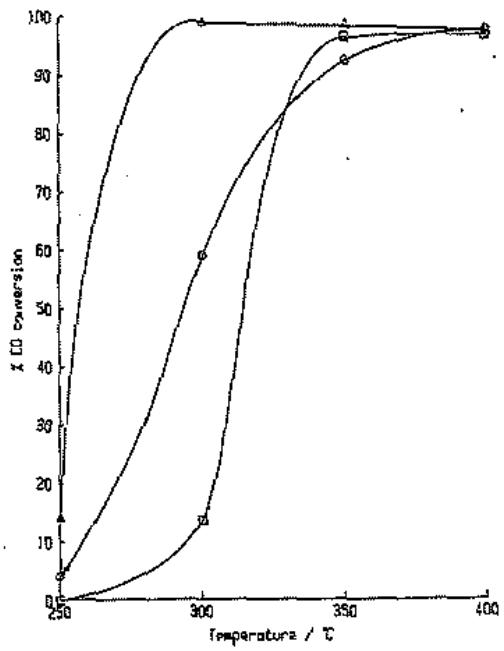
⊙ = Co : Cr = 3:1 + 2 % Mn

a : Temperature = 350°C ; CO GHSV = 510 h^{-1}

$CO:N_2:H_2O$ = 1:1:4.5

constituents of the catalyst to such an extent that MnO encapsulated some iron particles in extreme cases and thereby created a MnO promoted catalytic surface. This catalyst interacted with the reaction products CO_2

Figure 5.5 : Effect of introducing potassium or manganese on the water-gas shift activity over a Co:Cr = 3:1 catalyst



△ = Co : Cr = 3:1 + 0 % K ; ⊡ = Co : Cr = 3:1 + 1 % K

⊙ = Co : Cr = 3:1 + 2 % Mn

a : Temperature = 350°C ; CO GHSV = 510 h^{-1} ;

$CO:N_2:H_2O$ = 1:1:4.5

and H_2 in such a way as to depress hydrogen chemisorption and the secondary hydrogenation activity of olefins. It is therefore apparent that the addition of manganese to a supported metal oxide system (i.e. an

Fe-based FT catalyst) could promote the desired water-gas shift reaction and at the same time supress the formation of undesired methane by-product formation.

The effect on methane by-product formation and the resultant water-gas shift activity after introducing potassium and manganese onto the catalytic surface by the incipient wetness technique is shown in Figures 5.4 and 5.5 respectively.

Unfortunately, compared to the Co/MnO catalyst system, the addition of these promoters to the Co/Cr oxide catalysts gave no positive effect on the catalysts' methane production (Figure 5.4) or CO-shift activity (Figure 5.5). An explanation for this observation was found by analysing the catalysts' bulk structure and drawing parallels between the Co/Cr oxide and the Co/MnO systems. This discussion is presented in section 5.4.

5.4 Structural Studies

Analyses of the bulk structures of Co/Cr oxide catalysts was carried out by the following techniques:

- X-ray diffractometry (XRD)

and - Differential Scanning Calorimetry (DSC)

Table 5.3 Bulk structure of Co/Cr oxide catalysts[a]

Catalyst state	Phases present
Precipitated	Catalysts were totally amorphous
Calcined	$CoCr_2O_4$ spinel
Reduced	$CoCr_2O_4$ spinel (more crystalline)
	traces of Co metal were also detected
Used[b]	$CoCr_2O_4$ spinel

a : Results observed for Co:Cr = 1:10 ; 1:1 ; 3:1 and 10:1 as well as Co:Cr = 3:1 + 2 % (m/m) Mn^{2+} and Co:Cr = 3:1 + 1 % (m/m) K^+ catalysts

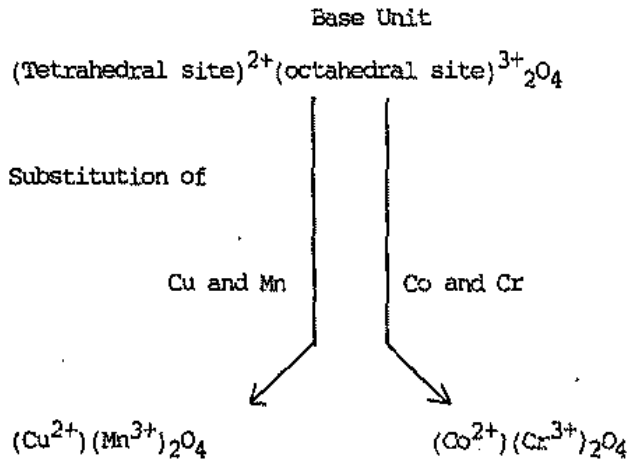
b : Data taken after catalysts had been on-line for about 600 hours

The bulk structures, as analysed by XRD, of the various Co/Cr oxide catalysts were found to consist mostly of a cobalt chromium spinel as is shown in Table 5.3 and it appeared that the $CoCr_2O_4$ spinel was the catalytically active species, as no other crystalline phases could be detected for the discharged catalyst. However, the possibility of an amorphous active phase co-existing with the crystalline active phase should not be ruled out, even though $CoCr_2O_4$ spinels have

been known to be the catalytically active component for other reactions. Kadenatsi et. al. (129, 144) as well as Fattakhova et. al. (126, 132) have both reported active $CoCr_2O_4$ spinel oxidation (CO and hydrocarbons) catalysts.

Again, structural similarities to the $CuMn_2O_4$ spinel already described in section 4.5.2 can be drawn, as one ion exclusively occupies the tetrahedral sites while the other ion exclusively occupy the octahedral sites. This point is further illustrated in Figure 5.6.

Figure 5.6 : A comparison of the $CuMn_2O_4$ spinel to the $CoCr_2O_4$ spinel



An explanation of the observation of exclusive substitution can be based on the knowledge that the

octahedrally coordinated Cr^{3+} is known to be the most stable state of chromium (145) and that Cr_2O_3 has been known to fuse with a number of M^{2+} oxides to give crystalline MCr_2O_4 compounds having a spinel structure with Cr^{3+} ions occupying the octahedral sites (146). Assuming that the above theory also holds for the $CoCr_2O_4$ spinel, it could then have been possible that Cr_2O_3 was a precursor in the formation of the $CoCr_2O_4$ spinel during the transition from the precipitated to the calcined state, even though it was not detected by the X-ray diffraction patterns.

However, the fact that Co metal was only present in trace levels for the active $CoCr_2O_4$ catalysts is in direct contrast with the results obtained for the structure of the Co/MnO catalysts (section 3.6), where Co metal supported on a MnO matrix was found to be the major phases present.

This fundamental difference in the structure of these two catalyst systems can also be considered to form the basis for the difference in the levels of CH_4 by-product observed over both the promoted and unpromoted $CoCr_2O_4$ catalysts. As the $CoCr_2O_4$ catalysts with high cobalt loadings were found to be more active than the catalysts with low cobalt

loadings, it must be concluded that cobalt appeared to be the active metal in the $CoCr_2O_4$ spinel. However, as the cobalt was present in a non-metallic state (i.e Co^{2+}), and since Copperthwaite et. al. (80) have shown (as discussed in section 3.6) that non-metallic cobalt appeared to be associated with CH_4 formation, it is not surprising that the $CoCr_2O_4$ catalyst produced significantly higher levels of CH_4 by-product as compared to the Co/MnO catalysts described in chapter 3.

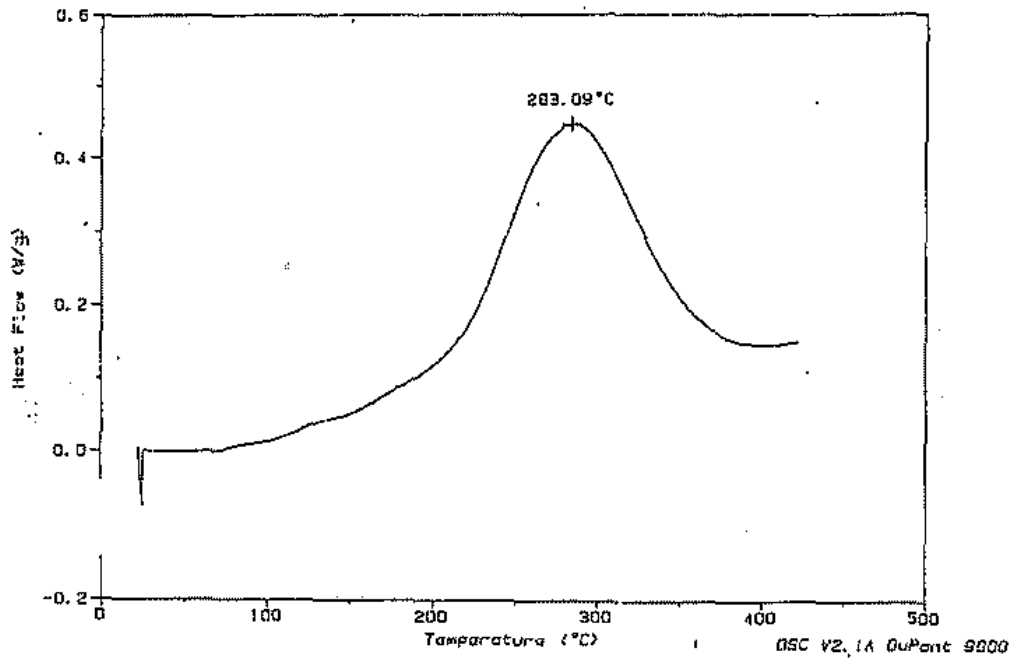
Taking into account that the addition of potassium tended to selectively poison catalytic sites associated with non-metallic cobalt as discussed for the Co/MnO catalysts in section 3.6, and extending the $CoCr_2O_4$ catalysts, one can visualise addition of any potassium promoter to a $CoCr_2O_4$ catalyst would only result in the poisoning of active sites, and thereby explain the slight decrease in water-gas shift activity observed in Figure 5.5 for a potassium promoted $CoCr_2O_4$ catalyst. Even though, these catalysts were found to produce CH_4 by-products, their rate of H_2 and CO_2 formation was still much larger as compared to the rate of CH_4 formation. As both CH_4 formation and the water-gas shift reaction are thought to take place on the same catalytic sites, it is not surprising that the addition

of a potassium promoter, only decreased the catalyst's water-gas shift activity to a minor extent, thereby explaining the results presented in Figure 5.4 for the potassium promoted $CoCr_2O_4$ catalyst.

Similar conclusions can be drawn for the manganese promoted $CoCr_2O_4$ catalyst, as the observed decrease in water-gas shift activity (Figure 5.5) also pointed towards a blocking (or poisoning) of the active sites. Whether this blocking was achieved by encapsulating the active species, in the way described by Kreitman et. al. (107) for the Fe-based FT catalyst, could not be ascertained as the X-ray diffraction patterns for the Mn promoted $CoCr_2O_4$ catalyst showed no differences as compared to the pattern for the unpromoted catalyst. It is also interesting to note that the levels of CH_4 by-product did not decrease upon promotion with 2 % (m/m) Mn (Figure 5.4). This result therefore indicates that even though the addition of Mn to a Fe-based FT catalyst had a chemical effect on the rate of CH_4 formation (107), no such effect was observed for the $CoCr_2O_4$ catalyst investigated.

The DSC technique was used to further investigate the effects of reducing a calcined $CoCr_2O_4$ catalyst under hydrogen, using the experimental conditions described in chapter 2. The DSC plot is shown in Figure 5.7.

Figure 5.7 : DSC plot for the reduction of a $CoCr_2O_4$ catalyst under hydrogen



From Figure 5.7, it can be seen that the reduction of the catalyst involved a single step process with an endotherm representing a phase change occurring at 283°C. As the calcined state of the catalyst comprised the $CoCr_2O_4$ spinel, and since only trace levels of Co metal had been detected upon reduction

under H_2 (Table 5.3), it can only be concluded that the endotherm observed in the DSC plot was due to the formation of additional $CoCr_2O_4$ spinels, probably from highly dispersed amorphous chromium oxides and cobalt oxides.

5.5 Summary

In this chapter, it was shown that $CoCr_2O_4$ catalysts with high cobalt loadings (i.e. Co : Cr = 3:1) displayed high and stable water-gas shift activity (i.e. 98 % CO conversion) at temperatures as low as 300°C. Activation energy calculations showed that the values obtained for the $CoCr_2O_4$ catalysts investigated were similar to the ones obtained by Chinchen et. al. (119) for the commercial Fe/Cr oxide based high temperature water-gas shift catalyst. It was thus concluded that , based on these calculations, the water-gas shift reaction would be expected to operate via similar mechanisms over both these catalysts.

It was also found that the $CoCr_2O_4$ formulations tested gave significant levels of CH_4 by-product (ca. 0.4 mole %) under water-gas shift reaction conditions. A structural analysis of the catalytic material showed that the crystalline phase of the active catalyst comprised the $CoCr_2O_4$ spinel and it was argued

that the presence of non-metallic cobalt in this active phase was the cause of the CH_4 by-product formation. The effect of various promoters (i.e. K^+ and Mn^{2+}) on the rate of CH_4 formation and water-gas shift activity over a Co : Cr = 3:1 catalyst was also investigated. It was found that while neither of these elements could significantly suppress the levels of CH_4 produced by the catalyst, they brought about a slight deactivation in the catalyst's water-gas shift activity. Both these observations were believed to have been caused by the blocking or poisoning of the non-metallic cobalt sites, which were thought to catalyse both the water-gas shift reaction and CH_4 by-product formation.

Nevertheless, the $CoCr_2O_4$ catalysts can be considered as a useful high activity water-gas shift catalyst, which could be particularly suited for a coal-based ammonia synthesis plant, which requires the conversion of high levels of carbon monoxide (eg. about 60 % (vol.)) prior to the actual ammonia synthesis cycle.

6. A KINETIC AND MECHANISTIC STUDY OF Co/Mn OXIDE, Cu/Mn OXIDE, AND Co/Cr OXIDE WATER-GAS SHIFT CATALYSTS

6.1 Introduction

A detailed description of the many mechanistic and kinetic studies dealing with water-gas shift reaction catalysts has already been presented in sections 1.5 and 1.6 respectively, of this Thesis. Summarising the mechanistic discussions presented in section 1.5, it was shown that two main types of mechanisms have become widely accepted for the more common water-gas shift catalysts. These mechanistic schemes can be distinguished in as far as that one involves a redox type mechanism by which an oxygen atom is transferred from the water molecule to the carbon monoxide molecule with the aid of a catalyst, which undergoes reduction and oxidation during the reaction cycle. This type of mechanism has been postulated for the iron-based catalysts (56,59), but has recently also been reported over the copper based low temperature water-gas shift catalyst (58,61,147).

The other, more general type of a water-gas shift mechanism, postulates the formation of a transition state (i.e. central intermediate), which is composed of

fragments of the reagent molecules. This central intermediate then decomposes to form carbon dioxide and hydrogen. A number of different intermediates have been proposed over various water-gas shift catalysts, and a description of their nature has been given in section 1.5.2. Furthermore, a survey on the various kinetic studies described in the literature was presented in section 1.6.

However, it should be mentioned that although a great number of papers have appeared in the literature dealing with kinetic and mechanistic aspects of commercial iron and copper based heterogeneous (and various homogeneous) water-gas shift catalysts, no reference could be found addressing these issues involving Co/MnO, Cu/MnO or $CoCr_2O_4$ catalysts operated under water-gas shift conditions. Thus, in this chapter, the mechanism of the water-gas shift reaction over these three catalyst systems is discussed using both kinetic and model reagent studies.

6.2 Experimental techniques

The kinetic studies were based on techniques described in the literature (148-150), by which the partial pressure of one of the reagents (eg. P_{CO} or P_{H2O}) was varied while keeping the partial pressure of the

other reagent (eg. P_{H2O} or P_{CO}) constant and in excess. An inert carrier gas was also used to keep the overall flow rate of the system constant and the rate of the water-gas shift reaction was monitored using the gas chromatographic techniques described in chapter 2.

Furthermore, it was decided to carry out the kinetic experiments at reduced temperatures (i.e. 275°C for the Co/MnO catalyst, 229°C for the Cu/MnO catalyst and 261°C for the $CoCr_2O_4$ catalyst)in order to eliminate any interference from the reverse water-gas shift reaction, which is favoured at higher temperatures.

The experimental results were used to obtain a graphical representation of the partial pressure of the various reagents as a function of the rate of the reaction. An empirical form of the rate law under these experimental conditions was thus predicted.

The evaluation of all catalysts for the model reagent studies was carried out, using the all-glass microreactor already described in section 2.3 of this Thesis. It should be noted that a similar design had been used by Hutchings et. al. (151) to feed reagents to a reactor, using controlled vaporisation in an inert carrier gas. Also, all products, both liquid and gaseous, were analysed by the gas chromatographic techniques described in section 2.4.

6.3 Kinetic Studies

6.3.1 The effect of the partial pressure of H_2O on the rate of the reaction

The effect of the partial pressure of H_2O on the rate of H_2O conversion (i.e. the rate of the reaction) was investigated for the following catalysts:

i) Co : Mn = 1:1

ii) Cu : Mn = 1:1

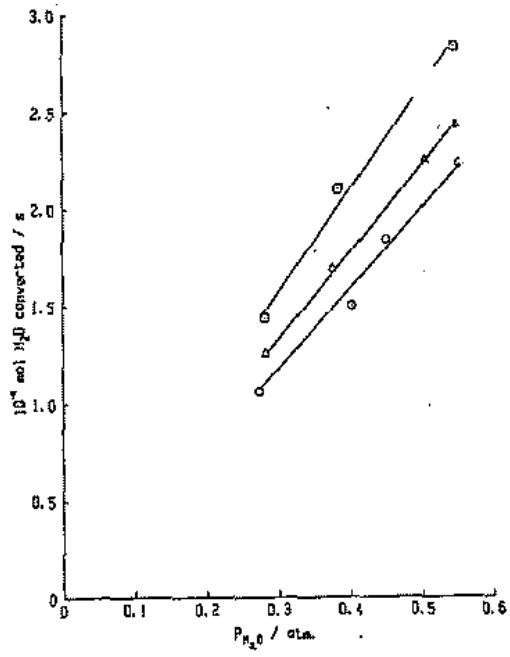
iii) Co : Cr = 3:1

The results for these set of experiments, which were carried out at a constant 28.4 kPa partial pressure of CO and a CO GHSV of 510 h^{-1} are shown in Figure 6.1.

The results shown in Figure 6.1 demonstrate that, for all three catalyst systems tested, the rate of H_2O conversion was found to be linearly dependent on the partial pressure of H_2O, indicating that in the concentration range investigated, the water-gas shift reaction was first order in water concentration over the Co : Mn = 1:1, the Cu : Mn = 1:1 and the Co : Cr = 3:1 catalysts.

As a first order rate dependence can be considered to be the simplest case in the maze of mathematical rate expressions, it could now be argued that in the

Figure 6.1 : Rate of H_2O conversion as a function of P_{H2O} for the various catalysts tested[a]



△ = Co : Mn = 1:1 ; ⊡ = Cu : Mn = 1:1 ;

⊙ = Co : Cr = 3:1

a : Co : Mn = 1:1 ; Temperature = 275°C

Cu : Mn = 1:1 ; Temperature = 229°C

Co : Cr = 3:1 ; Temperature = 261°C

P_{CO} = 28.2 kPa

presence of these catalysts, the water-gas shift reaction could be classified as a "simple" reaction of the form

$$A + B \longrightarrow \text{PRODUCTS}$$

which could proceed on the basis of a simple

bimolecular collision with the collision frequency being proportional to the concentration of both reagents A and B (152). This would thus imply the following rate law:

$$-\frac{d[A]}{dt} = k\,[A]\,[B] \qquad (6.1)$$

In our case, equation 6.1 holds true for the rate dependence of H_2O as determined experimentally.

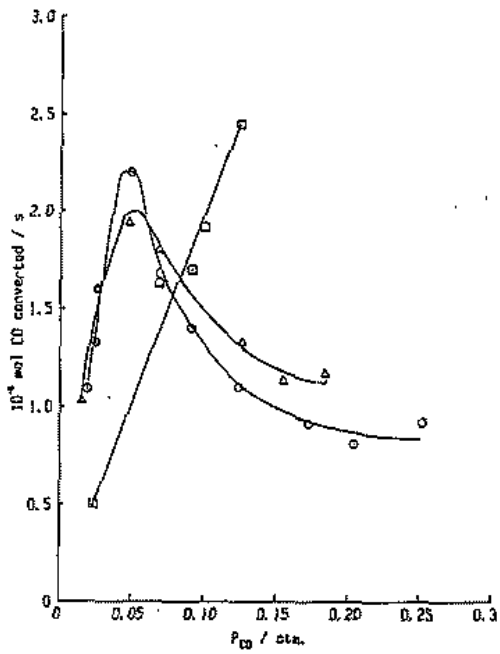
However, the interpretation of a rate law is full of pitfalls and one should not lose sight of the fact that one-step reactions could also result from a reaction scheme which is far more complex than just a simple bimolecular collision process. In order to make a deduction about the final form of the rate law, one first has to investigate the effects of all the other reagents on the overall rate of the reaction.

6.3.2 Effect of partial pressure of CO on the rate of the reaction

The effect of CO partial pressure on the rate of CO conversion was investigated for the various catalysts. The results for these sets of experiments, which were

carried out at a constant H_2O feed rate of 2.72 g (H_2O)/hour are shown in Figure 6.2.

Figure 6.2 : Effect of CO partial pressure on the rate of CO conversion for the various catalysts tested[a]



△ = Co : Mn = 1:1 ; ⊡ = Cu : Mn = 1:1 ;

⊙ = Co : Cr = 3:1

a : The temperatures at which these experiments were carried out are identical to the ones shown in Figure 6.1

H_2O feed rate = 2.72 g (H_2O)/hour

From the results presented in Figure 6.2, it is apparent, that the Cu:Mn = 1:1 catalyst displayed a different kinetic behaviour to both the Co:Mn = 1:1 and the Co:Cr = 3:1 catalysts, as the rate of CO conversion was found to be linearlly dependent on P_{CO} for the Cu:Mn = 1:1 catalyst, whereas for the other two catalyst systems, the rate of reaction initially increased with increasing CO partial pressure, but was then found to decline to a steady value.

Thus, considering only the Cu:Mn = 1:3 catalyst, the water-gas shift reaction could very well take place as a simple bimolecular collision reaction over this type of catalyst. The rate law can therefore mathematically be expressed as follows:

$$\text{Rate of reaction} = -\frac{d[CO]}{dt} = -\frac{d[H_2O]}{dt} = k[CO][H_2O]$$

The observation of the water-gas shift reaction kinetics being first order with respect to CO had already been reported for other catalyst systems, when Taqui Khan et. al. (153) showed this type of kinetic behaviour for the homogeneously catalysed water-gas shift reaction over a K[Ru (H EDTA) (CO)] catalyst under ambient temperature conditions.

On the other hand, the kinetic results for the Co:Mn = 1:1 and the Co:Cr = 3:1 catalysts, which reach a maximum rate with increasing CO partial pressure could possibly be indicative of a Langmuir-Hinshelwood type reaction mechanism.

6.3.2.1 The Langmuir-Hinshelwood mechanism

The Langmuir-Hinshelwood mechanism is based on the principles of localised chemisorption as first proposed by Langmuir (154) in 1917. The following is a simplified interpretation (155,156) of the Langmuir isotherm, which assumes that:

i) a gas molecule can only be adsorbed on a finite number of sites on the surface of the solid

ii) the quantum states of adsorbed gas molecules are the same for all sites and are independent of the effects (eg. pressure) of the neighbouring molecules

Using these assumptions, the well-known Langmuir isotherm can be derived in the following form:

$$\text{EXP}\left(-\frac{\Delta H}{RT} + \frac{S-S^{\circ}}{R}\right) P_{O} = \frac{\theta}{1-\theta} \qquad (6.2)$$

where θ = fractional coverage of gas molecules on the solid surface sites

P_o = equilibrium gas pressure

ΔH = molar heat of adsorption

S = entropy per mole of adsorbed molecules

S^o = entropy per mole of gas at unit pressure

If ΔH and S are both independent of θ, then equation 6.2 reduces to the following form :

$$b P_o = \frac{\theta}{1 - \theta} \qquad (6.3)$$

where b = constant = $EXP\ (-\frac{\Delta H}{RT} + \frac{S - S^o}{R})$

Solving this equation for θ one gets:

$$\theta = \frac{b P_o}{1 + b P_o} \qquad (6.4)$$

The catalysed water-gas shift reaction can be looked upon as involving the collision between CO and H_2O fragments adsorbed on the surface and can thus be expected to be second-order in the extent of surface coverage. The rate of these so-called

Langmuir-Hinshelwood types of reactions (157) can therefore be expressed as follows:

$$A + B \longrightarrow Products$$

$$-\frac{dP_A}{dt} = \text{rate of reaction} = k_s \theta_A \theta_B \qquad (6.5)$$

Applying equation 6.4 to the water-gas shift reaction one gets:

$$\text{Rate of reaction} = -\frac{dP_{CO}}{dt} = k_s \theta_{CO} \theta_{H_2O} \qquad (6.6)$$

where θ_{CO} = fractional coverage of CO molecules on the solid surface

θ_{H_2O} = fractional coverage of H_2O molecules on the solid surface

but $$\theta_{CO} = \frac{b P_{CO}}{1 + b P_{CO} + a P_{H_2O}} \qquad \text{(from 6.4)}$$

and $$\theta_{H_2O} = \frac{a P_{H_2O}}{1 + a P_{H_2O} + b P_{CO}} \qquad \text{(from 6.4)}$$

where a = *constant*

Thus, equation 6.6 becomes

$$-\frac{dP_{CO}}{dt} = \frac{k_s b a P_{H_2O} P_{CO}}{(1 + a P_{H_2O} + b P_{CO})^2} \qquad (6.7)$$

and at constant P_{H_2O} (as was the case for the experiments)

$$-\frac{dP_{CO}}{dt} = \frac{n\ P_{CO}}{(1 + m\ P_{CO})^2} \qquad (6.8)$$

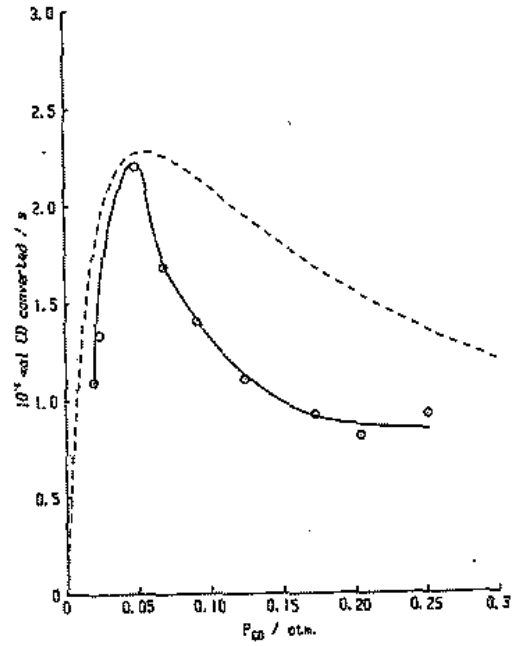
where $n = \frac{k_s\ b\ a\ P_{H_2O}}{(1 + a\ P_{H_2O})^2}$ = constant and $m = \frac{b}{1 + a\ P_{H_2O}}$ = constant .

Although expression 6.8 predicts a maximum for the rate of the reaction with increasing P_{CO}, it does not fit the experimental data for the Co:Mn = 1:1 and the Co:Cr = 3:1 catalysts shown in Figure 6.2 particularly well, as can be seen in Figure 6.3.

From Figure 6.3, it can be seen that the experimentally determined r_{CO} increased less rapidly than predicted by the Langmuir-Hinshelwood expression (equation 6.8). Furthermore, the experimental r_{CO} decreases rapidly to a steady value, whereas the theoretical expression predicts a gradual and steady decrease with increasing P_{CO}. The observed variation in r_{CO} as a function of P_{CO} is therefore not wholly consistent with a simple Langmuir-Hinshelwood bimolecular reaction mechanism on these catalysts.

The observed decline of the reaction rate to a steady

Figure 6.3 : A comparison between experimental and theoretical rates of CO conversion at constant H_2O partial pressure for the Co/MnO and $CoCr_2O_4$ catalysts



—— = mathematical expression

⊙ = Co : Mn = 3:1

$$r_{CO} = n\, P_{CO} / (1 + m\, P_{CO})^2$$

where n = 0.000164 mol CO converted / s / atm.

m = 18.0 /atm.

value with increasing P_{CO} could be indicative of a different reaction pathway occurring at these

conditions. It is possible that at high P_{CO}, a regenerative mechanism could occur in which the reaction proceeds in two steps:

$$H_2O\ (g) + * \rightleftharpoons H_2\ (g) + O\ (a)$$
$$CO\ (g) + O\ (a) \rightleftharpoons CO_2\ (g) + *$$

where * is a vacant surface site. This type of mechanism, which was first proposed by Temkin et. al. (59), has already been discussed in chapter 1 (section 1.5). The reaction rate for such a mechanism would depend on the availability of the H_2O and CO on the catalytic surface. At a high P_{CO}, the catalytic surface would become depleted of H_2O molecules, and thus the hydrogen production step for this type of mechanism would become the rate limiting step. The overall reaction rate would thus reach a steady value which would be equivalent to the rate of the hydrogen production cycle of this regenerative mechanism. Such a mechanism would be consistent with the observed constant r_{CO} at the high P_{CO} (45).

It is thus possible, that the water-gas shift reaction proceeds by means of at least two different mechanisms over the Co/MnO and the $CoCr_2O_4$ catalysts. At low P_{CO} the reaction was observed to obey the Langmuir-Hinshelwood behaviour to a reasonable extent,

whereas at a high P_{CO}, a regenerative mechanism could account for the kinetic results obtained.

Overall, the rate of the water-gas shift reaction can be mathematically expressed for the various catalysts tested as shown below:

$$-\frac{d[CO]}{dt} = -\frac{d[H_2O]}{dt} = k \cdot P_{H2O} \cdot P_{CO}$$

for the Cu/MnO catalyst

$$= k \cdot P_{H2O} \cdot \frac{a\, P_{CO}}{(1 + bP_{CO})^2}$$

for the Co/MnO and $CoCr_2O_4$ catalysts at low P_{CO}

$$= k \cdot P_{H2O} \cdot \text{constant}$$

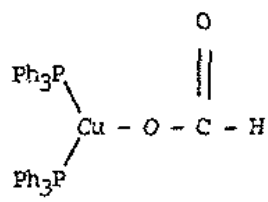
for the Co/MnO and $CoCr_2O_4$ catalysts at high P_{CO}

6.4 Model reagent mechanistic studies

The number of mechanisms accounting for the formation of CO_2 and H_2 from CO and H_2O have already been discussed in section 1.5, and can be summarised to either proceed via a redox regenerative mechanism or through the formation of a central intermediate.

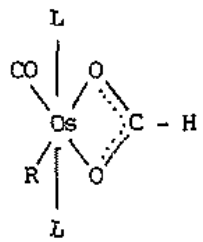
6.4.1 Reaction of formic acid over various catalyst systems

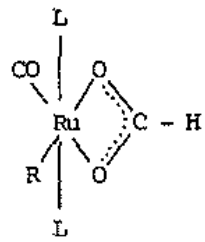
In section 1.5 of this thesis, the presence of a surface formate had been identified as the central intermediate for copper containing water-gas shift catalysts (61, 158). However, as there still exists uncertainty as to the exact co-ordination (mono- or bidentate) of these surface formate intermediates, researchers have generally omitted structural details when representing a surface formate. Using the field of organometallics as an analogy, both the formation of monodentate and bidentate formate species have been reported. For example, a monodentate formate intermediate has been reported by Beguin et. al. (159) on copper in the presence of phosphine ligands as shown below:



Further evidence for this type of co-ordination was given by Paonessa et. al. (160), who also reported the formation of a terminal formate over platinum.

In contrast, examples of stable bidentate formate intermediates have been reported by Roper and Wright (161) on osmium and ruthenium as shown below:





where L = PPh_3

In the field of heterogeneous catalysis, the subject of formate adsorption on catalytic surfaces has been discussed by Edwards et. al. (162), who provided evidence for the existence of a bidentate formate surface species over copper- containing heterogenous catalysts. In their publication, Edwards et. al. (162), used a Fourier Transform Infra Red (FTIR) spectrophotometer to characterise the various surface intermediates present during the synthesis of methanol from CO and H_2 over a Cu/Zn/Cr oxide catalyst. However, even though they proposed the formation of a bidentate intermediate in their overall reaction mechanism, their infra red spectra also showed a weak adsorption band (at 1470 cm^{-1}), which could be assigned to symmetric OCO stretching of a monodentate carbonate species (163).

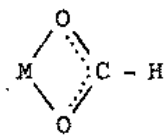
Thus, despite the fact that the formation of a bidentate formate intermediate on a heterogeneous catalyst surface has generally been accepted, one should nevertheless not exclude the possibility of the formation of a minor fraction of monodentate formate intermediates as well.

The formation of surface formate intermediates on heterogeneous catalysts presumably occurs by an oxidative addition reaction in which the H and the HCOO fragments add to the metal atom surface site. The decomposition of formic acid (to CO_2 and H_2), which is believed to occur via the formation of a surface formate, is well known over metals such as copper (164-166) or nickel (167). In order to test whether the water-gas shift reaction proceeded over the various catalyst systems investigated in this Thesis via formate fragments, it was decided to co-feed formic acid over these catalysts.

The formic acid was rigorously dried (using phthallic anhydride and then distilled under nitrogen) and was then reacted over the two catalyst systems investigated, using the experimental apparatus described in Chapter 2. The results of these studies are shown in Table 6.1. It can be seen that, under the conditions tested, formic acid did not react over either the Co/MnO or the $CoCr_2O_4$ catalyst systems

(i.e. no H_2 and CO_2 were produced). These results should be contrasted with those obtained by van Herwijnen et. al. (61, 158), who showed that formic acid decomposed at 150°C to form CO_2 and H_2 over a Cu/ZnO low temperature water-gas shift catalyst. These result can therefore be considered as an indication that the water-gas shift reaction proceeds via a different reaction mechanism over non-copper containing water-gas shift catalysts.

As the decomposition of formic acid over Cu-containing catalysts is generally considered to proceed via the formation of a bidentate surface intermediate, the mechanism of formic acid decomposition over a Cu/MnO catalyst (Figure 6.4) is believed to take place via the formation of the following intermediate:



where M = surface site

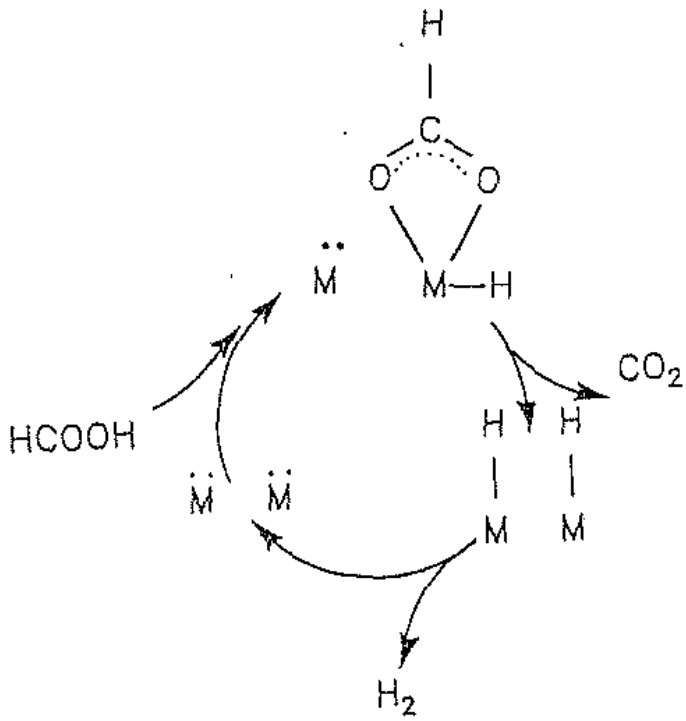
This decomposition mechanism is expected to involve oxidative addition and reductive elimination steps as depicted in Figure 6.4. However, one should also keep in mind that a monodentate formate intermediate could also be expected to be present on the surface to a minor extent. The decomposition of such an intermediate would take place by the same mechanistic steps outlined in Figure 6.4 for the bidentate intermediate.

Table 6.1 : Reaction of formic acid over the various catalysts tested

Catalyst System	Time on line / min.	% (mass) Selectivity				
		H_2	CO	CO_2	CH_4	HCOOH
Co/MnO	10	0.002	-	-	0.057	99.94
	54	0.005	-	-	0.068	99.92
Co:Mn =	134	0.003	-	-	0.043	99.95
1:1	260	0.003	-	-	0.025	99.97
$CoCr_2O_4$	12	0.004	-	-	0.102	99.89
	32	0.007	-	-	0.149	99.84
Co:Cr =	48	0.011	-	-	0.085	99.89
3:1	76	0.005	-	-	0.059	99.94
	129	0.003	-	-	0.046	99.95
Cu/MnO	60	0.200	-	1.97	0.018	97.65
	105	0.965	-	3.66	0.010	95.37
Cu:Mn =	120	2.12	-	4.01	0.007	93.86
1:3	180	3.01	-	3.69	-	93.03
	220	3.71	-	4.91	-	91.38
	245	2.72	-	3.72	0.008	93.56

Note : A "-" indicates that the compound was not detected.

Figure 6.4 : Decomposition of formic acid over metal oxide catalysts



Cotton and Wilkinson (168) have also described Cu-H as a borderline hydride with low stability, and Co-H, Cr-H as well as Mn-H as thermodynamically stable hydrides. Therefore, it can be envisaged that, upon formic acid co-feeding over the Co/MnO and the $CoCr_2O_4$

catalysts, the metal hydride, which had formed upon the dissociation of the formic acid on the active sites are too stable to decompose readily and could thereby block these sites. This theory therefore also aids in explaining the inactivity (and particularly the absence of any H_2 formation) of formic acid decomposition over these catalysts. However, as the Cu-H can decompose readily, no such blocking will occur and thus formic acid will decompose over these types of catalysts, resulting in the formation of H_2 as well as CO_2.

6.4.2 Reaction of methanol over the various catalysts systems

Due to similarities between CH_3OH and H_2O (i.e. -OH vs. $-CH_3$) methanol was used to further probe the reaction mechanisms of the water-gas shift reaction over the three catalysts investigated under a range of experimental conditions, and the results are given in Tables 6.2 and 6.3 respectively.

For CH_3OH-CO mixtures, methyl formate was observed as a significant product in the organic spectrum for all three catalysts investigated (Table 6.2). Even though the production of methyl formate was not particularly

Table 6.2 : Reaction of methanol over the various catalysts studied

i) Organic product distribution

Time on line/min	% Selectivity (mass) of gaseous organic phase			
	CH_4	CH_3OCH_3	MeOH	HCO_2CH_3
Co/MnO Co:Mn = 1:1 Temperature = 150°C				
9	2.68	1.53	81.8	14.0
24	0.63	4.17	67.7	27.5
41	0.31	2.22	81.8	15.6
59	0.67	3.72	95.6	-
90	0.14	0.61	99.2	-
$CoCr_2O_4$ Co:Cr = 3:1 Temperature = 150°C				
30	2.11	-	97.10	0.82
40	1.56	-	97.35	1.08
50	0.60	-	98.13	1.27
60	0.61	-	97.42	1.97
70	0.39	-	98.44	1.18
80	0.47	-	97.93	1.60
Cu/MnO Cu:Mn = 1:3 Temperature = 100°C				
20	0.02	-	99.02	0.95
30	0.31	-	85.72	10.34
40	0.68	-	84.46	14.85
50	0.35	-	86.93	12.70
70	0.40	-	86.83	12.75
90	0.23	-	92.29	7.46

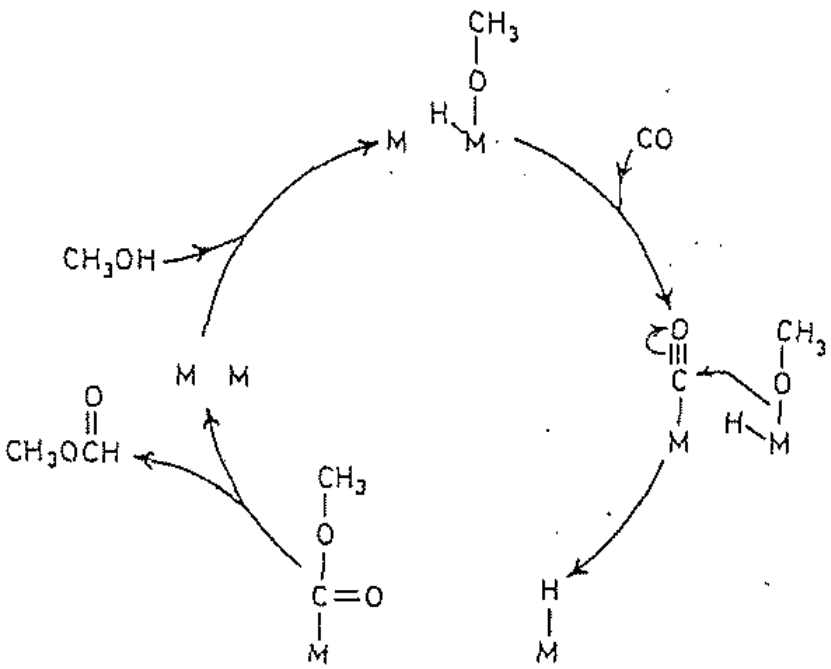
Table 6.3 : Reaction of methanol over the various catalysts studied

(ii) Inorganic product distribution

Time on line/min	% (vol) Selectivity of gaseous inorganic phase			
	H_2	N_2	CO	CO_2
Co/MnO ; Co:Mn = 1:1 ; Temperature = 150°C				
4	0.19	18.90	80.63	0.28
25	0.14	16.79	82.68	0.39
48	0.05	13.95	85.80	0.15
71	0.05	13.98	85.80	0.15
$CoCr_2O_4$; Co:Cr = 3:1 ; Temperature = 150°C				
10	0.03	19.10	80.87	0.01
37	0.04	18.67	81.29	-
82	0.04	17.33	82.63	-
Cu/MnO ; Cu:Mn = 1:3 ; Temperature = 100°C				
10	0.48	18.62	78.56	2.34
29	8.51	17.49	71.16	2.84
49	9.16	16.95	71.58	2.31
70	9.23	16.73	72.74	1.30
90	8.76	17.04	73.99	0.21

long lived (ca. 1.5 hours), it nevertheless was observed as the major product for all three catalysts. The formation of methyl formate from reaction of CH_3OH / CO is known for other catalyst systems, particularly at higher reaction pressures (169). Methyl formate is considered to be formed via the oxidative addition mechanism as shown in Figure 6.5.

Figure 6.5 : The formation of methyl formate over the various catalysts studied



In this mechanism, CH_3OH dissociatively adsorbs onto the surface to give a methoxy group, which subsequently reacts with co-adsorbed CO on an adjacent site to ultimately produce methyl formate.

High H_2 *and* CO_2 levels were observed for the CH_3OH co-feeding experiments over the Cu/MnO catalyst (Table 6.3). The decomposition of methanol is known to occur over copper containing catalyst systems (170, 171) and could thus account for the high H_2 levels observed. The process proceeds according to the reverse methanol synthesis reaction:

$$CH_3OH \rightleftharpoons 2\,H_2 + CO$$

The high levels of carbon dioxide observed for the Cu/MnO catalyst could be due to two possible *reactions:*

1) $CO + CO \rightleftharpoons CO_2 + C_s$

or 2) $CO + H_2O \rightleftharpoons CO_2 + H_2$

(the water-gas shift reaction)

It is unlikely that any CO_2 had formed by means of reaction 2 (i.e. the water-gas shift reaction) as the exclusion of water was ensured at all times. (i.e. all

experiments had been carried out under dry conditions and the methanol had been dried rigorously beforehand). Furthermore, the formation of water from methanol is unlikely under the experimental conditions used.

Reaction 1 would account for the decrease in the level of CO_2 with increased time-on-line (Table 6.3). Also, for reaction 1, the catalyst would become "coked up" and eventually lose its activity. An analysis revealed that the spent catalyst contained 3.4 % (m/m) carbon. This result thereby provided evidence that the disproportionation of CO to form CO_2 and C took place over the Cu/MnO catalyst during the methanol co-feeding experiments, resulting in the formation of CO_2. However, even though the deposition of carbon would be expected to deactivate the catalyst, it is interesting to note that the production of hydrogen and methyl formate was still being observed to a significant extent after 90 minutes on-line. As the levels of CO_2 formation decreased with time, an indication is therefore given that methanol decomposition and carbon formation took place on different catalytic sites (with the build up of carbon only deactivating the catalytic sites over which this reaction takes place).

From Table 6.2, it can also be seen that the levels of methyl formate produced during the methanol co-feeding experiments were found to be higher for the Cu/MnO catalyst than for both the Co/MnO and the $CoCr_2O_4$ catalysts. This observation explains why copper has been found to be the most active water gas shift metal (Grenoble et. al. (8)), as it readily adsorbs CO and thereby activates it.

6.5 Reaction Mechanism

The experiments carried out with the various model reagents are considered to be highly significant with respect to the mechanism of the water-gas shift reaction over the catalyst systems investigated. The major reaction product observed for the methanol co-feeding experiments was methyl formate, which formed from the insertion of a surface methoxy intermediate into a surface CO. Additional mechanistic evidence was obtained from co-feeding formic acid over the various catalysts. The decomposition of formic acid did not take place over the Co/MnO and the $CoCr_2O_4$ catalysts due to the formation of a bidentate surface formate intermediate. However, over the Cu/MnO catalyst formic acid was found to decompose to form CO_2 and H_2 due to the formation of a monodentate formate intermediate.

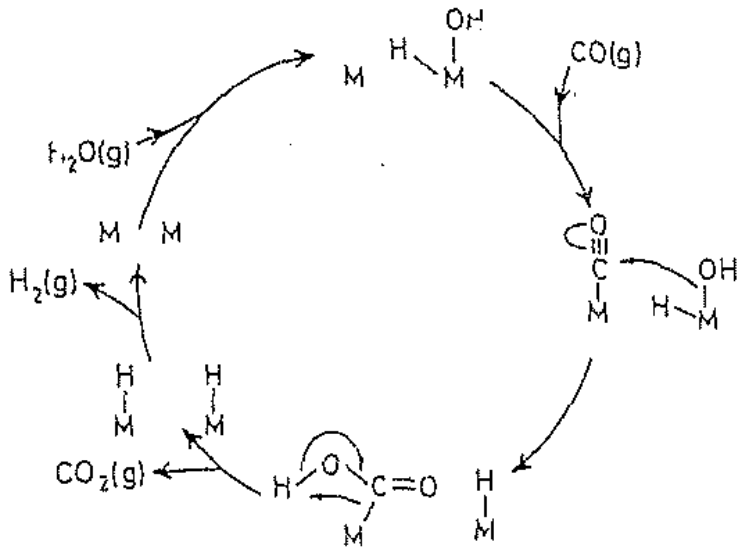
Based on these model reagent studies the water-gas shift reaction mechanism proposed in Figure 6.6 is thought to occur over the Co/MnO and the $CoCr_2O_4$ catalyst systems investigated

In this scheme, it is proposed that water adsorbs dissociatively onto a surface site with subsequent adsorption of CO onto an adjacent surface site. This is then followed by the insertion of the surface-bonded hydroxy group into the M-CO bond. The reaction of CH_3OH to form methyl formate is direct evidence for this proposed step and also insertion reactions are well known in analogous complexes in organometallic chemistry (172,173). Subsequent reaction would occur via a beta-elimination reaction to give gas-phase CO_2 and surface hydrides, which lead to hydrogen formation.

Such decomposition of a metallocarboxylic acid to yield CO_2 is also well supported in the reactions of numerous organometallic complexes (174-176), eg as was initially demonstrated for the organometallic complex $IrCl_2(CO_2H)(CO)(PMe_2Ph)_2$ (177).

The kinetic data obtained in the first part of this chapter supports such a reaction scheme. The key surface species derived from water is the surface hydroxy and the observed linear dependence of the

Figure 6.6 : Water-gas shift reaction mechanism over the Co/MnO and the $CoCr_2O_4$ catalyst systems investigated



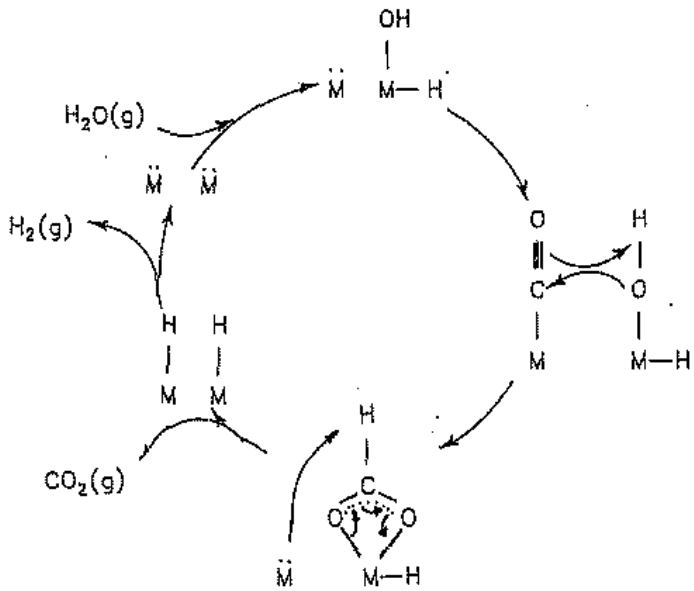
reaction rate on P_{H2O} (Figure 6.1) is consistent with this mechanistic step. The observation that r_{CO} reaches a maximum and then becomes constant at high P_{CO} for these two catalyst systems could be due to CO successfully competing with H_2O for adsorption sites. The concentration of surface hydroxy groups therefore becomes limited. Eventually, with increasing P_{CO}, it would no longer be possible to form a surface formate

intermediate, due to the lack of surface hydroxy species and this transition state type mechanism would break down. Hence, as stated previously (section 6.3.2.1) at high P_{CO}, a regenerative mechanism (*59, 60, 178, 179*)) may become a dominant reaction pathway, with the rate limiting step being the production of hydrogen. It is therefore possible for the Co/MnO and $CoCr_2O_4$ catalysts, that, at low P_{CO}, the proposed surface formate mechanism pathway is dominant, but at high P_{CO} the regenerative mechanism may also compete.

The proposed water-gas shift reaction mechanism over the Cu/MnO catalyst is shown in Figure 6.7. In this mechanism, water is again adsorbed dissociatively onto a surface site with the subsequent adsorption of CO onto an adjacent site. However, instead of the insertion by the surface bonded hydroxy species into the M-CO bond (as was shown for the Co/MnO and the $CoCr_2O_4$ catalysts) the CO is inserts into the O-H bond to form the bidentate formate intermediate, which is associated with copper-containing catalysts. Such insertion reactions involving copper complexes have been documented in the literature (180).

As the kinetics of such a reaction mechanism depend primarily on the availability of a surface hydroxy species, the rate of the reaction would hence be

Figure 6.7 : Water-gas shift reaction mechanism over the Cu/MnO catalyst system



directly proportional to number of adsorbed H_2O molecules (i.e. the $[H_2O]$). In Chapter 4, it was shown that the Cu/MnO catalyst system displayed the highest specific activity of all the three catalysts tested. This suggests that the Cu/MnO catalyst is capable of higher turnover frequencies than the Co/MnO or the $CoCr_2O_4$ catalysts. Hence, the competition (between CO and H_2O) for adsorption sites would only effect the reaction rate at a very high P_{CO} or P_{H2O}. One would therefore not expect the reaction rate to reach a maximum (as was observed for

the other two catalyst systems) except at very high P_{CO} or P_{H2O}. Thus, the high specific activity of the Cu/MnO catalyst could explain the observed first order rate dependence on CO under the experimental conditions employed.

6.5 Summary

In this chapter, an investigation of the water-gas shift reaction over three different catalyst systems has been described using both kinetic and model reagent studies. The results obtained lead to the derivation of kinetic expressions and mechanistic reaction schemes. The kinetics of the various catalyst systems investigated can be mathematically expressed as follows:

i) Cu/MnO catalysts :

$$r_{CO} = k \cdot P_{CO} \cdot P_{H2O}$$

ii) Co/MnO and $CoCr_2O_4$ catalysts:

$$r_{CO} = k \cdot P_{H2O} \cdot \frac{a\, P_{CO}}{(1 + b\, P_{CO})^2} \qquad \text{at low } P_{CO}$$

$$= k \cdot P_{H2O} \cdot \text{constant} \qquad \text{at high } P_{CO}$$

Based on the model reagent studies, mechanisms for the water-gas shift reaction have been proposed for all three catalyst systems for which it is considered that the following sequence takes place:

i) water dissociatively adsorbs to form a surface hydroxy and hydride species

ii) subsequent adsorption of CO

iii) insertion of CO into (a) the O-H of the surface hydroxy species over the Cu/MnO catalyst or (b) insertion of the surface hydroxy species into the metal carbonyl over the Co/MnO and $CoCr_2O_4$ catalysts to form surface intermediates

iv) decomposition of the surface intermediates to form gaseous CO_2 and surface hydrides

v) combination of the surface hydrides to form gaseous H_2

The mechanistic sequence discussed in this chapter showed much promise for explaining the route of the water-gas shift reaction over the three catalyst systems studied, thereby helping to explain the complex interaction of catalyst surface sites on reagent molecules in the ultimate production of CO_2 and H_2.

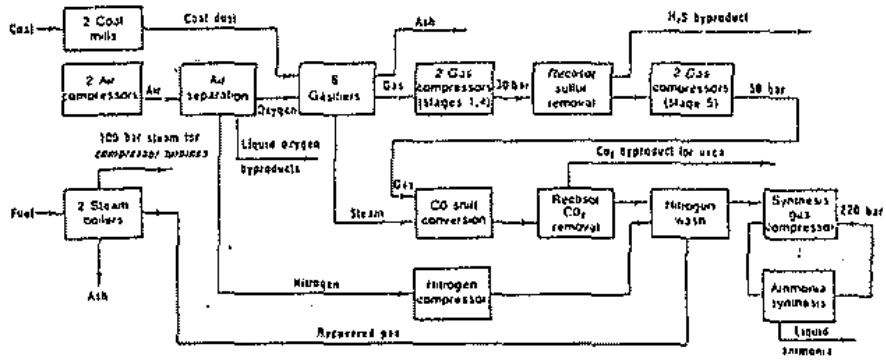
7. SULPHUR POISONING OF THE VARIOUS CATALYSTS INVESTIGATED

7.1 Introduction

Sulphur is considered to be one of the most common catalyst poisons (181) as it not only alters the catalyst's surface but also its bulk structure and hence its overall activity and selectivity. Due to the commercial interest in the subject, it is not surprising that a great deal of research work has been dedicated to sulphur poisoning (5, 181-183). Feed gases containing sulphur impurities (even in ppm levels) drastically reduce the activity of most metal-containing industrial catalysts. On plants which utilise coal-derived synthesis gas to produce chemicals or fuels, sulphur removal units have to be incorporated (Figure 7.1) in order to protect various catalysts from the relatively high levels of H_2S (about 0.4 %) and COS (about 0.04 %) present in the feed gases (184, 185).

There still exists a fair degree of uncertainty about the mechanism by which metal catalysts are poisoned by sulphur, but it is believed that both thermodynamic (i.e. bulk characteristics) as well as surface

Figure 7.1 : Schematic diagram of a coal based ammonia synthesis plant



interactions are involved (182). From the thermodynamic results presented in Table 7.1, it can be seen that most metals have a very high affinity for sulphur and hence it is very difficult to avoid sulphur poisoning of transition metal catalysts. Due to the low electronegativity of sulphur, metal-sulphur bonds are mainly non-ionic, thereby explaining the many metal sulphide phases (some of which can also be present in a nonstoichiometric form) which can exist. It is not difficult to envisage that the formation of such metal

sulphides alters the bulk structure of metal catalysts and hence their catalytic properties.

Table 7.1 : Free energies of formation of various metal sulphides [a]

Element	Metal Sulphide	ΔG_f (kJ/mol)	
		300 K	600 K
Co	CoS	- 54.0	- 47.7
	Co_2S_3	- 69.8	-
	Co_4S_{3-x}	- 39.3	- 39.8
	Co_9S_8	- 65.3	- 55.3
Cr	CrS	-110	-108
Cu	CuS	- 55.4	- 62.3
	CuS_2	- 44.4	- 60.7
	Cu_2S	- 46.5	- 52.3
Fe	FeS	- 58.2	- 57.3
	FeS_2	- 75.8	-
Mn	MnS	-185	-180
	MnS_2	-116	-128
Zn	ZnS	-168	-152

a : Data computed from reference 181 and 186 and based on the following stoichiometry:

$$(x/y)\ M + H_2S \rightleftharpoons (1/y)\ M_xS_y + H_2$$

Oudar (182) has shown that the enthalpy of adsorption

of sulphur-containing compounds onto most catalytically active metals (i.e Ni, Cu, Fe, Cr and Pt) is directly related to the enthalpy of bulk sulphide formation. At a 50 % adsorption layer, he concluded that the enthalpy of formation for a surface sulphide species is between 20 and 40 % higher than the enthalpy of formation for the most stable bulk sulphide. Evidence was thereby presented that sulphur poisoning should not just be considered to modify the bulk characteristics of a catalyst, but that it also alters the surface structure significantly.

The effect of strong sulphur adsorption on metal catalysts are far reaching, particularly if one considers that sulphur-containing molecules (i.e. H_2S) have been known to adsorb dissociatively onto a copper surface (187). The build-up of metal sulphides not only prevents the adsorption of reagent molecules, but can also markedly affect the selectivity of reactions. A typical example of an extreme case of catalyst poisoning by sulphur exists in the Fischer-Tropsch process. There, a fused iron catalyst has been found to loose about three orders of magnitude specific activity when ppb levels of sulphur impurities had been present in the feed stream (181). Furthermore, evidence in the open literature was presented that sulphur containing feed gases brought about an increase

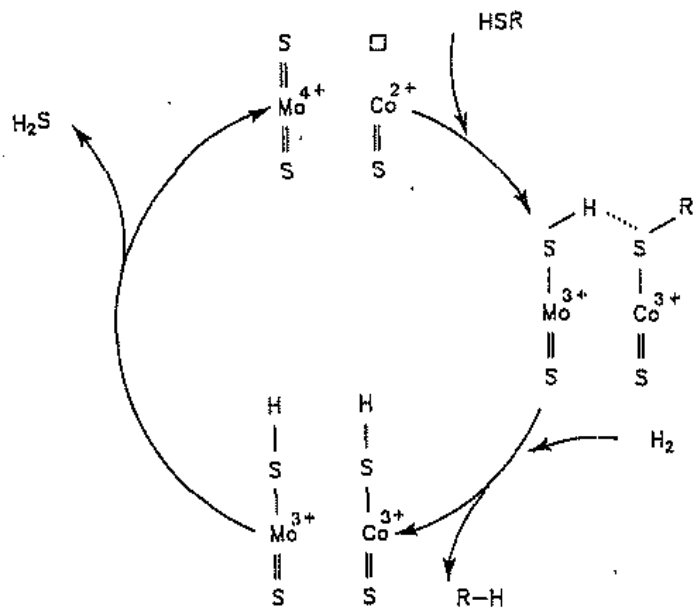
in the yield of liquid hydrocarbons and a decrease of gaseous hydrocarbons when CO and H_2 were fed over a Co/ThO_2/kieselguhr catalyst.

Another type of catalyst, which is prone to sulphur poisoning is the nickel-containing methanation catalyst, which has been reported to seriously deactivate when the sulphur content in the feed gases exceeded about 0.1 % (188).

However, sulphur must not always be considered as a catalyst poison. There are certain catalysts which depend on high sulphur levels to remain active. These are the so-called "CoMox" catalysts which are mainly used for hydrodesulphurisation (HDS) processes (189-193); but have also been known to catalyse the water-gas shift reaction (section 1.4.3) In spite of the great commercial significance of these catalysts, little is understood regarding their activity in terms of mechanistic features. Different mechanistic models have been suggested to explain the catalyst's hydrodesulphurisation activity (194,195) but no such information is available to explain its water-gas shift activity. Topsoe et.al. (195) give a good insight of how the interaction between the catalytic structure of a sulphided CoMox catalyst accounts for its desulphurisation activity. From their proposed reaction

sequence (shown in Figure 7.2), one can see that sulphur forms part of the catalyst's active structure. Even though the Co and Mo have to change oxidation states twice in order to complete the reaction cycle, their role as a sulphur support is also vital to the catalyst's activity. Thus, the presence of sulphur containing compounds would not poison this type of catalyst, but rather keep it active.

Figure 7.2 : Hydrodesulphurisation reaction sequence over a CoMox catalyst proposed by Topsoe et. al. (195)



where □ = vacant anion site

From the discussion presented in this section, it can be seen that sulphur compounds must not always be regarded as deactivating agents, but that they can also act as building blocks to ensure the catalytic activity of certain materials. However, no theoretical method exists for the prediction of whether sulphur will poison or promote a certain reaction over catalytically active material. Thus, the only means of obtaining such information is by experimentation, which involves the feeding of gases containing a known quantity of sulphur into a controlled reaction environment. The effect of this modified feed gas on the catalytic performance can then be monitored and the results can then be compared to those done with pure feed gas.

7.2 Experimental

Desulphurised feed gases for the water-gas shift reactor of a coal-based ammonia plant were obtained from AECI Ltd., Modderfontein, South Africa and spiked with a known quantity of H_2S. The overall composition of the gas is shown in Table 7.1.

The following catalysts were tested for water-gas shift activity :

1 - Co/MnO : Co : Mn = 3:1

2 - $CoCr_2O_4$: Co : Cr = 3:1

3 - Cu/MnO : Cu : Mn = 1:3

All catalysts investigated were prepared, pretreated and tested in the manner described in chapter 2.

Table 7.1 : Composition of sulphur containing feed gas

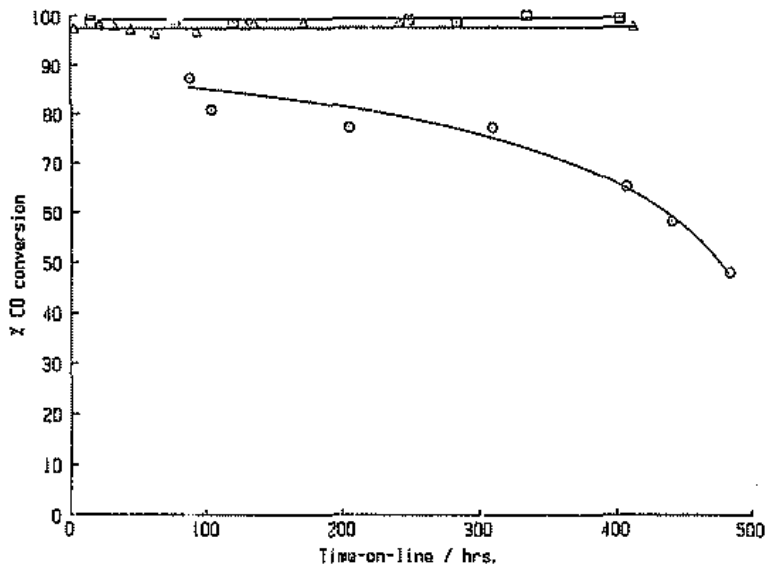
Component	% (mol)	
	Cylinder 1	Cylinder 2
H_2	30.6	31.5
N_2	4.2	3.8
CO	56.8	57.9
CO_2	8.4	6.7
Total sulphur (H_2S +COS)	0.00011	0.024

7.3 Results

From the results shown in Figures 7.3 (carried out using Cylinder 1) and 7.4 (carried out using Cylinder 2), it can be seen that both the Co/MnO and the $CoCr_2O_4$ catalysts not only displayed high water-gas shift activity under these conditions, but they also maintained this activity over an extended period of time. These observations suggest that both catalysts do not appear to be poisoned by the sulphur containing components present in the feed gas. X-ray diffraction analysis of the bulk structure of both catalysts showed

that no detectable changes in the individual phases present in each of the catalysts as compared to the sulphur-free laboratory gas studies (section 3.3.1 and section 5.2.2) were observed.

Figure 7.3 : Stability studies of various catalysts using coal derived feed gas containing 1 ppm sulphur[a]

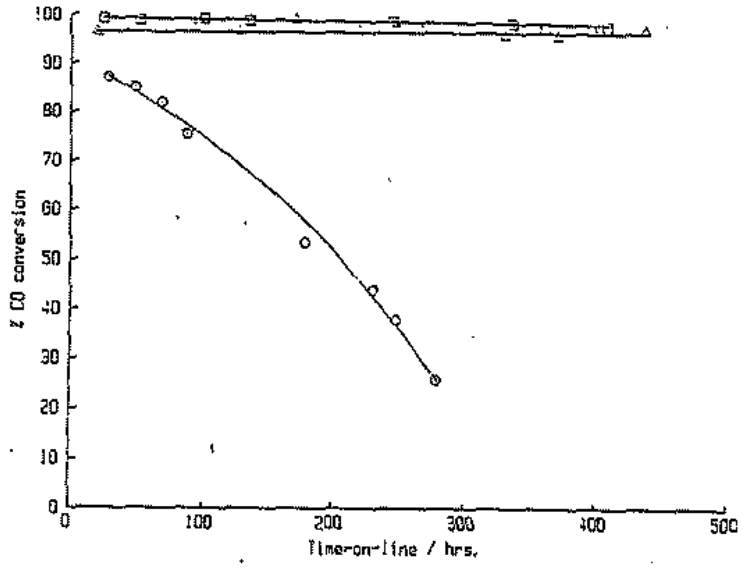


△ = Co : Mn = 3:1 ; ⊡ = Co : Cr = 3:1 ;

⊙ = Cu : Mn = 1:3

a : all catalysts were tested at CO GHSV = 510 h^{-1}, Temperature = 350°C for the Co/MnO and $CoCr_2O_4$ catalyst and 400°C for the Cu/MnO catalyst, CO : H_2O = 1:4.5

Figure 7.4 : Stability studies of various catalysts using coal derived feed gas containing 240 ppm sulphur[a]



△ = Co : Mn = 3:1 ; ⊡ = Co : Cr = 3:1 ;

⊙ = Cu : Mn = 1:3

a : all catalysts were tested at the same conditions shown in Figure 7.3

7.4 Discussion

7.4.1 The Co/Mn oxide and Co/Cr oxide catalyst systems

From the figures presented in Table 7.1, it can be seen that large differences exist among the various metal

sulphides in terms of their thermodynamic stabilities. For example, metals such as Co or Fe have a significantly lower free energy of formation for their various bulk sulphides as compared to metals such as Cr or Mn, which have much higher free energies of formation of their bulk sulphides. Thus, it was suggested that sulphur poisoning over Co- or Fe-containing catalysts could be reduced by combining these metals with other metals such as Cr or Mn. As the formation of Cr or Mn sulphides would thus be thermodynamically more favourable, cobalt would not preferentially sulphide, assuming negligible kinetic control (181). This "protection mechanism", thus allows the Co-containing catalysts to remain active for the desired water-gas shift reaction. This theory, which has been discussed in the literature (196), would thus explain the experimental results shown in Figures 7.3 and 7.4 for the Co/MnO and the $CoCr_2O_4$ catalysts.

7.4.2 The Cu/Mn oxide catalyst system

The conversion of sulphur-containing feed gases by means of the water-gas shift reaction over a Cu/MnO catalyst, led to severe catalyst deactivation at both

sulphur levels (Figures 7.3 and 7.4). This observation suggests that the Mn part of the catalysts did not provide protection from sulphur poisons, even though MnS is more stable than Cu_2S (ΔG^{o} = -185 kJ/mol for MnS and ΔG^{o} = -55.4 kJ/mol for CuS). It can therefore be concluded that the thermodynamic information provided failed to rationalise the experimental observations. However, as catalytic reactions primarily occur on the surface, one should look at explaining the experimental data by analysing the events that occurred on the surface of the Cu/MnO catalyst during the sulphur poisoning experiments.

In section 7.3.1 it was shown that the formation of MnS from H_2S was thermodynamically more favourable than the formation of CuS and should thereby provide a protective mechanism to sulphur poisoning. Yet, in contrast to the Co/MnO catalyst, the Cu/MnO catalyst tested was found to deactivate after prolonged sulphur exposure (Figures 7.3 and 7.4). However, a distinct difference in the magnitude of the surface areas of the Co/MnO and the Cu/MnO catalysts was found after these catalysts had been exposed to the sulphur containing feed gases. These surface area results are presented in Table 7.2.

Table 7.2 : Surface area determined by the BET method for the various manganese oxide catalysts after sulphur exposure experiments[a]

Sulphur content / ppm	Surface area / m^2g^{-1}	
	Co/MnO catalyst	Cu/MnO catalyst
0	64.0	10.1
1.1	30.8	3.7
240	25.7	2.1

a : Surface areas were determined after the catalysts had been on-line for ca. 600 hours

Now, combining both the thermodynamic results and the surface area observations, the sulphur poisoning process for a Cu/MnO catalyst can be envisaged as follows :-

Firstly, the MnO component of the catalyst allows the catalyst to absorb sulphur, by the thermodynamically favourable reaction to form manganese sulphides and H_2O.

eg. $H_2S + MnO \rightleftharpoons MnS + H_2O$.

$\Delta G = -185\ kJmol^{-1}$

This reaction step takes place on the surface of the MnO crystals. However, the large sulphide anions can geometrically block the passage of reagent gas (eg. CO or H_2O) to the remaining active Cu centres in the structure of the catalyst. The observed distinct loss in surface area (Table 7.2) upon sulphur exposure to the Cu/MnO catalyst confirms that the pore structure of this catalyst had been adversely affected by the S-containing molecules.

Thus, the Cu/MnO catalyst can be considered to have been poisoned primarily by the geometric blocking of the active sites by adsorbed sulphur, which resulted in the thermodynamically favoured formation of manganese sulphide. Support for such a sulphur poisoning mechanism can also be found in the literature (5, 181)

7.5 Summary

Sulphur poisoning studies were carried out over the $CoCr_2O_4$, Co/MnO and the Cu/MnO catalysts by feeding gases containing different levels of sulphur (1 ppm and 240 ppm). The results obtained indicated that only the Cu/MnO catalyst was found to deactivate after prolonged exposure of either of the sulphur containing feed

gases. It was found that the formation of manganese sulphides and chromium sulphides were thermodynamically more favourable than the formation of either copper sulphides or cobalt sulphides. Thus the manganese and the chromium catalyst supports were protecting the active components of the catalyst from deactivation. The fact that the Cu/MnO catalyst was nevertheless found to deactivate even after low level sulphur exposure, was believed to have been due to the geometric blocking of the active Cu sites by the manganese sulphide product. A distinct loss of the catalyst's surface area after exposure to the sulphur-containing gases and similar observat.ons and results reported by other researchers were found to support this theory.

8. CONCLUSION

This Thesis has endeavoured to cover several important aspects water-gas shift catalysis. In Chapter 1, a historical overview of the development of various water-gas shift reaction catalysts and their mechanistic and kinetic workings was presented. Furthermore, the need to develop a novel stable and sulphur tolerant high activity water-gas shift catalyst was identified. Theoretical and practical developments for the identification, preparation and characterisation of such catalyst systems were described in Chapter 2.

These developments led to the identification of three novel high activity water-gas shift catalyst systems (i.e. i) Co/MnO ; ii) Cu/MnO ; iii) $CoCr_2O_4$). Optimisation studies for the Co/MnO catalyst system (which were presented in Chapter 3) indicated that a 1 % (m/m) Co/MnO catalyst with a Co:Mn ratio of 3:1 exhibited its highest CO conversion activity with minimum CH_4 by-product formation at 350°C. Furthermore, experimental data was presented in Chapter 3 to show that the water-gas shift reaction and the CO hydrogenation reaction, to produce C^{2+} products, did not proceed simultaneously over this catalyst system.

A comparison of other manganese oxide containing water-gas shift catalysts, was presented in Chapter 4 and revealed the following specific (i.e. corrected for surface area) reactivity pattern :

$$Cu/MnO > Co/MnO >> Fe/MnO$$

In contrast to the Co/MnO catalyst system, Cu/MnO was found to display the highest water-gas shift activity at low Cu loadings (i.e. Cu:Mn = 1:3). Although, the Cu/MnO catalysts had the highest specific activities of all the MnO containing catalysts tested, they nevertheless lost their catalytic activity when operated continuously at their optimum operating temperature of 400°C.

A third novel high activity water-gas shift catalyst system was also identified in the form of $CoCr_2O_4$. This catalyst was found to give an optimum CO conversion activity at high temperatures (350-400°C) and high cobalt loadings (Co:Cr = 3:1). However, it was also found that the $CoCr_2O_4$ formulations tested produced significant levels of CH_4 by-product which was believed to have formed on the non-metallic Co sites.

In order to obtain a better understanding of the events occurring on the catalysts' surfaces, both kinetic and mechanistic model reagent studies lead to the

derivation of mathematical rate laws as well as the proposal of mechanistic reaction cycles (Chapter 6). Based on the results obtained for the model reagent studies, the water-gas shift reaction was found to proceed via the formation of various surface formate intermediates for all three catalyst systems studied. However, the kinetic results obtained for the Co/MnO and the $CoCr_2O_4$ catalysts showed that the reaction could also proceed via a regenerative "Temkin" type mechanism at a high partial pressure of CO.

Finally, sulphur poisoning experiments clearly indicated that, with the exception of the Cu/MnO catalyst system, all the novel high activity catalysts developed were found to be sulphur tolerant under water-gas shift reaction conditions and sulphur levels up to 220 ppm. Hence the work presented in this Thesis has laid the foundations to further industrial scale developments in the field of substitute high activity water-gas shift shift catalysts, which can also be operated in a plant utilising coal-derived synthesis gas.

REFERENCES

1) G.C. Bond , Heterogeneous Catalysis , 2nd. Ed. Clarendon Press , Oxford , (1987)

2) C.L. Thomas , Catalytic Processes and Proven Catalysts , Academic Press , New York , (1970)

3) H.S. Taylor , Industrial Hydrogen , The Chemical Catalog Company , (1921)

4) Reed , British Patent 3776 , (1885)
Mond and Langer , British Patent 12608 , (1888)

5) P.N. Hawker , Hydrocarbon Process., Int. Ed. , 61 , 183 , (1982)

6) S. Strelzoff , Technology and Manufacture of Ammonia , 177-192 , John Wiley and Sons , New York (1981)

7) D.S. Newsome , Catal. Rev. - Sci. Eng. , 21 , 275 , (1980)

8) D.C. Grenoble, M.M. Estadt, and D.F. Ollis, J. Catal. , 67 , 90 , (1981)

9) F. Ono and T. Toshihiro , Japanese Patent 62,148,593 ; (1987)

10) A. Warshaw , J.S. Negra and J.F. Tourtlellotte U.S. Patent 3,956,189 , (1976)

11) A. Nishino , H. Kumano and K. Sonetaka , Japanese Patent 18,786 , (1974)

12) P. Escaffre, A.Thorez and P. Kalck, J. Mol. Catal., 33 , 87 , (1985)

13) J.M. Moe , Am. Chem. Soc. , Div. Pet. Chem. Prepr., 8 , B29 , (1963)

14) P.W. Sherwood , Petroleum (London) , 24 , 338 , (1961)

15) M.I. Markina , G.K. Boreskov , F.P. Ivanovskii and B.G. Ludkovskaya , Kinet. Katal. , 2 , 867 , (1961)

16) C.P.P. Singh and D.N. Saraf , Ind. Eng. Chem. , Process Des. Dev. , 16 , 313 , (1977).

17) M.A. Vannice , J. Catal. , 37 , 449 , (1975)

18) J.C. Gonzalez , M.A. Gonzalez , M.A. Laborde and N. Moreno , Appl. Catal. , 2 , 3 , (1986)

19) H. Bohlbro and M.H. Jorgensen , Chem. Eng. World , 5 , 46 , (1970)

20) M.D. Newton , AECI Ltd. , Personal Communications , (1986)

21) P. Mars , Chem. Eng. Sci. , 14 , 375 , (1961)

22) J. Haber and N. Denisyk , Angew. Chem. , 51 , 507 , (1939)

23) S. Ahmad and P. Sen , Chem. Age India , 34 , 459 , (1983)

24) G.C. Chinchen , R.A. Logan and M.S. Spencer , Appl. Catal. , 12 , 89 , (1984)

25) R.P. Prokopowicz , P.L. Silvestri , R.R. Hudgins and D.E. Irish , React. Kinet. Catal. Lett. , 37 , 63 , (1988)

26) G.C. Chinchen , P.J. Denny , J.R. Jennings , M.S. Spencer and K.C. Waugh , Appl. Catal. , 36 , 1 , (1988)

27) M. Bowker , R.A. Hadden , H. Houghton , J.N.K. Hyland and K.C. Waugh , J. Catal. , 109 , 263 (1988)

28) S. De Rossi , G. Ferraris and R. Mancini , Appl. Catal. , 38 , 359 , (1988)

29) H. Uchida , N. Isogai , M. Oba and T. Hasegawa , Bull. Chem. Soc. Jpn. , 40 , 1981 , (1967)

30) F. Garbasri and G. Petrini , J. Catal. , 90 , 106 , (1984)

31) G. Petrini , F. Montino , A. Bossi and F. Garbassi in Preparation of Catalysts , 3 , by G. Poncelet Elsevier Science Publishers , Amsterdam , (1983)

32) J.S. Campbell , Ind. Eng. Chem. , Process Des. Develop. , 9 , 588 , (1970)

33) H. Uchida , M. Oba , N. Isogai and T. Hasegawa , Bull. Chem. Soc. Jpn. , 41 , 479 , (1968)

34) D. Kitchen , Low temperature shift catalyst developments and related process effects , presented at Nitrogen'88 , (1988)

35) J.J. Carberry , J. Catal. , 107 , 248 , (1987)

36) D.B. Dadyburjor , Stud. Surf. Sci. Catal. , 34 , 21 , (1987)

37) J. Dewing and D.S. Davis Adv. Catal. , 24 , 221 , (1975)

38) F.E. Massoth , Adv. Catal. , 27 , 265 , (1978)

39) F. Casbas , D. Du Prez and J. Olliver , Appl. Catal. , 50 , 87 , (1989)

40) A.W. Sleight , Science , 208 , 895 , (1980)

41) P. Hou , D. Meeker and H. Wise , J. Catal. , 80 , 280 , (1983)

42) K.S. Chung and F.E. Massoth , J. Catal. , 64 , 332, (1980)

43) I. Wender , H.W. Sternberg and M. Orchin in Catalysis , 5 , by P.H. Emmett , Rheinhold Publishing Corporation , (1958)

44) J.W. Reppe and E. Reindl , Liebigs Ann. Chem. , 582 , 120 , (1953)

25×

45) R.M. Laine and R.B. Wilson in Aspects of Homogeneous Catalysis , 5 , by R. Ugo , (1985)

46) R. Eisenberg , C.H. Cheng and D.E. Hendriksen , J. Am. Chem. Soc. , 99 , 2791 , (1977)

47) H.C. Kang , C.H. Mauldon , T. Cole , W. Slegeir , K. Cann and R. Petit , J. Am. Chem. Soc. , 99 , 8323 , (1977)

48) R.M. Laine, R.G. Rinker and P.C. Ford , J. Am. Chem. Soc. , 99 , 2791 , (1977)

49) C.H. Cheng and R. Eisenberg , J. Am. Chem. Soc. , 100 , 5968 , (1978)

50) T. Yoshida , Y. Veda and S. Otsuka , J. Am. Chem. Soc. , 100 , (1978)

51) P. Grannoccaro , G. Vasapollo and A. Sacco , J. Am. Chem. Soc. , Chem. Commun. , 1136 , (1980)

52) J.W. Moore and R.G. Pearson in Kinetics and Mechanism , 3rd. Ed. , John Wiley and Sons , New York , (1981)

53) F. Basolo and R.G. Pearson in Mechanisms of Inorganic Reactions" , 2nd. Ed. , John Wiley and Sons , New York , (1958)

54) M.I. Temkin , Adv. Catal. , 28 , 263 , (1979)

55) P.C. Ford , Acc. Chem. Res. , 14 , 31 , (1981)

56) T. Salmi , S. Bostroem and L.-E. Lindfors , J. Catal. , 112 , 345 , (1988)

57) T. Salmi , S. Bostroem and L.-E. Lindfors , Chem. Eng. Sci. , 41 , 929 , (1986)

58) T. Salmi and R. Hakkarainen , Appl. Catal. , 49 , 285 , (1989)

59) M.I. Temkin and N.V. Kul'kova , Zh. Fiz. Chim. , 23 , 695 , (1949)

60) G.K. Boreskov , T.M. Yur'eva and A.S. Sergeeva , Kinet. Katal. , 11 , 1476 , (1970)

61) T. van Herwijnen and W.A. de Jong , J. Catal. , 63 , 83 , (1980)

62) T.M. Yur'eva , G.K. Boreskov and V. Sh. Gruver , Kinet. Katal. , 10 , 862 , (1969)

63) M.A. Vannice , J. Catal. , 50 , 228 , (1977)

64) E.F. Armstrong and T.P. Hilditch , Proc. Roy. Soc. Ser. , A97 , 265 , (1920)

65) Y. Amenomiya and G. Pleitzer , J. Catal. , 76 , 345 , (1982)

66) D. Shopov and A. Andreev , Kinet. Katal. , 28 , 152 , (1987)

67) K. Tamaru , Trans. Faraday Soc. , 63 , 3081 , (1967)

68) P.C. Ford , Prepr.-Am. Chem. Soc. , Div. Pet. Chem. 29 , 567 , (1984)

69) D.C. Elliot , R.T. Hallen and L.J. Sealock jr. , Ind. Eng. Chem. , Prod. Res. Dev. , 22 , 431 , (1983) An Investigation on the Kinetics of

70) H. Bohlbro , An Investigation on the Kinetics of the Conversion of Carbon Monoxide with Water Vapour over Iron Oxide Based Catalysts , 2nd. Ed. , Gjellerup , Copenhagen , (1969)

71) R.N. Sahay , K. Prasad , S. Ahmed and N.B. Bhattacharyya , Fertilizer Technology , 20 , 78 , (1983)

72) M.I. Temkin , N.M. Morozov and G.G. Shibrya , Kinet. Katal. , 6 , 1057 , (1965)

73) G.C. Chinchen , R.H. Logan and M.S. Spencer , Appl. Catal. , 12 , 97 , (1984)

74) R.G. Copperthwaite , G.J. Hutchings and M. van der Riet , S. Afr. J. Sci. , 82 , 596 , (1986)

75) J.W. Geus , Stud. Surf. Sci. Catal. , 16 , 1 , (1983)

76) G.J. Hutzler in Encyclepedia of Chemical Technology 2nd Ed. , 4 , 534-586 , by R.E. Kirk and D.F. Othmer , John Wiley and Sons , New York , (1964)

77) Y.J.R. Huang , The effect of catalyst preparation on catalytic activity , from Diss. Abstr. Int. B , 49 , 2285 , (1989)

78) G.C. Bond and P.A. Sermon , New Methods of Catalyst Preparation , Elsevier Scientific Publishers , Amsterdam , (1988)

79) M. van der Riet , G.J. Hutchings and R.G. Copperthwaite , J. Chem. Soc. Chem. Commun. , 798 , (1986)

80) M. van der Riet , R.G. Copperthwaite , G.J. Hutchings and J.R. Woodhouse , Ind. Eng. Chem. Res. , 26 , 869 , (1987)

81) M. van der Riet , PhD Thesis , University of the Witwatersrand , (1988)

82) K. Klier, R.G. Herman, G.W. Simmons, B.P. Finn and J.B. Bulko , J. Catal. , 56 , 407 , (1979)

83) N. Ray, S.K. Nath, B. Yadava, A.R.N. Sahay and P. Sen , Fert. Technol. , 20 , 35 , (1983)

84) N. Singh, B. Yadava and J.S. Tiwari , Fert. Technol. , 19 , 39 , (1982)

85) C.J. Korf and R. Espinoza , CSIR (CERG) Report , CSIR , Pretoria , South Africa , 584 , (1982)

86) W.A. Dietz , J. of Gas Chromatogr. , 68 (1967)

87) R.L. Varma , L. Dan-Chu , J.F. Mathews and N.N. Bakhshi , Can. J. Chem. Eng. , 63 , 72 , (1985)

88) J.S. Negra , British Patent 1,318,477 , (1973)

89) J.S. Negra , U.S. Patent 3,740,349 , (1973)

90) A.S Ivanova , V.A. Dzis'ko , E.M. Moroz and S.P Noskova , Kinet. Katal. , 27 , 428 , (1986)

91) M. Kantschewa , F. Delannay , H. Jeziorowski , D. Delgado , S. Eder , G. Ertl and H. Knoezinger , J. Catal. , 87 , 482 , (1984)

92) K. Klier , Chyl-Woel Young , and J.G. Nuan , Ind. Chem. Eng. Fundam. , 25 , 36 , (1986)

93) K. Klier , Appl. Surf. Sci. , 19 , 267 , (1984)

94) A.K. Brewer , J. Am. Chem. Soc. , 53 , 74 , (1931)

95) A.V. Kryhru , L.O Kuznetsov and I.N. Konguklwvu , Kinet. Katal. , 5 , 948 , (1964)

96) H. Kobel and N.K.H. Muller , Ber Bunsenger Phys. Chem. , 67 , 212 , (1963)

97) F.A. Cotton and G. Wilkinson , Advanced Inorganic Chemistry , 5th Ed. , 58-60 , John Wiley & Sons , New York , (1988)

98) G. Blyholder , J. Phys. Chem. , 79 , 756 , (1975)

99) G. Doyen and G. Ertl , Surf. Sci. , 43 , 197 , (1974)

100) L.S. Cederbaum , W. Domcke , W. von Niessen and W. Brenig , Z. Phys. , B21 , 381 , (1975)

101) L. Lloyd and M.V. Twigg , Nitrogen , 118 , 30 , (1979)

102) V. Ponec and Z.J. Knor , J. Catal. , 10 , 73 , (1968)

103) J.E. Crowell , E.L. Garfunkel and G.A. Somorjai Surf. Sci. , 303 , (1982)

104) M.E. Dry , T. Shingles , L.T. Boshoff and G.J. Oosthuizen , J. Catal. , 15 , 190 , (1969)

105) L.I. Kuznetsova , A.R. Suzdorf , I.V. Usmanova , G.A. Moiseeva and V.G. Chumakov , Kinet. Katal. , 29 , 491 , (1988)

106) W.D Deckwer and Y. Serpemen , Ind. Eng. Chem. Process Res. Dev. , 21 , 222 , (1982)

107) K.M. Kreitman , M. Baerns and J.B. Butt , J. Catal. , 105 , 319 , (1987)

108) S. Ledakowicz , R. Kokuun and W.D Deckwer , Ger. Chem. Eng , 9 , 299 , (1986)

109) U. Lochner , H. Papp and M. Baerns , Appl. Catal. 23 , 339 , (1986)

110) M.E. Dry , T. Shingles and L.J.J. Boshoff , J. Catal. , 25 , 99 , (1972)

111) S.B. Kanungo , J. Catal. , 58 , 419 , (1979)

112) V. Di Castro , C. Furlani , M. Gargano and M. Rossi , Appl. Surf. Sci. , 28 , (1987)

113) V. Dondur , S. Lampa and D. Vucelic , Geterog. Katal. , 4 , 151 , (1979)

114) V. Dondur , S. Lampa and D. Vucel . Chem. Soc. , Faraday Trans 1 , 79 , 163

115) L.I. Gvasaliya and M.A. Kurashivili , Izv. Akad. Nauk. Gruz. SSR , Ser. Khim. , 8 , 211 , (1982)

116) S. B. Kanugo , Proc. Symp. Sci. Catal. Its Appl. Ind. , 476 , (1979)

117) J.M. Thomas and W.J. Thomas, Introduction to Heterogenous Catalysis , Academic Press , London , (1967)

118) M.A. Baltans , A.B. Stiles and J.R. Katzer , Appl. Catal. , 20 , 31 , (1986)

119) G.C. Chinchen , R.M. Logan and M.S. Spencer , Appl. Catal. , 12 , 69 , (1984)

120) C.T. Campbell and K.A. Daube , J. Catal. , 104 , 109 , (1987)

121) J.Gazo , Coord. Chem. Rev. , 18 ,253 , (1976)

122) B.J. Hathaway and D.E.Billig , Coord. Chem. Rev. , 5 ,143 , (1970)

123) F.A. Cotton and G. Wilkinson , Advanced Inorganic Chemistry , 4th Ed. , 811-812 , John Wiley and Sons , New York , (1980)

124) R.C. Weast and M.J. Astle , Handbook of Chemistry and Physics , 62 nd. Ed. , F 175 , CRC Press Inc., Boca Raton, Florida , (1981)

125) A.S. Ivanova , V.A. Dzis'ko , E.M. Moroz and S.P. Noskova , Kinet. Katal. 27 , 428 , (1986)

126) Z.T. Fattakhove , A.A Ukharskii , P.A. Shiyaev and A.D. Berman , Kinet. Katal. , 27 , 884 , (1986)

127) O.N. Kovalenko , P.G. Tsyrul'nikov , V.V. Popovskii , E.M. Moroz and N.N. Boldyreva , Zh. Prikl. Khim. , 57 , 793 , (1984)

128) T.N. Tay'or and W.P. Ellis , Energy Res. , 3 , Abstr. No. 15600 , (1978)

129) B.M. Kadenatsi , K.N. Spiridonov , M.D. Shibanova and M.Ya. Kushnerev , Kinet. Katal. , 19 , 1259 , (1978)

130) C.M. Stander , S. African Patent No. 7,205,654 , (1974)

131) M.P. Senes , M. Pottler and J.F. Gourdier , Ger. Offen. Patent 2,329,962 , (1974)

132) Z.T. Fattakhova , A.D. Berman and B.M. Kadenatsi , Kinet. Katal. , 20 , 651 , (1979)

133) L.A. Kennedy , Energy Res. , 8 , Abstr. No. 45776 (1983)

134) V.N. Vorob'ev , Sh. A. Isandarov , M.F. Abidova and G. Sh. Talipov , Kinet. Katal. , 15 , 1045 , (1974)

135) J.F. Roth , U.S. Patent 3,493,325 , (1970)

136) E. Koberstein and E. Lakatos , Ger. Patent 1,283,247 , (1968)

137) H. Mckinzie , J.E. Lester and F.C. Palilla , U.S. Patent 4,147,763 , (1979)

138) D.P. Rajwar , A.K. Ghosh and Dipak Guha , Adv. Catal. (Proc. Natl. Symp. Catal.) , 7th , 573 , Ed. T. Prasada Rao , S.R. Wiley , New York , (1985)

139) D. Mekhandzhiev , E. Zhecheva , Z.T. Fattakhova and A.D. Berman , Kinet. Katal. , 27 , 889 , (1986)

140) Badische Anilin und Soda Fabrik A.G. , Fr. Demande Patent 2,004,844 , (1969)

141) A.V. Andreev , V. Idakiev , D. Mihajlova and D. Shopov , Appl. Catal. , 22 , 385 , (1986)

142) W.M.H. Sachtler , Proc. 8th Intl. Congr. on Catalysis , Berlin , 151 , Dechema , Weinheim , (1984)

143) O.V. Krylov , Int. Chem. Eng. , 29 , 246 , (1989)

144) B.M. Kadenatsi , K.N. Spiridonov , M.D. Shibanova and D. Mekhandzhiev , Geterog. Katal. , 4 , 379 (1979)

145) F.A. Cotton and G. Wilkinson , Advanced Inorganic Chemistry , 4th Ed. , 720 , John Wiley and Sons , New York , (1980)

146) F.A. Cotton and G. Wilkinson , Advanced Inorganic Chemistry , 4th Ed. , John Wiley and Sons , New York , 723 , (1980)

147) E. Fiolitakis and H. Hofmann , J. Catal. , 80 , 328 , (1983)

148) S.W. Benson , The Foundations of Chemical Kinetics 81-82 , McGraw-Hill Book Company , London , (1960)

149) J.P. Bromberg , Physical Chemistry , 2nd. Ed. , 891 , Allyn and Bacon Inc. , Boston , (1984)

150) W.C. Gardiner , Jr. , Rates and Mechanisms of Chemical Reactions , 46 , W.A. Benjamin Inc. , New York , (1969)

151) G.J. Hutchings , M.V. Hall , F.M. Gottschalk and R. Hunter, J. Chem. Soc. , Faraday Trans. 1 , 83 , 571 , (1987)

152) P.W. Atkins , Physical Chemistry , 934-935 , 2nd Ed. , Oxford University Press , London , (1983)

153) M.M. Taqui Khan , S.B. Halligadi and S. Shukla , Angew. Chem. Int. Ed. Engl. , 27 , 1735 , (1988)

154) I. Langmuir , Trans. Faraday Soc. , 17 , 621 , (1917)

155) K. Denbigh , The Principle of Chemical Equlibrium 4th Ed. , 436-438 , Cambridge University Press , Cambridge , (1981)

156) Everett , Trans. Faraday Soc. , 46 , 942 , (1950)

157) P.W Atkins , Physical Chemistry , 2nd Ed. , 1030-1033 , Oxford University Press , London , (1983)

158) T. van Herwijnen , R.T. Guczalski and W.A. de Jong J. Catal. , 63 , 94 , (1980)

159) B. Beguin , B. Denise and R.P.A. Sneeden , J. Organnomet. Chem. , 208 , C18 , (1981)

160) R.S. Paonessa and W.C. Trogler , J. Am. Chem. Soc. 104 , 3529 , (1982)

161) W.R. Roper and L.J. Wright , J. Organnomet. Chem. 234 , C5 , (1982)

162) J.F. Edwards and G.L. Schrader , J. Catal. , 94 , 175 , (1985)

163) K. Nakamoto , Infra Red and Raman Spectra of Inorganic and Coordination Compounds , 3rd Ed. , John Wiley and Sons , New York , (1978)

164) G. Riednaecker and H. Bremer , Z. Anorg. Allg. Chem. , 272 , 126 , (1953)

165) K. Tamaru , Trans. Faraday Soc. , 55 , 1191 , (1959)

166) G.M. Schwab and A.M. Watson , Trans. Faraday Soc. 60 , 1833 , (1964)

167) H.S. Inglis and D. Taylor , J. Chem. Soc. A , 5248 (1965)

168) F.A. Cotton and G. Wilkinson , Advanced Inorganic Chemistry , 4 th Ed. , 247-252 , John Wiley and Sons , New York , (1980)

169) A. Peltzman , Oil Gas J. , 79 , 103 , (1981)

170) J.C. Amphlett , M.J. Evans , R.F. Mann and R.D. Weir , Can. J. Chem. Eng. , 63 , 605 , (1988)

171) J.C. Amphlett , R.F. Mann and R.D. Weir , Can. J. Chem. Eng. , 66 , 950 , (1988)

172) D.J. Darensbourg and R.A. Kudaroski in Advances in Organnometallic Chemistry , 22 , 129-168 , by F.G.A. Stone and R. West , Academic Press , New York , (1983)

173) D.F. Shriver , ACS Symp. Ser. , 152 , 1 , (1981)

174) N. Grice , S.C. Kao and R. Pettit , J. Am. Chem. Soc. , 101 , 1627 , (1979)

175) M. Catellani and J. Halpern , J. Inorg. Chem. , 19 566 , (1980)

176) J.R. Sweet and W.A.G. Graham , Organnometallics , 1 , 982 , (1982)

177) A.J. Deeming and B.L. Shaw , J. Chem. Soc. A , 443 (1969)

178) G.C. Chinchen , M.S. Spencer , K.C. Waugh and D.A. Whan , J. Chem. Soc., Faraday Trans 1 , 83 , 2193 (1987)

179) J.E. Kubsh and J.A. Dumesic , AIChE J. , 28 , 793 (1982)

180) T. Tsuda , Y. Chujo and T. Saegusa , J. Am. Chem. Soc. , 102 , 431 , (1980)

181) C.H. Bartholomew , P.K. Agrawal and J.R. Katzer , Adv. in Catal. , 31 , 135 , (1982) (check year)

182) J. Oudar , Catal. Rev. - Sci. Eng. , 22 , 171 , (1980)

183) R.J. Madon and H. Shaw , Catal. Rev. - Sci. Eng. , 15 , 69 , (1977)

184) A.D. Engelbrecht and L.J. Partidge , Technol. , 113 , Feb. 9 (1981)

185) M.D. Newton , AECI Ltd. , Personel Communications (1989)

186) M. Kh. Karapet'yants and M.K. Karapet'yants , Handbook of Thermodynamic constants of Inorganic and Organic Compounds , Ann Arbor-Humphrey Science Publishers , London , (1970)

187) J.M. Saleh , Trans. Faraday Soc. , 68 , 1520 , (1972)

188) J.S. Campbell , P. Craven and P.W. Young Catalyst Handbook , Wolfe Scientific Books , London (1970)

180) T. Tsuda , Y. Chujo and T. Saegusa , J. Am. Chem. Soc. , 102 , 431 , (1980)

181) C.H. Bartholomew , P.K. Agrawal and J.R. Katzer , Adv. in Catal. , 31 , 135 , (1982) (check year)

182) J. Oudar , Catal. Rev. - Sci. Eng. , 22 , 171 , (1980)

183) R.J. Madon and H. Shaw , Catal. Rev. - Sci. Eng. , 15 , 69 , (1977)

184) A.D. Engelbrecht and L.J. Partidge , Technol. , 113 , Feb. 9 (1981)

185) M.D. Newton , AECI Ltd. , Personel Communications (1989)

186) M. Kh. Karapet'yants and M.K. Karapet'yants' , Handbook of Thermodynamic constants of Inorganic and Organic Compounds , Ann Arbor-Humphrey Science Publishers , London , (1970)

187) J.M. Saleh , Trans. Faraday Soc. , 68 , 1520 , (1972)

188) J.S. Campbell , P. Craven and P.W. Young Catalyst Handbook , Wolfe Scientific Books , London (1970)

189) K-I Tanaka and T. Okuhara , Catal. Rev. - Sci. Eng. , 15 , 249 , (1977)

190) F. Mauge , A. Vallet , J. Bachelier , J. Duchet and J.C. Lavalley , Catal. Lett. , 2 , 157 , (1989)

191) V.H.J. de Beer and G.C.A. Schuit in Preparation of Catalysts , 343 by B. Delmon , P.A. Jacobs and G. Poncelet , Elsevier Scientific Publishing Company Amsterdam , (1976)

192) S.C. Schuman and H. Shalit , Catal. Rev. , 4 245 , (1970)

193) T. Ohtsuka , Catal. Rev. - Sci. Eng. , 16 , 291 , (1977)

194) R.J.H. Voorhoeve and J.C.M. Stuiver , J. Catal. , 13 , 243 , (1971)

195) H. Topsoe , B.S. Clausen , R. Candia , C. Wivel and S. Morup , J. Catal. , 68 , 433 , (1981)

196) J.T. Richardson , Hydrocarbon Process. , 52 , 91 , (1973)

APPENDIX 1

Co-precipitation method

The methods used were based on the work of van der Riet et. al. (79-81), who prepared various manganese oxide supported catalysts for Fischer-Tropsch synthesis. All work was carried out using the experimental equipment shown in Figure 2.1. Routine experiments were carried out to optimise the parameters (viz. temperature, pH or precipitating agent) used to prepare the various catalyst systems studied. This apparatus was used in such a way that it allowed for the simultaneous precipitation of two metal nitrates. Variations in the ratio of mixing these metal nitrate solutions determined the final active component : support ratio of the catalyst. It was found that for all catalysts prepared a direct correlation between these ratios existed.

The mixed metal nitrate solutions (0.75 M ; Merck Chemicals) were then preheated in the temperature controlled water bath to the required precipitation temperature as detailed in Table 2.1. A peristaltic pump (Gilson Minipuls 2) was used to transfer the solutions of nitrates as well as the precipitating agent to the reaction vessel. The flow rates of both solutions were kept at 5.0 ml/min. It should be noted

at this point that different experimental conditions were used to prepare the various catalysts tested. A detailed breakdown of these conditions can be found in Table 2.1.

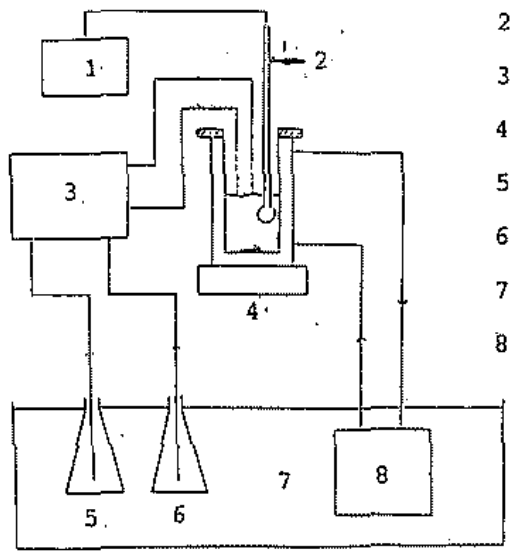
Table 2.1 : Experimental parameters used for the preparation of the various catalyst systems tested

	Catalyst system		
	Co/Mn oxide	Cu/Mn oxide	Co/Cr oxide
Temperature /^{o}C	70	25	70
[Metal nitrate] /mol/l	0.75	0.75	0.75
Precipitating agent	30 % (vol) NH_3	1 M Na_2CO_3	30 % (vol) NH_3
pH	8.30	8.70	9.30

The pH of the solution was continuously monitored (Swiss Lab digital pH meter connected to a Ross Orion sleeveless junction electrode) and maintained to an accuracy of 0.01 pH units during the preparation procedure by manually adding either dilute nitric acid or ammonia solutions. The precipitating solution was constantly stirred magnetically.

Reaction time was about 1 hour and yielded about 5 g of solid material suspended in solution. The solution was then vacuum filtered at the reaction temperature (Whatman No. 31 paper) and washed repeatedly with distilled water to remove any nitrates or carbonates. The co-precipitated material was dried at 110 ^{o}C under vacuum (5 kPa) for 16 hours.

Figure 2.1 : Schematic representation of the experimental set-up used for the co-precipitation method



Key : 1 = pH meter
2 = pH electrode
3 = pump
4 = magnetic stirrer
5 = ammonia solution
6 = metal nitrate solution
7 = water bath
8 = heater / pump

The catalyst material was analysed to determine the metal ratios using atomic absorption spectroscopy (AAS)

(Varian Techtron AA4). This was done by dissolving about 0.100 g of material in boiling aqua regia and diluting it 100 times with distilled water. Calibration curves were then obtained and the concentrations of the various metal components were determined from these curves. Typical results obtained showed that if the metal nitrates of cobalt and manganese were mixed in a 1 : 1 ratio, then the final co-precipitated catalyst as prepared by the method outlined in this section had a cobalt : manganese ratio of 1 : 0.98. Similar results were obtained for the other catalyst systems tested.

APPENDIX 2

Impregnation or "Incipient Wetness" method

This method was used to introduce a small amount (viz. 0.5 - 2. % (m/m)) of a third metal component (eg. potassium, manganese, or vanadium) to the pores of the co-precipitated catalysts. These components were added to a dried catalyst by just wetting it with the minimum volume of a solution containing these promoters. The wetted catalyst was then dried under vacuum (5 kPa), and the third metal component remained in the catalyst's pores.

A typical example of the method followed to introduce potassium to a Co/Mn oxide catalyst will now be given. In order to prepare any other three-component catalyst system, this method was only modified by making the required changes to the amount or nature of the third component to be added.

It was found that 0.612 g of water just wetted 1.000 g of co-precipitated, dried, Co/Mn oxide catalyst. Thus, in order to add 1 % (m/m) of K to 2.000 g of Co/Mn oxide catalyst, 0.141 g of K_2CO_3 were dissolved in 1.224 g of water and this solution was contacted with the Co/Mn oxide catalyst. The wetted catalyst was then dried at 110°C under vacuum (5 kPa) for 16 hours.

All promoted catalysts were prepared according to similar procedures using the following metal salts: $K_2C_$, and $Mn(NO_3)_2 \cdot 4H_2O$.

Again, the use of salts containing sulphur or chlorine was avoided since these elements are potential catalyst poisons.

APPENDIX 3

Catalyst pretreatment

The dried co-precipitated catalytic material, which was produced in powder form, was pressed (20 tons/cm^2) in order to obtain a hard pelleted disc. This disc was broken down and sieved to obtain catalyst particles of the size 0.500 mm - 1.180 mm. These particles were then further treated, based on procedures outlined in the literature (79,82-84).

Table 2.2 : Calcination temperatures[a] during catalyst pretreatments

Catalyst system		
Co/Mn oxide	Co/Cr oxide	Cu/Mn oxide
500°C isothermal for 16 hours	500°C isothermal for 16 hours	increased from 150 to 350°C within 2.5 hours 350°C for 3.0 hours

a: all calcination was carried out in air

The calcination and reduction conditions used for the Co/Mn and Co/Cr oxide catalyst systems were adopted

from work carried out by van der Riet et. al. (79). For the Cu/Mn oxide catalyst system, work done by Klier et. al. (82), Ray et. al. (83) as well as Singh et. al. (84) formed the basis for choosing the relevant calcination and reduction conditions. The exact parameters for the calcination and reduction of the various systems are shown in Tables 2.2 and 2.3 respectively. A lower calcination and reduction temperature was used for the Cu/Mn oxide catalysts as compared to the Co/Mn oxide and the Co/Cr oxide catalysts to prevent sintering during these pretreatment stages.

Table 2.3 : Reduction conditions for the various catalysts tested

	Catalyst system		
	Co/Mn oxide	Co/Cr oxide	Cu/Mn oxide
Gas used	H_2	H_2	2 % (vol) H_2 98 % (vol) N_2
G H S V /h^{-1}	200	200	1000
Temperature /^oC	isothermal 400 for 16 hours	isothermal 400 for 16 hours	from 150 to 250 in 2 hours and then 250 for 16 hours

APPENDIX 4

Stainless steel reactor assembly used for catalyst testing

A schematic representation of the reactor assembly is given in Figure 2.2. This set-up allowed for the simulation of the catalysed water-gas shift reaction on a laboratory bench scale (eg. 2.0 g).

It should be noted that all equipment, except the feed gas and the analysis section was triplicated in order to allow three catalysts to be tested simultaneously. What follows will be a description of the function and operation of one of such reactor units. Using this arrangement, carbon monoxide and nitrogen (>99.9 % purity, supplied by Afrox, South Africa) were fed to the evaporator part of the reactor assembly. Nitrogen was introduced as an inert tracer gas as well as a catalyst coolant as the water-gas shift reaction is an exothermic reaction. Gas flow control, at a manifold pressure of 100 kPa was carried out using Aalborg standard flow meters (0-2 l gas/hour). Water from the reservoir was introduced by means of a peristaltic pump (Gilson Minipuls 2) capable of flow rates as low as 0.60 g/hr. The evaporator was designed and manufactured in the University workshops and a detailed schematic diagram is shown in Figure 2.3.

Figure 2.2 : Stainless steel reactor assembly layout

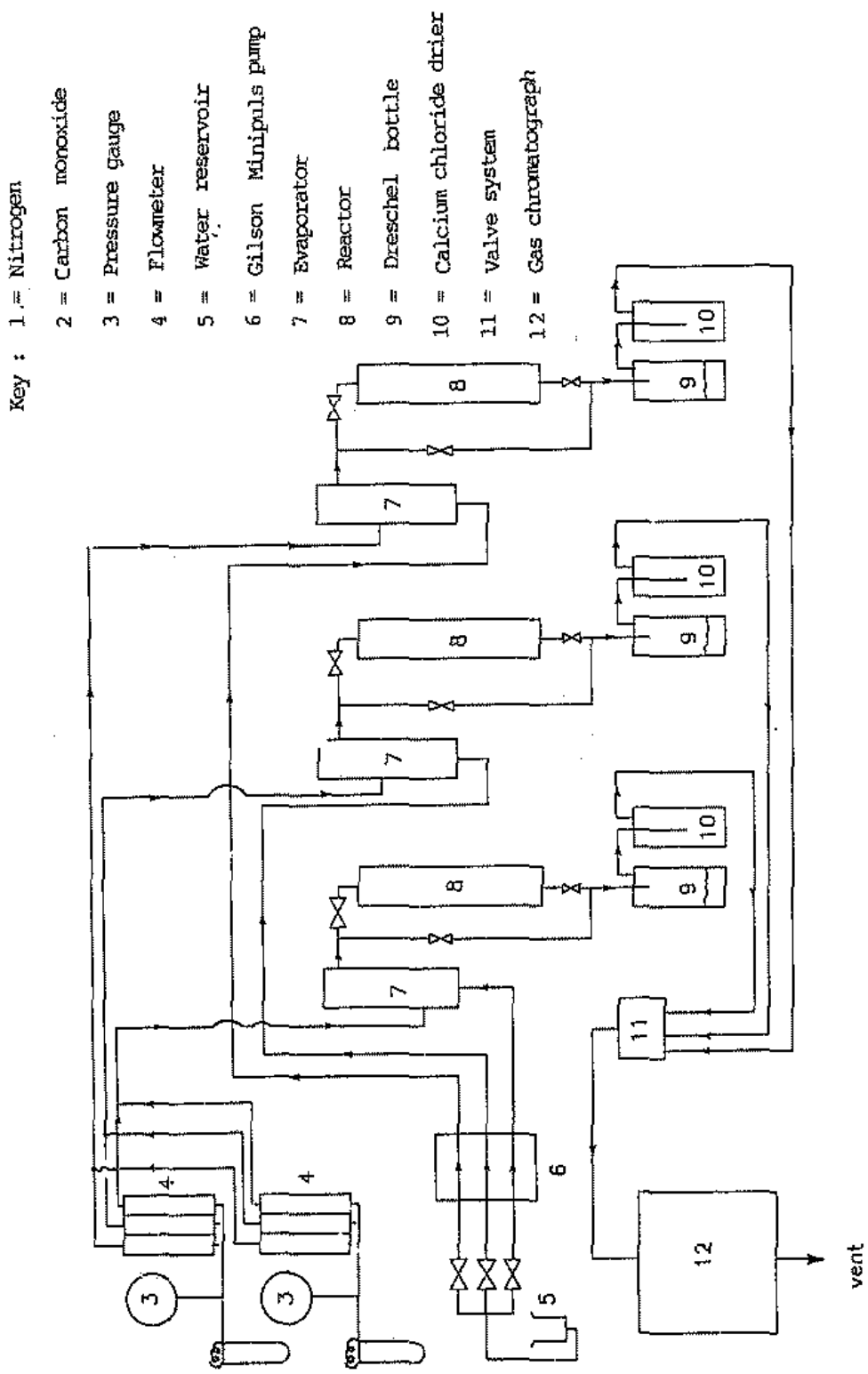
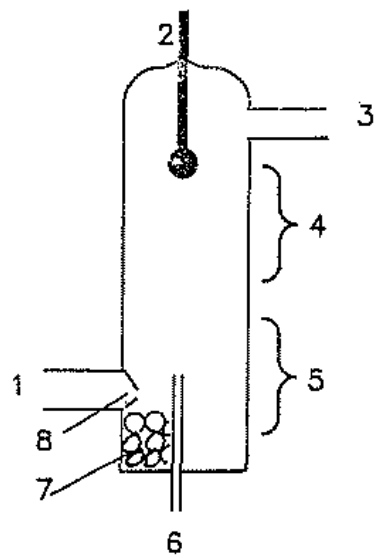


Figure 2.3 : Schematic diagram of evaporator



Key : 1 = 1/4" gas inlet tube
2 = Thermocouple
3 = 1/4" gas outlet tube
4 = Evaporating section
5 = Preheating section
6 = 1/8" H_2O inlet tube
7 = metal beads
8 = 1/16" restriction

The evaporator was heated to 110 ^{o}C using a thermostatically controlled electric heating tape (Electric Elements , South Africa). The temperature of the water, which was introduced to the evaporator via the 1/8" stainless steel tube was first increased in the preheating section and finally converted to steam in the evaporating section. The steam was then homogenised with the nitrogen and carbon monoxide feed gases in the upper mixing section. The final nitrogen, carbon monoxide and steam mixture was then channelled to the 1/4" stainless steel outlet tube. It was found that this evaporator design allowed for the evaporation of water, even at flow rates as high as 10 g H_2O/hr.

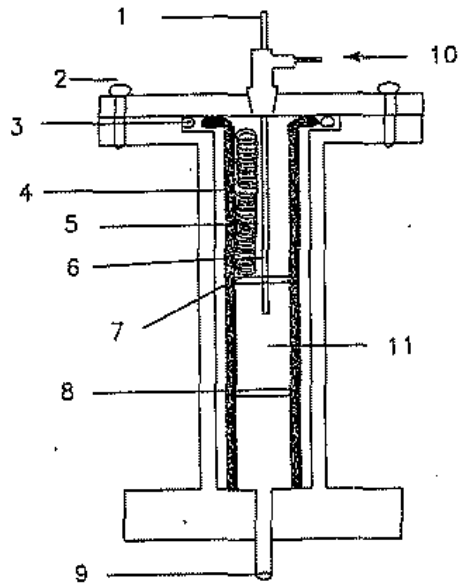
Thus this design was considered satisfactory for the testing of the various catalysts. The outlet line of the evaporator was connected to the inlet of the microreactor and in order to avoid water condensing inside this line it was electrically heated using a rheostat control, which kept the temperature between 150°C and 180°C.

The reactor design was very similar to the one used by van der Riet (81) for his Fischer-Tropsch catalyst studies and was originally based on a design by Karf and Espinoza et. al. (85). A detailed layout of this design is given in Figure 2.4.

The reactor consisted of two main sections:
The first section was the preheater and here the reagent gas temperature was slowly brought up to the catalyst bed temperature. The second part was the catalyst bed, in which about 2.0 g of catalytic material was supported on a metal grid. With the reagent gases entering the reactor at the top and the catalyst supported in the centre of the reactor, it can be said that the reactor design was of a fixed bed down-flow microreactor type and it exhibited plug flow characteristics.

Electric heating tapes, governed by a temperature

Figure 2.4 : Details of reactor design



Key : 1 = Thermocouple
2 = Nut
3 = Stainless steel seal
4 = Reactor insert
5 = Preheating section
6 = Thermocouple holder
7 = Top plate
8 = Bottom plate
9 = Reactor outlet
10 = Reactor inlet
11 = Catalyst bed

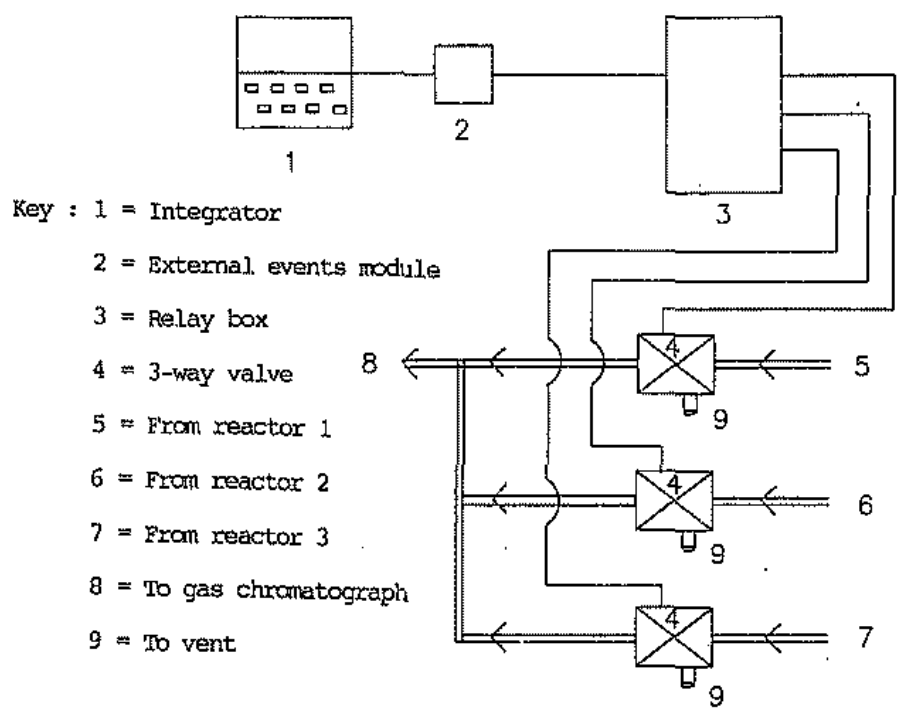
controller (RKC Instruments), allowed for an accurate temperature control of +/- 1.0°C. The controller monitored the catalyst temperature by means of a thermocouple with an iron/copper-nickel junction (type J). This thermocouple was fitted into a well, which extended into the centre of the catalyst bed.

A dual-trap system removed any unreacted water from the product gas mixture before analysis. This was found necessary as water could have damaged the gas chromatographic columns used to carry out the product

identification. The trap system consisted of two 500 ml Dreschel bottles which were kept at room temperature. The unreacted water was condensed in the first trap and the complete water removal was achieved in the second trap, which contained anhydrous calcium chloride drying agent.

A computer controlled valve system selected the individual product streams, which were analysed. This system used 1/8" brass ASCO on/off valves which could be individually switched on and off through the controls on the Spectraphysics SP 4290 integrator, via an external events module. A schematic representation of this operation is given in Figure 2.5.

Figure 2.5 : *Valve system used to select individual product streams*



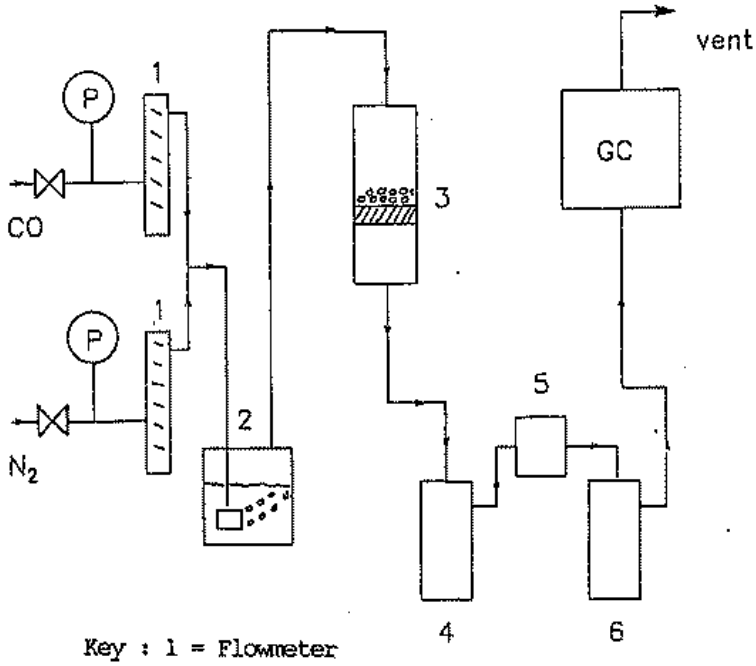
Key : 1 = Integrator
2 = External events module
3 = Relay box
4 = 3-way valve
5 = From reactor 1
6 = From reactor 2
7 = From reactor 3
8 = To gas chromatograph
9 = To vent

Appendix 5

Glass reactor assembly for the mechanistic co-feeding experiments

The basic reactor design of this apparatus was essentially the same as the one described in Appendix 4. Figure 2.6 gives an overall layout of the individual components used for this reactor assembly.

Figure 2.6 : Glass reactor used for mechanistic studies



Key : 1 = Flowmeter

2 = Evaporator containing organic liquid

3 = Reactor

4 = Trap 1 ($0^{o}C$)

5 = Gas sample point

6 = Trap 2 ($-30^{o}C$)

The manifold section used for the introduction of the feed gases was identical to the one employed in the stainless steel reactor assembly. However, instead of introducing water to the system, organic liquids, required for the mechanistic experiments (eg. methanol, and formic acid) were co-fed. These liquids were introduced by means of a bubbler system, in which a controlled flow of feed gases (eg. nitrogen or carbon monoxide) were passed through a Dreschel bottle containing the liquid. To further control the amount of liquids to be evaporated, the Dreschel bottle was electrically heated, by means of a temperature controller similar to that described in Appendix 4.

The cylindrical reactor (400mm long ; 15mm inner diameter) was made from quartz glass, containing a porous sintered disk in the centre to support the catalyst particles. Temperature control was again carried out by means of a thermostatically controlled heating tape, which had been wrapped around the reactor.

The trap system was slightly modified, to allow for the complete removal of any organic components. The liquids produced during the course of the reactions were condensed in a two stage trap consisting of Dreschel bottles. The first trap was kept at room temperature

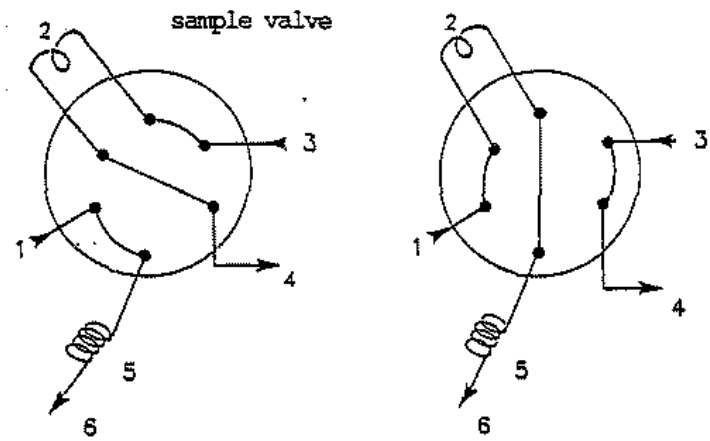
and the second trap was cooled down to -30°C, using a liquid nitrogen/ acetone mixture. On-line gas chromatographic analysis was used to identify the inorganic products. The organic fraction was analysed using off-line gas chromatography. Gas samples were taken after the first trap and analysed by the techniques described in Appendix 6.

Appendix 6

Product analysis

A pneumatically operated six port sample valve (Valco, Switzerland), containing a 2.0 ml sample loop was used to inject the various gas samples into the on-line gas chromatograph. A diagram of the valve's operation is given in Figure 2.7.

Figure 2.7 : Pneumatically operated gas chromatographic sample valve



sample position inject position

Key : 1 = GC carrier gas 4 = Vent
2 = Sample loop (1.0 ml) 5 = GC column
3 = From reactor 6 = To detector

The valve was switched by commands sent from the Spectra-Physics 4290 integrator. This set-up allowed

for programmable gas sample injection into the on-line Hewlett Packard 5730A gas-solid chromatograph, which contained a 3 m X 1/8" Carbosphere column (Alltech Associates, 60-80 mesh). This column was found to separate H_2, N_2, CO, CH_4 and CO_2 very well. It should be noted that the separation of N_2 and O_2 could not be achieved with this column. However, a separate off-line analysis, using a molecular sieve column confirmed that the O_2 levels were less than 0.001 % for all work carried out. The carbosphere column was operated isothermally at 60°C using argon as a carrier gas (20 ml/min) and utilising a thermal conductivity detector (TCD). The detector output was connected to an electronic integration system (Spectraphysics SP 4290), which allowed for accurate and reproducible data collection.

Hydrocarbon and organic oxygenate analysis (C_1-C_7) was carried out using an off-line Pye Unicam 204 temperature programmable gas chromatograph, containing a 2 m X 1/8" Porapak Q column (Waters Associates Inc., 80-100 mesh), using nitrogen as a carrier gas (20 ml/min) and a flame ionisation detector (FID) unit. A similar gas sample valve as for the on-line unit was used to introduce the gas mixtures to be analysed, but the valve was manually operated. Liquid samples were injected with a microsyringe into a preheated injector

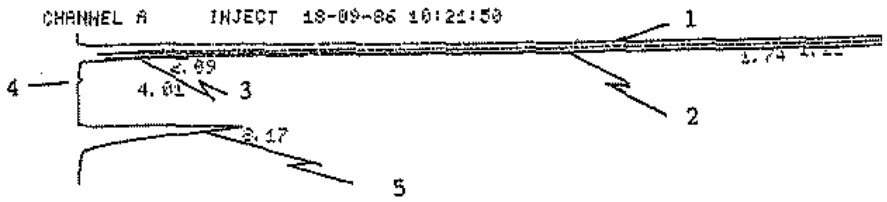
block, where evaporation took place and the carrier gas then fed the sample into the column. Data acquisition was carried out using the second channel of the electronic integrator, whose operation will be described later.

Appendix 7

Data evaluation and calculations

The signal from the thermal conductivity detector was transferred to the Spectra-Physics SP 4290 electronic integrator, which converted it to an area count for the various components analysed for. The integrator also provided a gas chromatographic trace of retention time versus detector response as shown in Figure 2.8 for a typical analysis.

Figure 2.8 : Chromatogram of a typical permanent gas analysis



FILE 1. METHOD 1. RUN 96 INDEX 96

NAME	%	RT	AREA	BC	RF
HYDROGEN	30.722	1.21	1937577	03	0.084
NITROGEN	35.216	1.74	186685	06	1.
C.MONOX.DE	2.609	2.89	14548	07	0.926
METHANE	0.062	4.01	1126	01	0.288
C DIOXIDE	31.381	0.17	195024	01	0.899
TOTALS	100.		2328291		

1 = Hydrogen 2 = Nitrogen

3 = Carbon Monoxide 4 = Methane

5 = Carbon Dioxide

A normalisation method was used to obtain quantitative results, after correcting for detector response of the various components. The method of correcting for detector response of the individual components was outlined by Dietz (86), who tabulated the response factors for many organic and inorganic compounds. However, from experiments performed in our laboratories, it was found that Dietz's response factors were considered too inaccurate for the work presented in this thesis. Thus, a standard pre-calibrated gas mixture, containing known quantities of all the components analysed for was obtained from Afrox's special gas division and injected into the gas chromatograph. The individual response factors were then calculated from the area counts obtained for each component and normalised using nitrogen as the base.

The factors were then entered into the integrator's data evaluation program which was used to calculate the volume % of each component using the following formula:

$$\%\ \text{vol}\ (i) = \frac{\text{Area count}\ (i) \times RF(i)}{\sum_{i=1}^{n} (\text{Area count}\ (i) \times RF(i))} \times 100$$

where % vol (i) = volume percent of component i

RF (i) = response factor of component i

Area count (i) = area count of component i

Flame ionisation detector (FID) response was also converted to an area count using the second input channel of the integrator, which monitored and recorded the both the TCD and the FID signals simultaneously. The integrated FID data was corrected for detector response, by using the literature correction factors (86). For compounds not covered in the literature, a known volume of the compound was injected into the gas chromatograph and the relevant response factor was then calculated. Once the corrected area counts were obtained, the results for all the organic compounds were normalised and a % selectivity on a mass basis was obtained and reported.

All catalyst activities were expressed as % CO conversion, which was calculated using the following formula:

$$\% \text{ CO conversion} = \frac{\text{moles CO in} - \text{moles CO out}}{\text{moles CO in}} \times 100$$

Appendix 8

Catalyst characterisation

Powder X-ray diffractometry (XRD) was used to determine the crystalline bulk structure of the various catalyst precursors investigated. The instrumentation included a Phillips PW 1050 diffractometer, which incorporated a copper anode and a graphite monochromator. The peaks of the individual spectra obtained were manually assigned using data in the JCPD file.

BET surface area measurements were determined with a Carlo Erba Sorptomatic Series 1800 analyser. The samples analysed were heated and degassed at 110°C for 8 hours under nitrogen and adsorption isotherms were plotted and the surface area was calculated using the BET equation.

In order to supplement the XRD data obtained, DSC and TGA were also undertaken. These experiments were carried out using a Dupont 9900 thermal analysis system, which was linked to a 910 DSC as well as a 951 TGA module.

The various catalysts investigated were heated from ambient temperature to 550°C at a steady rate of

5°C/min, in the presence of various gases hydrogen. These techniques allowed for the detection of phase changes (DSC) as well as weight changes (TGA) in the catalysts, which could be interpreted as changes in the bulk structures at specific temperatures.

Appendix 9

List of Publications

1) F.M. Gottschalk and G.J. Hutchings
Cobalt Manganese Oxide: A Novel High Activity Water Gas Shift Catalyst
J. Chem. Soc., Chem. Commun., 123 , (1988)

2) F.M. Gottschalk, R.G.Copperthwaite,M. van der Riet and G.J. Hutchings
Cobalt Manganese Oxide Water-Gas Shift Catalysts: Competition Between Carbon Monoxide Hydrogenation and Water Gas Shift Activity
Appl. Catal. , 38 , 103 , (1988)

3) G.J. Hutchings, F.M. Gottschalk, R.Hunter and S.W. Orchard
Cobalt Manganese Oxide Water-Gas Shift Catalysts: A Kinetic and Mechanistic Study
J. Chem. Soc.,Faraday Trans. 1 , 85 , 363 , (1989)

4) G.J. Hutchings and F.M. Gottschalk
Cobalt Manganese Oxide Water-Gas Shift Catalysts: Comparison with Copper Manganese and Iron Manganese Catalysts
Submitted to Appl. Catal. , (1989)

LIST OF PUBLICATIONS (continued)

5) F.M. Gottschalk and G.J. Hutchings
Catalyst Material
South African Patent No. 9002 , (1987)

6) F.M. Gottschalk and G.J. Hutchings
Catalyst Material
South African Patent No. 5269 , (1988)

7) F.M. Gottschalk, T. Sangiorgio and G.J. Hutchings
Method for the conversion of CO
South African Patent No. 0644 , (1989)

25×

Author Gottschalk Frank Michael
Name of thesis Water-gas Shift Reaction Over Supported Metal Oxides With Special Reference To The Cobalt Manganese Oxide System. 1989

PUBLISHER:
University of the Witwatersrand, Johannesburg
©2013

LEGAL NOTICES:

Copyright Notice: All materials on the University of the Witwatersrand, Johannesburg Library website are protected by South African copyright law and may not be distributed, transmitted, displayed, or otherwise published in any format, without the prior written permission of the copyright owner.

Disclaimer and Terms of Use: Provided that you maintain all copyright and other notices contained therein, you may download material (one machine readable copy and one print copy per page) for your personal and/or educational non-commercial use only.

The University of the Witwatersrand, Johannesburg, is not responsible for any errors or omissions and excludes any and all liability for any errors in or omissions from the information on the Library website.